

**STUDY OF UTILIZING PALM AND BAGASSE ASH
AS ADDITIVES IN DRILLING MUDS**



**A Thesis Submitted in Partial Fulfillment of the Requirements for the
Degree of Master of Engineering in Geotechnology
Suranaree University of Technology
Academic Year 2016**

การศึกษาการใช้เก้าอี้ปัดน้ำมันและเก้าอี้ขานอ้อยเป็นสารเติมแต่ง
ในน้ำโคลนขุดเจาะ



วิทยานิพนธ์นี้เป็นส่วนหนึ่งของการศึกษาตามหลักสูตรปริญญาวิศวกรรมศาสตรมหาบัณฑิต
สาขาวิชาเทคโนโลยีธรณี
มหาวิทยาลัยเทคโนโลยีสุรนารี
ปีการศึกษา 2559

**STUDY OF UTILIZING PALM AND BAGASSE ASH AS
ADDITIVES IN DRILLING MUDDS**

Suranaree University of Technology has approved this thesis submitted in partial fulfillment of the requirements for a Master's Degree.

Thesis Examining Committee



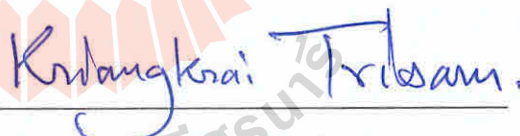
(Prof. Dr. Kittitep Fuenkajorn)

Chairperson



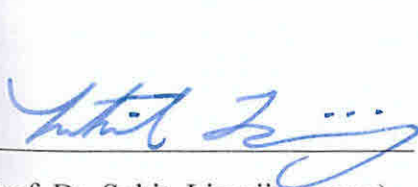
(Asst. Prof. Dr. Bantita Terakulsatit)

Member (Thesis Advisor)



(Assoc. Prof. Kriangkrai Trisarn)

Member



(Prof. Dr. Sukit Limpijumnong)

Vice Rector for Academic Affairs
and Innovation



(Assoc. Prof. Flt. Lt. Dr. Kontorn Chamniprasart)

Dean of Institute of Engineering

อารดา แสงดี : การศึกษาการใช้เถ้าปาล์มน้ำมันและเถ้าชานอ้อยเป็นสารเติมแต่งใน
น้ำโคลนขุดเจาะ (STUDY OF UTILIZING PALM AND BAGASSE ASH AS
ADDITIVES IN DRILLING MUDS) อาจารย์ที่ปรึกษา : ผู้ช่วยศาสตราจารย์
ดร.บัณฑิตา ชีระกุลสถิตย์, 185 หน้า.

งานวิจัยนี้มีวัตถุประสงค์เพื่อศึกษาคุณสมบัติทางเคมีและกายภาพของเถ้าปาล์มน้ำมันและ
เถ้าชานอ้อยและน้ำโคลนขุดเจาะผสมเถ้าปาล์มน้ำมันและเถ้าชานอ้อย น้ำโคลนขุดเจาะผสมด้วย
สารเติมแต่งที่มีความเข้มข้นร้อยละ 1, 3 และ 5 โดยน้ำหนัก ซึ่งทดสอบที่อุณหภูมิ 25, 50 และ 80
องศาเซลเซียส โดยเฉพาะการใช้เถ้าปาล์มน้ำมันและเถ้าชานอ้อยเป็นสารเติมแต่งเพื่อช่วยปรับปรุง
คุณสมบัติด้านวิทยาการกระแส เช่น การเพิ่มค่าความหนืดและลดการสูญเสียของของไหลในน้ำโคลน
ขุดเจาะ การทดสอบคุณสมบัติทางเคมีพบว่าองค์ประกอบทางเคมีของเถ้าปาล์มน้ำมันส่วนใหญ่
ประกอบด้วยซิลิกา โปแทสเซียม แคลเซียมและคลอไรด์ แร่ประกอบที่พบส่วนใหญ่คือแร่ซิลิไท์
ควอตซ์ อะนอร์ไทท์ เคโอลิไนท์และยิปซัม จากโครงสร้างจุลภาคของเถ้าปาล์มน้ำมันแสดงลักษณะ
กลม รูปร่างไม่แน่นอนและเป็นเหลี่ยมมุม ขณะที่อนุภาคบางส่วนมีลักษณะกลมและต่อเนื่อง เถ้า
ชานอ้อยพบว่ามีปริมาณของซิลิกาสูงถึงร้อยละ 88.38 และธาตุประกอบอื่นๆ เล็กน้อย แร่ประกอบที่
สำคัญคือแร่ควอตซ์ แบไรต์ แคลไซต์ อะนอร์ไทท์ เคโอลิไนท์และยิปซัม ลักษณะของรูปร่าง
อนุภาคของเถ้าชานอ้อยแสดงรูปร่างไม่แน่นอน พื้นผิวขรุขระและพื้นผิวมีรูพรุนขนาดเล็ก จากผล
การวิเคราะห์คุณสมบัติทางเคมีพบว่าอุณหภูมิในการทดสอบไม่มีผลต่อการเปลี่ยนแปลงธาตุและแร่
ประกอบ และ โครงสร้างของแร่ในน้ำโคลนขุดเจาะ ทั้งนี้ น้ำโคลนขุดเจาะหลังการผสมเถ้าปาล์ม
น้ำมันและเถ้าชานอ้อยจะเกิดการเปลี่ยนแปลงองค์ประกอบทางเคมีและแร่ประกอบโดยขึ้นกับอัตรา
ส่วนผสมของเถ้าปาล์มและเถ้าชานอ้อย การทดสอบคุณสมบัติทางกายภาพประกอบด้วยความ
หนาแน่น ความหนืด การซึมผ่าน ความเป็นกรด-ด่าง ความต้านทาน ไฟฟ้า และปริมาณของแข็งของ
น้ำโคลนขุดเจาะ โดยทำการทดสอบตามขั้นตอนมาตรฐาน API RP 13B-1 จากผลการเปรียบเทียบ
คุณสมบัติทางด้านวิทยาการกระแส ซึ่งประกอบด้วย ความหนืดปรากฏ ค่าความหนืดพลาสติก จุดคราก
และความแข็งแรงของเจลของน้ำโคลนขุดเจาะ พบว่าน้ำโคลนขุดเจาะผสมเถ้าปาล์มน้ำมันสามารถ
เพิ่มคุณสมบัติทางด้านวิทยาการกระแสได้สูงกว่าน้ำโคลนขุดเจาะผสมเถ้าชานอ้อยในทุกอุณหภูมิของ
การทดสอบ ทั้งนี้ที่ความเข้มข้นร้อยละ 3 โดยน้ำหนักของเถ้าปาล์มน้ำมันเป็นอัตราผสมที่เหมาะสม
สำหรับการนำไปใช้เพื่อเพิ่มคุณสมบัติทางด้านวิทยาการกระแส ขณะที่น้ำโคลนขุดเจาะที่ผสมเถ้าชาน
อ้อยในทุกอุณหภูมิตดสอบมีคุณสมบัติทางด้านการป้องกันการสูญเสียของของไหลและความหนา
ของชั้นผนังโคลนได้อย่างมีประสิทธิภาพ ซึ่งดีกว่าน้ำโคลนขุดเจาะผสมเถ้าปาล์มน้ำมันและ
น้ำโคลนขุดเจาะมาตรฐาน ที่อุณหภูมิ 25 องศาเซลเซียส ความเข้มข้นร้อยละ 1 โดยน้ำหนักของ

เจ้าชานอ้อย พบว่ามีคุณสมบัติในการป้องกันการสูญเสียของของไหลและความหนาของชั้นผนังโคลนได้ดีที่สุด จากการเปรียบเทียบราคาของเจ้าปาล์มน้ำมันและเจ้าชานอ้อยกับสารเติมแต่งอื่นๆ พบว่าต้นทุนสุทธิของเจ้าปาล์มน้ำมันและเจ้าชานอ้อยนั้นมีราคาสูงกว่าสารเติมแต่งอื่นๆ อย่างไรก็ตามหากมีการนำเจ้าปาล์มน้ำมันและเจ้าชานอ้อยมาผลิตเป็นสารเติมแต่งในเชิงพาณิชย์ จะสามารถช่วยลดราคาต้นทุนของเจ้าเหล่านี้ลงได้ ดังนั้นเจ้าปาล์มน้ำมันเหมาะสมในการนำมาใช้เป็นสารเติมแต่งเพื่อปรับปรุงคุณสมบัติทางด้านวิทยากระแสน้ำโคลนขุดเจาะ ในขณะที่เจ้าชานอ้อยเหมาะสมในการนำมาใช้เป็นสารเติมแต่งเพื่อปรับปรุงคุณสมบัติทางด้านป้องกันการสูญเสียของของไหล



สาขาวิชาเทคโนโลยีธรณี

ปีการศึกษา 2559

ลายมือชื่อนักศึกษา _____

ลายมือชื่ออาจารย์ที่ปรึกษา _____

ARADA SAENGDEE : STUDY OF UTILIZING PALM AND BAGASSE
ASH AS ADDITIVES IN DRILLING MUDS. THESIS ADVISOR :
ASST. PROF. BANTITA TERAKULSATIT, Ph.D., 185 PP.

PALM OIL FUEL ASH/ SUGARCANE BAGASSE ASH/ DRILLING MUDS

The objective of this study is to determine the chemical and physical properties of water based drilling mud mixed with palm and bagasse ash. The drilling mud is mixed with 1, 3 and 5 percent by weight of additives with testing temperatures at 25, 50 and 80°C. Particularly, the palm and bagasse ash as additive used for enhancing the rheological properties, such as increasing of viscosity and decreasing fluid loss. The chemical property analysis indicates that the palm ash comprises mainly of silica, potassium oxide, calcium oxide and chloride. The minerals that have the greatest amount are sylvite, quartz, anorthite, kaolinite and gypsum. The microstructure of palm ash shows round, irregular and angular shaped particles, while some particles are rounded and contiguous clusters. The bagasse ash shows a high amount of silica of 88.38% and slight other element. The major minerals dominantly comprise quartz, barite, calcite, anorthite, kaolinite and gypsum. The particle shape of bagasse ash shows an irregular shape with rough surfaces and small porous textures. The results of chemical analysis show that the testing temperature has no effect on the elemental and mineral compositions, and mineral structures in drilling mud. However, the drilling mud after mixed with additive changes the contents in chemical and minerals which depend on the mixed ratio. The physical property includes the density, viscosity, filtration, pH, resistivity and solid content according with API RP 13B-1 standard.

Comparison of rheological property, including apparent viscosity, plastic viscosity, yield point and gel strength between drilling mud mixed with palm ash and bagasse ash, present that the palm ash is generally greater than bagasse ash for rheological property of drilling mud throughout a temperature range. The drilling mud mixed with 3% of palm ash, gives appropriate rheological properties. The drilling mud mixed with bagasse ash in all testing temperatures shows high potential filtrate volume and mud filter cake thickness, representing better filtration control characteristics than these of palm ash and water based mud. At the temperature of 25°C, 1% of bagasse ash shows the best filtration control characteristics with minimal filtrate volume and thinner and consistent mud filter cakes. Comparative cost of palm and bagasse ash with other additives found that the net cost of palm and bagasse ash still are expensive than chemical additives. However, if the palm and bagasse ash could be produced in commercial, which it could be able to reduce the cost use these materials as additive in drilling mud. Therefore, the palm ash is suitable for additive enhancement of rheological properties in drilling mud. Meanwhile, bagasse ash is appropriate to be additive for fluid loss control properties.

School of Geotechnology

Academic Year 2016

Student's Signature _____

Advisor's Signature _____

ACKNOWLEDGEMENT

First and foremost, I wish to express my sincere thanks to my thesis advisor, Asst. Prof. Dr. Bantita Terakulsatit for her invaluable help and constant encouragement throughout the course of this research. I am most grateful for her teaching and advice, not only the research methodologies, but also many other methodologies in life. I would not have achieved this far and this thesis would not have been completed without all the support that I have always received from her.

I would like to thank the lectures in the school of geotechnology: Assoc. Prof. Kriangkrai Trisarn, Asst. Prof. Dr. Akkhapun Wannakomol and many others for suggestions and all their help.

In addition, I am grateful to the technicians and personnel at the geotechnology laboratory for their suggestions and help. My special thanks go to Ms. Supharapon Sakulpakdee for her full support.

Finally, I am most grateful to my parents and my friends for all their support throughout the period of this research.

Arada Saengdee

TABLE OF CONTENTS

	Page
ABSTRACT (THAI).....	I
ABSTRACT (ENGLISH).....	III
ACKNOWLEDGEMENTS.....	V
TABLE OF CONTENTS.....	VI
LIST OF TABLES.....	XI
LIST OF FIGURES.....	XII
SYMBOLS AND ABBREVIATIONS.....	XVIII
CHAPTER	
I INTRODUCTION.....	1
1.1 Rational and background.....	1
1.2 Research Objective.....	3
1.3 Scope and limitation of the study.....	3
1.4 Thesis contents.....	4
II LITERATURE REVIEW.....	5
2.1 Introduction.....	5
2.2 Palm oil fuel ash.....	5
2.2.1 Physical properties of palm oil fuel ash.....	6
2.2.2 Chemical compositions of palm oil fuel ash.....	8
2.2.3 Development of concrete by palm oil fuel ash.....	9

TABLE OF CONTENTS (Continued)

	Page
2.3 Sugarcane bagasse ash.....	10
2.3.1 Properties of sugarcane bagasse ash.....	11
2.3.2 Development of concrete by sugarcane bagasse ash.....	12
2.4 Drilling mud.....	13
2.5 Functions of drilling mud.....	14
2.6 Drilling mud improvement.....	15
2.7 Drilling mud rheology.....	18
2.7.1 Newtonian fluid model.....	18
2.7.2 Non-Newtonian fluid.....	20
2.7.2.1 Bingham plastic model.....	20
2.7.2.2 Power law model.....	22
2.7.2.3 Herschel-Bulkley model.....	25
2.8 API recommended practices.....	26
III METHODOLOGY.....	28
3.1 Introduction.....	28
3.2 Research methodology.....	28
3.2.1 Literature review.....	28
3.2.2 Collecting the samples of POFA and SCBA.....	29
3.2.3 Preparing and analysis of POFA and SCBA.....	29
3.2.3.1 Chemical properties tests.....	30

TABLE OF CONTENTS (Continued)

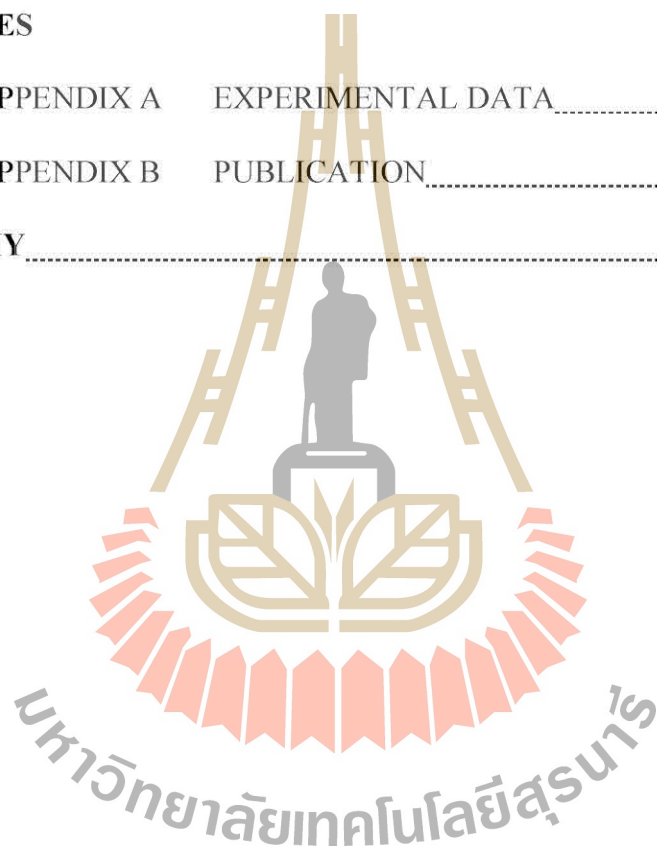
	Page
3.2.3.2 Physical properties tests.....	30
3.2.4 Collection data and testing results.....	30
3.2.5 Discussions, conclusions and thesis writing.....	31
3.3 Sample collection.....	31
3.4 Sample preparation.....	32
3.5 Chemical properties tests.....	35
3.5.1 X-ray Fluorescence.....	35
3.5.2 X-ray Diffraction.....	37
3.6 Physical properties tests.....	38
3.6.1 Density.....	38
3.6.2 Rheology.....	39
3.6.3 Filtration.....	46
3.6.4 Hydrogen ion concentration.....	47
3.6.5 Resistivity.....	48
3.6.6 Solid content.....	49
3.6.7 Scanning Electron Microscope.....	51
3.6.8 Field Emission Scanning Electron Microscope.....	52
IV RESULTS AND DISCUSSIONS.....	55
4.1 Introduction.....	55
4.2 Chemical properties.....	55

TABLE OF CONTENTS (Continued)

	Page
4.2.1 Chemical composition.....	55
4.2.2 Mineral composition.....	59
4.3 Physical properties.....	66
4.3.1 Density properties.....	66
4.3.2 Rheology properties and parameters.....	69
4.3.3 Rheological behavior of drilling mud.....	78
4.3.4 Filtration properties.....	93
4.3.5 Hydrogen ion concentration properties.....	101
4.3.6 Resistivity properties.....	107
4.3.7 Solid content properties.....	115
4.3.8 Morphology properties.....	118
4.4 Cost analysis.....	121
4.5 Summary of chemical and physical properties of drilling mud mixed with POFA and SCBA.....	123
V CONCLUSIONS AND RECOMMENDATIONS.....	132
5.1 Introduction.....	132
5.2 Conclusions.....	132
5.2.1 Chemical property.....	132
5.2.2 Physical property.....	133
5.2.3 Cost analysis.....	136

TABLE OF CONTENTS (Continued)

	Page
5.3 Recommendations.....	137
REFERENCES	139
APPENDICES	
APPENDIX A EXPERIMENTAL DATA.....	146
APPENDIX B PUBLICATION.....	183
BIOGRAPHY	185



LIST OF TABLES

Table	Page
2.1 Physical properties of POFA (after Safiuddin et al., 2011).....	6
2.2 Chemical compositions of POFA (after Safiuddin et al., 2011).....	8
2.3 Chemical compositions of SCBA (after Cordeiro et al., 2004).....	11
2.4 Physical properties of SCBA (after Cordeiro et al., 2004; Goyal et al., 2007).....	12
3.1 Bentonite water based suspension.....	34
3.2 Composition of POFA mud samples.....	34
3.3 Composition of SCBA mud samples.....	35
4.1 Chemical compositions of various materials.....	57
4.2 Chemical compositions of drilling mud mixed with additives.....	58
4.3 Mineral compositions of various materials.....	61
4.4 Mineral compositions of drilling mud mixed with additives.....	62
4.5 Results of shear stress and shear rate of water based drilling mud.....	69
4.6 Rheological parameters of drilling mud.....	76
4.7 Cost of drilling mud chemicals.....	122
4.8 Summarized comparison of the chemical and physical properties of drilling mud mixed with POFA and SCBA additives.....	125

LIST OF FIGURES

Figure	Page	
2.1	Ideal consistency curves for common flow models (after Caenn et al., 2011).....	19
2.2	Flow curve for a Newtonian fluid (after Caenn et al., 2011).....	20
2.3	Flow curve for a Bingham plastic model (after Baker Hughes, 2006).....	22
2.4	Flow curve for a Power law model (after Baker Hughes, 2006).....	23
2.5	Flow Behavior for Power law model (after Baker Hughes, 2006).....	24
3.1	Research methodology.....	29
3.2	Retsch sieve shakers.....	32
3.3	Yield curve for typical clays (after Gatlin, 1960).....	33
3.4	Hamilton Beach commercial mixer 3 speed mixer with 1 spindle.....	35
3.5	Horiba XGT-5200 X-ray Fluorescence.....	36
3.6	Bruker-D2 Phaser X-ray Diffraction.....	38
3.7	Fann model 140 mud balance.....	39
3.8	Fann model 35SA viscometer.....	40
3.9	Plastic viscosity and yield point values from two measurements (after Baker Hughes, 2006).....	42
3.10	Plastic viscosity and yield point ranges for water base drilling mud (after MI Swaco, 1998).....	42
3.11	Log plot of Power law models (after Baker Hughes, 2006).....	46

LIST OF FIGURES (Continued)

Figure	Page
3.12 Fann series 300 API filter press.....	47
3.13 Oakton pH 700 benchtop meter.....	48
3.14 Fann model 88c resistivity meter.....	49
3.15 Fann retort oil and water 50 ml kit.....	51
3.16 JEOL JSM-6010LV Scanning Electron Microscope.....	52
3.17 Carl Zeiss Auriga Field Emission Scanning Electron Microscope.....	54
4.1 XRD pattern of POFA.....	64
4.2 XRD pattern of SCBA.....	65
4.3 Density of base mud mixed with POFA versus temperature.....	67
4.4 Density of base mud mixed with SCBA versus temperature.....	67
4.5 Density of drilling mud versus additive concentration at (a) 25°C, (b) 50°C and (c) 80°C.....	68
4.6 Consistency plot of base mud with a linear correction.....	70
4.7 Consistency plot of base mud with a power correction.....	70
4.8 Consistency plot of base mud mixed with POFA at 25°C.....	71
4.9 Consistency plot of base mud mixed with POFA at 50°C.....	72
4.10 Consistency plot of base mud mixed with POFA at 80°C.....	72
4.11 Consistency plot of base mud mixed with SCBA at 25°C.....	73
4.12 Consistency plot of base mud mixed with SCBA at 50°C.....	73
4.13 Consistency plot of base mud mixed with SCBA at 80°C.....	74

LIST OF FIGURES (Continued)

Figure	Page
4.14 Consistency plot of drilling mud at 25°C.....	74
4.15 Consistency plot of drilling mud at 50°C.....	75
4.16 Consistency plot of drilling mud at 80°C.....	75
4.17 Apparent viscosity of drilling mud versus POFA concentration.....	80
4.18 Apparent viscosity of drilling mud versus SCBA concentration.....	80
4.19 Apparent viscosity of base mud mixed with (a) POFA and (b) SCBA versus temperature.....	81
4.20 Plastic viscosity of drilling mud versus POFA concentration at (a) 25°C, (b) 50°C and (c) 80°C.....	82
4.21 Plastic viscosity of drilling mud versus SCBA concentration at (a) 25°C, (b) 50°C and (c) 80°C.....	83
4.22 Plastic viscosity of base mud mixed with POFA versus temperature; (a) base mud, (b) base+ 1% POFA, (c) base+ 3% POFA and (d) base+ 5% POFA.....	84
4.23 Plastic viscosity of base mud mixed with SCBA versus temperature; (a) base mud, (b) base+ 1% SCBA, (c) base+ 3% SCBA and (d) base+ 5% SCBA.....	85
4.24 Yield point of drilling mud versus POFA concentration.....	87
4.25 Yield point of drilling mud versus SCBA concentration.....	87

LIST OF FIGURES (Continued)

Figure	Page
4.26 Yield point of base mud mixed with (a) POFA and (b) SCBA versus temperature.....	88
4.27 Initial gel strength of drilling mud versus POFA concentration.....	89
4.28 Initial gel strength of drilling mud versus SCBA concentration.....	89
4.29 Initial gel strength of base mud mixed with (a) POFA and (b) SCBA versus temperature.....	90
4.30 10 minutes gel strength of drilling mud versus POFA concentration.....	91
4.31 10 minutes gel strength of drilling mud versus SCBA concentration.....	91
4.32 10 minutes gel strength of base mud mixed with (a) POFA and (b) SCBA versus temperature.....	92
4.33 Static filtration and time of base mud.....	94
4.34 Static filtration of base mud mixed with POFA versus time at 25°C.....	95
4.35 Static filtration of base mud mixed with POFA versus time at 50°C.....	95
4.36 Static filtration of base mud mixed with POFA versus time at 80°C.....	96
4.37 Static filtration of base mud mixed with SCBA versus time at 25°C.....	97
4.38 Static filtration of base mud mixed with SCBA versus time at 50°C.....	97
4.39 Static filtration of base mud mixed with SCBA versus time at 80°C.....	98
4.40 API filtrate volume at 30 minutes of base mud mixed with POFA.....	99
4.41 API filtrate volume at 30 minutes of base mud mixed with SCBA.....	99
4.42 Mud filter cake of base mud mixed with POFA versus temperature.....	100

LIST OF FIGURES (Continued)

Figure	Page
4.43 Mud filter cake of base mud mixed with SCBA versus temperature.....	101
4.44 pH of base mud versus temperature.....	102
4.45 pH of base mud mixed with POFA versus temperature.....	103
4.46 pH of base mud mixed with SCBA versus temperature.....	103
4.47 pH of drilling mud versus additive concentration at (a) 25°C, (b) 50°C and (c) 80°C.....	104
4.48 pH of mud filtrate of base mud mixed with POFA versus temperature.....	105
4.49 pH of mud filtrate of base mud mixed with SCBA versus temperature.....	105
4.50 pH of mud filtrate versus additive concentration at (a) 25°C, (b) 50°C and (c) 80°C.....	106
4.51 Resistivity of base mud versus temperature.....	108
4.52 Resistivity of base mud mixed with POFA versus temperature.....	108
4.53 Resistivity of base mud mixed with SCBA versus temperature.....	109
4.54 Resistivity of drilling mud versus additive concentration at (a) 25°C, (b) 50°C and (c) 80°C.....	110
4.55 Resistivity of mud filtrate of base mud mixed with POFA versus temperature.....	111
4.56 Resistivity of mud filtrate of base mud mixed with SCBA versus temperature.....	111

LIST OF FIGURES (Continued)

Figure	Page
4.57 Resistivity of mud filtrate versus additive concentration at (a) 25°C, (b) 50°C and (c) 80°C.....	112
4.58 Resistivity of mud filter cake of base mud mixed with POFA versus temperature.....	113
4.59 Resistivity of mud filter cake of base mud mixed with SCBA versus temperature.....	113
4.60 Resistivity of mud filter cake versus additive concentration at (a) 25°C, (b) 50°C and (c) 80°C.....	114
4.61 Solid content of base mud mixed with POFA versus temperature.....	116
4.62 Solid content of base mud mixed with SCBA versus temperature.....	116
4.63 Solid content of drilling mud versus additive concentration at (a) 25°C, (b) 50°C and (c) 80°C.....	117
4.64 SEM image of mud filter cake (size 1 µm) formed by base mud on at (a) 25°C, (b) 50°C and (c) 80°C.....	118
4.65 SEM image of POFA size (a) 100 µm and (b) 20 µm.....	119
4.66 SEM image of mud filter cake (size 50 µm at temperature 25°C) formed by (a) base+ 1% POFA, (b) base+ 3% POFA and (c) base+ 5% POFA.....	120
4.67 SEM image of SCBA size (a) 10 µm and (b) 1 µm.....	120
4.68 SEM image of mud filter cake (size 10 µm at temperature 25°C) formed by (a) base+ 1% SCBA, (b) base+ 3% SCBA and (c) base+ 5% SCBA.....	121

SYMBOLS AND ABBREVIATIONS

ROMAN ABBREVIATIONS:

%w/w	=	Percentage of weight by weight
AV	=	Apparent viscosity
cP	=	Centipoise
FE-SEM	=	Field Emission Scanning Electron Microscope
g	=	Gram
Gel ₁₀	=	10 minutes gel strength
Gel _{in}	=	Initial gel strength
K	=	Fluid consistency index
ml	=	Milliliter
mm	=	Millimeter
n	=	Flow behavior index
OBM	=	Oil based mud
POFA	=	Palm oil fuel ash
PV	=	Plastic viscosity
rpm	=	Rotational speed
SCBA	=	Sugar cane bagasse ash
SEM	=	Scanning Electron Microscope
Temp.	=	Temperature
WBM	=	Water based mud
XRD	=	X-ray Diffraction

SYMBOLS AND ABBREVIATIONS (Continued)

XRF = X-ray Fluorescence

YP = Yield point

GREEK ABBREVIATIONS:

μ = Viscosity

μ_a = Apparent viscosity

μ_m = Micrometer

μ_p = Plastic viscosity

γ = Shear rate

γ_p = Yield point

θ = Mud viscometer dial readings

θ_{300} = Mud viscometer dial readings at 300 rpm

θ_{600} = Mud viscometer dial readings at 600 rpm

τ = Shear stress

τ_0 = Yield stress

τ_y = Yield point

ω = Mud viscometer RPM

ω_{300} = Mud viscometer RPM at 300 rpm

ω_{600} = Mud viscometer RPM at 600 rpm

CHAPTER I

INTRODUCTION

1.1 Background and rationale

A successful drilling procedure depends on the appropriate mixture and supervision of the drilling mud. The immense mass of petroleum explorations is majorly accomplished by applying water based drilling mud. Drilling mud which represents about one-fifth (15-18%) of the total cost of petroleum well drilling, must generally comply with three important requirements, they should be easy to use, not too expensive and environmentally friendly. The complex drilling mud plays several functions simultaneously. They are intended to clean the well, hold the cuttings in suspension, prevent caving, ensure the tightness of the well wall and form an impermeable cake near the wellbore area (Khodja et al., 2010). The significant factors in distinguishing the assets of a drilling mud are gel strength, viscosity (apparent and plastic viscosity), specific weight, pH, thermal stability and the filtration function (Caenn et al., 2016).

Many researches have used locally available materials as additives for drilling mud for fluid loss control agent, such as fly ash, cassava derivative, periwinkle shell ash (PSA). These materials are effective in the fluid loss control in various concentrations and temperature (Korsinwattana and Terakulsatit, 2014; Samavati et al., 2014; Igwe and Kinate, 2015).

Palm oil fuel ash (POFA) is a by-product from the palm oil industry. The palm oil industry is one of the most important agro industries in Thailand. The production of crude palm oil, a large amount of solid waste of palm oil residues, such as palm fiber, shells and empty fruit bunches is produced. Utilization of POFA is minimal and unmanageable, while its quantity increases annually and most of the POFA are disposed of as waste in landfills causing environmental and other problems. Likewise, Sugarcane is one of the foremost crops grown in all over countries and its entire production is over 1,500 million tons. After the extraction of all economical sugar from sugarcane, about 40-45% fibrous residue is obtained, this is reused in the same industry as fuel in boilers for heat generation leaving behind 8-10% ash as waste, known as sugarcane bagasse ash (SCBA) depending on the quality and type of the boiler (Modani and Vyawahare, 2013). The disposal of this material is already causing environmental problems around the sugar factories. While the quantity of the SCBA is increasing annually, but the utilization of the SCBA is minimal, unmanageable and causing environmental problems.

Most technical applications of POFA and SCBA has been in the area of civil engineering, using POFA and SCBA as partial replacement of cement in concrete (Sata et al., 2004; Tangchirapat et al., 2007; Chusilp et al., 2009; Srinivasan and Sathiya, 2010; Abbasi and Zargar, 2013). The successful applications of POFA and SCBA in concrete should encourage research on its applicability in other areas of engineering. However, these materials are never applied using in the drilling mud. Therefore, this work intends about the possibility to use POFA and SCBA as additives for enhancement the rheological properties, especially in the increasing of viscosity, thickener and decreasing fluid loss.

1.2 Research objectives

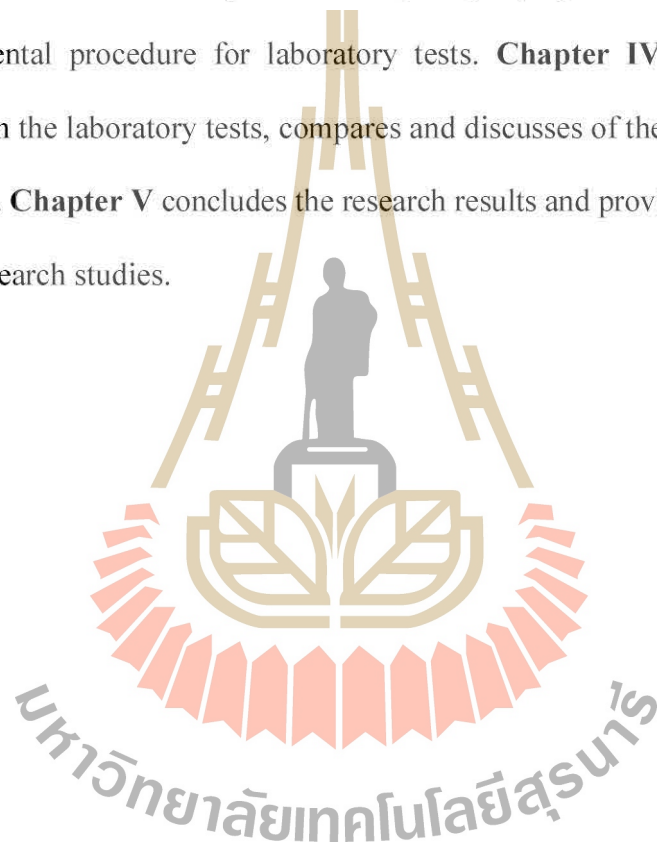
The main aim of this research is to enhance the efficiency of water based drilling mud using POFA and SCBA additives. Some more objectives are (1) determining the physical and chemical properties of POFA and SCBA and water based drilling mud mixed with POFA and SCBA, (2) studying the effects of temperature and mixing ratio of the rheological properties of drilling mud mixed with these additives, and (3) comparing the rheological properties of drilling mud mixed with different additives.

1.3 Scope and limitation of the study

This research is aimed to study the chemical and physical properties of water based drilling mud using POFA and SCBA additives when the POFA and SCBA concentration and temperature were changed. The chemical properties of additives are analyzed both before and after mixed with drilling mud via using X-ray Fluorescence (XRF) and X-ray Diffraction (XRD). The rheological properties tests are on a laboratory scale that is not a real borehole condition and ignoring the influence of pressure. The test procedures had been followed the API RP 13B-1 (1997) including density, rheology, filtration, hydrogen ion, resistivity and solid content of drilling mud. Moreover, analyzed both before and after mixed with drilling mud by using Scanning Electron Microscope (SEM) and Field Emission Scanning Electron Microscope (FE-SEM).

1.4 Thesis contents

Chapter I introduce the thesis by briefly describing the rationale and background. The research objectives and scope and limitation are identified. **Chapter II** summarizes results of the literature review to improve an understanding of water based drilling mud characteristics and the factor that affects to mud properties. **Chapter III** describes the sample collection, sample preparation, test instruments and the experimental procedure for laboratory tests. **Chapter IV** presents the results obtained from the laboratory tests, compares and discusses of the results between each mud formula. **Chapter V** concludes the research results and provides recommendations for future research studies.



CHAPTER II

LITERATURE REVIEW

2.1 Introduction

Relevant topics and previous research results are reviewed to improve understanding of water based drilling mud and applications, using of additives in drilling mud, POFA and SCBA properties and API recommended practices. This chapter also describes the drilling mud rheology which has played important roles for mud characteristic. The sources of information are from journals, researches, dissertation and books. The results of the review are summarized as follows.

2.2 Palm oil fuel ash

Malaysia, Indonesia and Thailand are amongst the countries in the equatorial belt that cultivate oil palm and palm oil products. The palm oil industry is one of the major agro-industries in Thailand. POFA is a by-product produced in palm oil industry. After palm oil is extracted from the palm oil fruit, both palm oil husks and palm oil shell are burned as fuel in the boiler of palm oil mill at a temperature of 800-1000°C. The burning process results in an ash, which is referred to as palm oil fuel ash (POFA). After combustion in the steam boiler, about 5% POFA by weight of solid wastes is produced (Sata et al., 2004). The ash produced sometimes varies in tone of color from whitish gray to darker shade based on the carbon content in it. POFA causes a nuisance to the environment. Since the tropical countries are continuously increasing the production of palm oil, the quantity of POFA is also increasing and

thus creating a large environmental load (Abdullah et al., 2006). Due to the absence of sufficient nutrients required for a fertilizer, POFA is mostly dumped in an open field near palm oil mills without any profitable return, thus causing environmental pollution and health hazard (Sumadi and Hussin, 1995; Tonnayopas et al., 2006).

2.2.1 Physical properties of palm oil fuel ash

The physical properties of POFA are greatly influenced by the burning condition, particularly burning temperature (Abdullah et al., 2006). A number of physical properties of unground and ground POFA used in various studies are shown in Table 2.1.

Table 2.1 Physical properties of POFA (after Safiuddin et al., 2011).

Properties	Unground POFA	Ground POFA
Color	light gray/whitish	dark gray
Specific gravity	1.78-1.97	2.22-2.78
Median particle size, d_{50} (μm)	54.3-183	7.2-10.1
% Passing through 45 μm sieve (% mass)	5.6-58.8	97-99
Specific surface area, Blaine (m^2/kg)	796	882-1244

Color

Generally, unground POFA is light gray in color. This is due to the unburned carbon content left at relatively low burning temperature. The unburned carbon content becomes very low when the burning temperature is high. Unground POFA can be whitish in the absence of unburned carbon (Abdullah et al., 2006). The color becomes dark gray in a case of ground POFA.

Specific gravity

The specific gravity of unground POFA generally varies in the range of 1.78-1.97. After the grinding process, the specific gravity of POFA increases and is found to be in the range of 2.22-2.78 (Sata et al., 2004; Tangchirapat et al., 2009). This is because the grinding process decreases the porosity with reduced particle size.

Particle shape and size

The particle shape and size of ground and unground POFA are different. From SEM, it was found that the unground POFA particles are mostly large, spherical and porous. In contrast, the ground POFA generally consists of crushed particles with irregular and angular shape (Chindapasirt et al., 2007).

The median particle size (d_{50}) of unground POFA varies in the range of 54.3-183 μm . After grinding, the median particle size of POFA can be reduced to 7.2-10.1 μm (Sata et al., 2004; Chindapasirt et al., 2008).

Fineness

The particle size of POFA can be reduced by the grinding process in ball mills (Sata et al., 2007; Tangchirapat et al., 2007; Tangchirapat et al., 2009). POFA may also be ground in a Los Angeles abrasion machine using mild steel bar (12 mm diameter and 800 mm long) instead of steel ball (Abdullah et al., 2006; Awal and Hussin, 1999; Hussin and Awal, 1996). The grinding process reduces not only the particle size, but also the porosity of POFA (Kiattikomol et al., 2001). After grinding, POFA can be less porous with smaller particles (Payá et al., 1996).

The fineness of POFA can also be expressed with regard to the percentage mass passing through or retained on sieve No.325 (45 μm opening). The percentage mass passing sieve No.325 can be in the range of 5.6-58.8% for unground

POFA whereas it can be 97-99% for ground POFA. Both specific surface area and percentage mass passing sieve No.325 reveal that the surface area of POFA becomes higher after grinding.

2.2.2 Chemical compositions of palm oil fuel ash

The chemical compositions of POFA reported in various studies are summarized in Table 2.2.

Table 2.2 Chemical compositions of POFA (after Safiuddin et al., 2011).

Chemical components	Weight fraction (%)
SiO ₂	44-66
Al ₂ O ₃	1.5-11.5
Fe ₂ O ₃	1.5-5.5
SiO ₂ +Al ₂ O ₃ +Fe ₂ O ₃	55-70
CaO	4-8.5
MgO	2-6.5
K ₂ O	2-8.5
Na ₂ O	0.1-3.5
SO ₃	0.2-3.0
Loss on ignition (LOI)	0.1-21.5

The major chemical component of POFA is SiO₂, which varies in the range of 44-66%. The other pozzolanic components are Al₂O₃ and Fe₂O₃. The loss on ignition (LOI) and SO₃ are in the range of 0.1-21.5% and 0.2-3%, respectively. There are many arguments in justifying the classification of POFA based on its chemical

composition. This is possibly due to the variability in the nature of the product, and also because of various burning conditions. Hence, more study is needed to avoid this contradiction by establishing a proper classification.

2.2.3 Development of concrete by palm oil fuel ash

Many researchers (Tay, 1990; Sumadi and Hussin, 1995; Hussin and Awal, 1996; Sata et al., 2010) have found that POFA can be used in the construction industry, specifically as a supplementary cementitious material in concrete.

Tay (1990) investigated the use of ash derived from oil palm waste incineration in making blended cement, the results showed that replacing 10-50% ash by weight of cementitious material in blended cement had no significant effect on segregation, shrinkage, water absorption, density or soundness of concrete. Within the 20-50% replacement rate range, the decrease in the compressive strength of concrete at various ages was almost proportional to the amount of ash in the blended cement, with the exception of 10% replacement.

Sumadi and Hussin (1995) unground POFA, used up to 20% as a cement replacement, has no adverse effect on the strength characteristics and has a durability factor that is at least comparable to that of Portland cement (OPC) concrete. Ground POFA provides much higher compressive strength than unground POFA because of significant differences in particle size and fineness. The ground POFA with high fineness is a reactive pozzolanic material and can be used to make high-strength and high-performance concrete.

Hussin and Awal (1996) studied the compressive strength of concrete containing POFA at various replacement levels of 10, 20, 30, 40, 50 and 60% by weight of ordinary Portland cement. The results revealed that it was possible to

replace at a level of 40% POFA without affecting compressive strength. The maximum compressive strength gain occurred at a replacement level of 30% by weight of binder.

Sata et al. (2010) investigated the strength development of POFA concretes with water/binder ratios of 0.50, 0.55 and 0.60 tended to be in the same direction. At early ages, concretes containing POFA as a cement replacement of 10, 20 and 30% had lower strength development than control concretes while at a later age (>28 days), the replacement at rates of 10 and 20% yielded higher strength development. The temperature rise of fresh concrete decreased as POFA content increased. For concrete with a water/binder ratio of 0.50, the use of 30% POFA as a cement replacement had the lowest peak temperature rise.

2.3 Sugarcane bagasse ash

Sugarcane is one of the foremost crops grown in all over countries and its entire production is over 1500 million tons. After the extraction of all economical sugar from sugarcane, about 40-45% fibrous residue is obtained, which is reused in the same industry as fuel in boilers for heat generation leaving behind 8-10% ash as waste, known as sugarcane bagasse ash (SCBA) depending on the quality and type of the boiler, modern boiler release lower amount of bagasse ash (Modani and Vyawahare, 2013). At present, SCBA waste is ultimately disposed of as soil fertilizer in many sugarcane-producing countries. However, this option has three disadvantages: (1) it causes significant changes in the physical and chemical properties of soils, (2) it contributes to environmental pollution and (3) it may have a strong negative impact on human health. Thus, the SCBA waste production presents a serious waste

management problem for the sugarcane industry (Schettino and Holanda, 2015).

2.3.1 Properties of sugarcane bagasse ash

The sugarcane bagasse consists approximately 50% of cellulose, 25% of hemicelluloses and 25% of lignin. Each ton of sugarcane generate approximately 26% of bagasse (at a moisture content of 50%) and 0.62% of residual ash. The residue after combustion presents a chemical composition dominated by silicon dioxide (SiO_2) (Srinivasan and Sathiya, 2010). The chemical and physical properties are given in Table 2.3 and 2.4.

Table 2.3 Chemical compositions of SCBA (after Cordeiro et al., 2004).

Chemical components	Weight fraction (%)
SiO_2	78.34
Al_2O_3	8.55
Fe_2O_3	3.61
CaO	2.15
Na_2O	0.12
K_2O	3.46
MnO	0.13
TiO_2	0.50
MgO	1.65
BaO	< 0.16
P_2O_5	1.07
Loss on ignition (LOI)	0.42

Table 2.4 Physical properties of SCBA (after Cordeiro et al., 2004; Goyal et al., 2007).

Properties	SCBA
Color	Reddish gray
Specific gravity	2.20-2.52
Median particle size, d_{50} (μm)	28.90-45
% Passing through 45 μm sieve (% mass)	8.40
Specific surface area, Blaine (m^2/kg)	308-514

2.3.2 Development of concrete by sugarcane bagasse ash

Chusilp et al. (2009) examined the importance of bagasse ash for development as pozzolanic materials in concrete. The physical properties of concrete containing ground bagasse ash, including compressive strength, water permeability and heat evolution were investigated and all tests were done in accordance with American Standards. When bagasse ash is ground up into small particles, the compressive strength of concrete containing this ground bagasse ash improves significantly. The low water permeability values of concretes containing ground bagasse ash at 90 days were mostly caused by the pozzolanic reaction. The higher the replacement fraction of Portland cement by ground bagasse ash, the longer the delay time to obtain the highest temperature rise. Concrete containing up to 30% ground bagasse ash had a higher compressive strength and lower water permeability than the control concrete, both at ages of 28 and 90 days.

Srinivasan and Sathiya (2010) studied chemical and physical characterization of SCBA and partial replacement of cement at the ratio of 0, 5, 10, 15 and 25% by weight. The experimental study examines the compressive strength, split

tensile strength, flexural strength, young's modulus and density of concrete at the age of 7 and 28 days were obtained as per Indian Standards. It was found that the cement could be advantageously replaced with SCBA up to a maximum limit of 10%. Therefore, it is possible to use SCBA as cement replacement material to improve quality and reduce the cost of construction materials such as concrete.

Abbasi and Zargar (2013) studied the moisture percentage and the method of burning bagasse, physical characteristics, chemical combination (XRF test), crystal fixtures (XRD test) and specific area of bagasse ash and compared with cement. The burning of bagasse will produce very viscous smoke that causes difficulties for producers and near a residential building. Replacing cement by 10% of bagasse ash by fine grade, the workability and flowbility are optimized and there compressive strength at 28 days was increased by 25% in comparison with normal concrete specimens. Use of bagasse ash in concrete as 10% cement replacement causes slump increase and compressive strength and delayed in initial and final setting time.

2.4 Drilling mud

Drilling mud is the material created for the purpose of drilling oil and natural gas wells; the “mud” is pumped into the hole during the drilling process to help cool and lubricate the bit, suspend cuttings, seal the formation and control wellbore pressure. During this process, the mud is continuously recycled to remove solids until it can no longer be utilized for drilling. Options for disposal include injection wells, pits and land application.

The initial mud (prior to use in drilling) contains several chemical additives. These may include bentonite clay (soil mineral), sodium carbonate, lime, barium

sulfate, lignite and “loss circulation materials” such as ground peanut shells, mica, cellophane, walnut shells, plant fibers and cottonseed hulls.

There are two main types of drilling mud that are produced and land applied: water based mud (WBM) and oil based mud (OBM). The main difference between WBM and OBM is the solvent (liquid) used as the “base.” For WBM, the solvent is water and for OBM it is diesel. WBM is more common and is typically utilized in the shallow (0 to 3,000 feet) vertical portion of the well drilling and OBM is used in the deeper and horizontal portions (Penn and Zhang, 2013).

2.5 Functions of drilling mud

Drilling mud serves many purposes. All of these functions may not be simultaneously achievable in any particular situations. However, the program must be designed while prioritizing the most important required properties on the prospect well. The major functions are (1) to remove the cuttings from the bottom of the hole and transport them to the surface. Mud circulation velocity, higher mud density and higher viscosity are some factors required for efficient cuttings removal, (2) to cool and lubricate the bit and drilling. Lubrication is normally achieved by adding bentonite, oil and various emulsifying agents and graphite, etc. to the mud, (3) to wall the borehole with an impermeable mud cake. This property can be obtained by adding bentonite and chemically treating the mud to improve deflocculation and solids distribution. Starch or other fluid loss additive may also be added, (4) to control subsurface pressure. An increase in mud weight is required to slightly overbalance the hydrostatic pressure achieved by adding barite. In practice, an overbalance of 100-200 psi is normally adequate for safer drilling, (5) to hold cuttings and weight material in

suspension when circulation is interrupted. This depends on the gel strength of the mud, (6) to release sand and cuttings at the surface. The sand content at the pump suction should be kept below 2%, (7) to support part of the weight of drillpipe and casing. Increased mud weight results in a considerable reduction in total weight, which the surface equipment must support, (8) to reduce to a minimum any adverse effects upon the formation adjacent to the hole, i.e., minimizing formation damage, (9) to transmit hydraulic horsepower to the bit and improve drilling rates and (10) to minimize torque, drag, and pipe sticking (Mian, 1992).

2.6 Drilling mud improvement

Petchote and Sikong (2005) studied the properties of drilling mud blended with dolomite powder and fly ash in order to improve the formula of drilling mud with low cost. Furthermore, the properties of dolomite and fly ash affected on the properties of drilling were also investigated such as particle size distribution, density, pH, viscosity and dispersion of drilling mud. It was found that drilling mud which has the properties of barite: dolomite: fly ash. The good suspension property of drilling mud is 70:10:20 and 70:30:0 of barite: dolomite: fly ash; respectively, when the 3% weight of bentonite was added. The formula of 70:5:25 and 70:0:30 were also good suspension when the 3% by weight of bentonite and 0.6 grams/liter of CMC were added. Drilling mud of 4 formulas above research the drilling mud properties of API standard.

Meng et al. (2012) indicated the rheological properties of bentonite dispersion with carbon ash are improved markedly in yield point and especially for the low solid content of bentonite dispersion. The filtration and density test are also carried out using

an API Filter Press and mud balancer respectively. From the results, it could be observed that the filtrate loss and filter cake thickness increase dramatically, whereas the density of bentonite dispersion decrease slightly as the addition of carbon ash increases. Furthermore, the stability of bentonite dispersion incorporated with carbon ash is evaluated. The experimental results indicate that carbon ash is better than rheological modifier instability. Through this study, carbon ash is an excellent potential additive for improving the rheological properties of water based drilling mud.

Mahto (2013) studied the effect of activated charcoal on the rheological and filtration properties of water based drilling mud, base drilling mud combinations were prepared using xanthan gum, polyanionic cellulose, pregelatinized starch and potassium chloride. The rheological and filtration properties were measured using API standard methods. The experimental investigation in spite of the lower concentration of activated charcoal used in the drilling mud than the calcium carbonate, the charcoal based drilling mud has less a fluid loss and filter cake thickness which shows that activated charcoal is more effective bridging agent than the calcium carbonate. The activated charcoal shows better filtration loss control at lower concentration than the calcium carbonate and hence it may be the substitute of calcium carbonate for the development of water based drilling mud.

Mahto and Jain (2013) investigate the effect of fly ash on the rheological and filtration properties of water based drilling mud with the different drilling mud combinations were prepared using carboxy methyl cellulose (low viscosity grade), polyanionic cellulose, xanthan gum and potassium chloride. From the results, these drilling muds show very good rheological behavior, but poor filtration loss characteristics and when fly ash was added in these drilling mud combinations, a

nanoparticles fluid system was established which has better control of filtration properties without affecting the rheological properties. The experimental results indicate that the filtration properties were improved with the increase in a concentration of the fly ash and reducing the cake thickness and filter loss. Fly ash may compete with other bridging agents due to its best efficiency, availability, better environmental effects and low cost factor. It should be utilized as well as it is the waste product of the industries in huge amount.

Korsinwattana and Terakulsatit (2014) studied the physical and chemical properties of drilling mud mixed with fly ash, various 3, 5 and 7% of weight by volume of fly ash at 30, 60 and 90°C. The element of fly ash dominantly consists of 34.9% SiO₂, 18.98% Al₂O₃, 16.57% CaO, 15.51% Fe₂O₃ and 8.40% SO₃. The physical properties were tested based on API RP13B-1 standard. The result of the drilling mud mixed with concentration 3% of weight by volume of the fly ash at 30°C testing is a high potential additive for enhancement the rheological properties of water based drilling mud, especially in the increasing of apparent viscosity, yield point, gel strength and pH, and high efficiency of resistivity reduction. However, the high concentration of fly ash affects to the increasing of the filtrate loss, mud cake thickness and sand content.

Igwe and Kinate (2015) experimental assessment of the suitability of Periwinkle Shell Ash (PSA) for use as filtration loss control additive in water based drilling mud. The PSA was then sieved through BS sieve (75 µm) to obtain a fine ash (nanoparticles). The filtration characteristics of the formulated mud samples were tested using API filter press and in accordance to API recommended practice for field testing water based drilling mud (API RP 13B-1). This research has shown that PSA

has good filtration (fluid loss) control properties. The addition of PSA to the various mud samples improved the filtration characteristics of the formulated water based drilling mud with respect to reduced filtrate volume and thinner and consistent mud filter cakes. Mud sample formulated with 2.0 grams of PSA exhibited the best filtration control characteristics with minimal filtrate volume of 6.7 milliliters after 30 minutes of filtration. Physical examination of the mud filter cakes formed after 30 minutes of the filtration shows that sample produced the best filter cake with the minimum thickness of 0.75 mm. PSA has proved to possess good filtration (fluid loss) control properties.

2.7 Drilling mud rheology

Rheology is the study of deformation and flow of matter, including liquid and solid. Rheological models provide an approximate description of the behavior of fluids by expressing a mathematical relationship between shear stress and shear rate. In general, drilling mud is divided into two groups: Newtonian fluids and non-Newtonian fluids. Most drilling mud is non-Newtonian fluids, either viscosity changes with shear rate (i.e. Power law model or Herschel-Bulkley model), or a plastic yield must be overcome (i.e. Bingham plastic model) are shown in Figure 2.1 (Baker Hughes, 2006).

2.7.1 Newtonian fluid model

The Newtonian Fluid Model is the basis from which other fluid models are developed. The flow behavior of Newtonian fluids has been discussed and it can be seen from this equation that the shear stress-shear rate relationship is given by:

$$\tau = \mu \times \gamma \quad (2.1)$$

where τ = shear stress, $\text{lb}_f/100 \text{ ft}^2$
 μ = viscosity, cp
 γ = shear rate, sec^{-1}

At a constant temperature, the shear stress and shear rate are directly proportional. The proportionality constant is the viscosity (μ). Figure 2.2 illustrates the flow curve of a Newtonian fluid, the flow curve is a straight line which passes through the origin (0,0) and the slope of the line is the viscosity (μ).

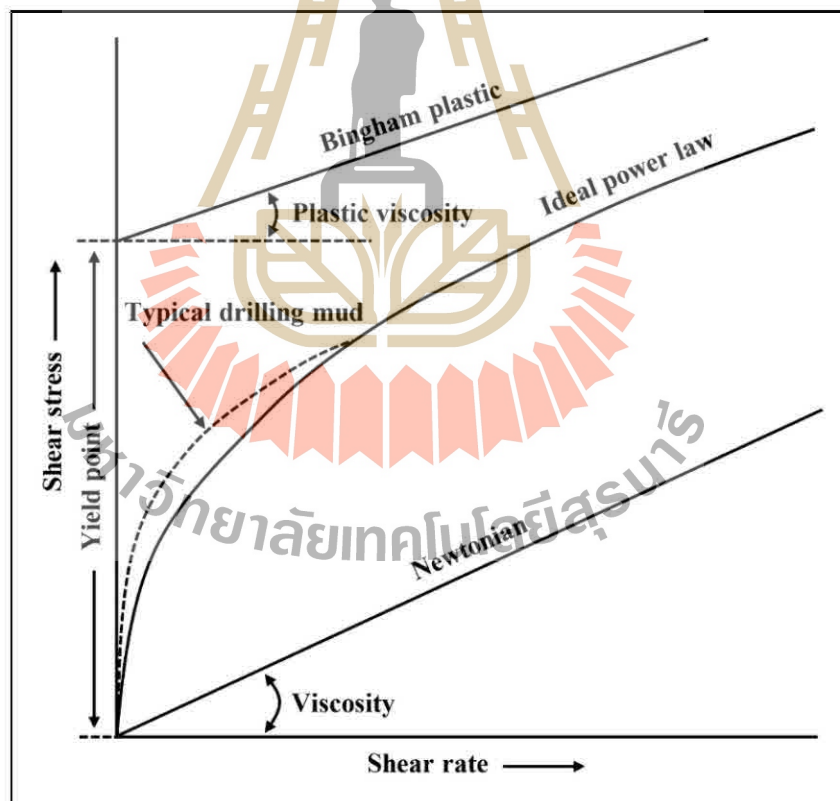


Figure 2.1 Ideal consistency curves for common flow models

(after Caenn et al., 2011).

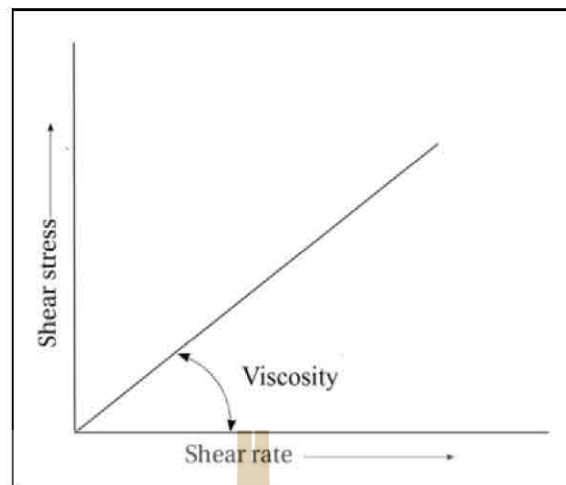


Figure 2.2 Flow curve for a Newtonian fluid (after Caenn et al., 2011).

2.7.2 Non-Newtonian fluid

The non-Newtonian models of particular interest in the context of this work are the Bingham plastic model, Power law model and Herschel-Bulkley model. The concepts introduced in the previous sections were valid for Newtonian fluids. A non-Newtonian fluid may exhibit a yield stress, which is the amount of stress required in order to get the material moving. Below this yield stress, the material behaves as solid and no flow can be initiated, or a non-linear viscosity characteristic or both (Fitton, 2007).

2.7.2.1 Bingham plastic model

In the early 1900s, E.C. Bingham first recognized that some fluids exhibited a plastic behavior, distinguished from Newtonian fluids, in that they require a yield stress to initiate flow. No bulk movement of the fluid occurs until the applied force exceeds the yield stress. The yield stress is commonly referred to as the yield point. The shear stress/shear rate relationship for the Bingham plastic model is given by:

$$\tau = \tau_y + \mu_p \gamma \quad (2.2)$$

where	τ	=	shear stress, lb _f /100 ft ²
	τ_y	=	yield point or shear stress at zero shear rate (Y-intercept), lb _f /100 ft ²
	μ_p	=	plastic viscosity or rate of increase of shear stress with increasing shear rate (slope of the line), cP
	γ	=	shear rate, sec ⁻¹

The flow curve for a Bingham plastic fluid is illustrated in Figure 2.3. The effective viscosity, defined as the shear stress divided by the shear rate, varies with shear rate in the Bingham plastic model. The effective viscosity is visually represented by the slope of a line from the origin to the shear stress at some particular shear rate. The slopes of the dashed lines represent effective viscosity at various shear rates. As can be seen, the effective viscosity decreases with the increased shear rate. As discussed in the viscosity section, this is referred to as shear thinning.

As shear rates approach infinity, the effective viscosity reaches a limit called the plastic viscosity (PV). The PV of a Bingham plastic fluid represents the lowest possible value that the effective viscosity can have at an infinitely high shear rate, or simply the slope of the Bingham plastic line. The Bingham plastic model and the term PV and yield point (YP) are used extensively in the drilling mud industry. PV is used as an indicator of the size, shape, distribution and quantity of solids and the viscosity of the liquid phase. The YP is a measure of electrical attractive forces in the drilling mud under flowing conditions.

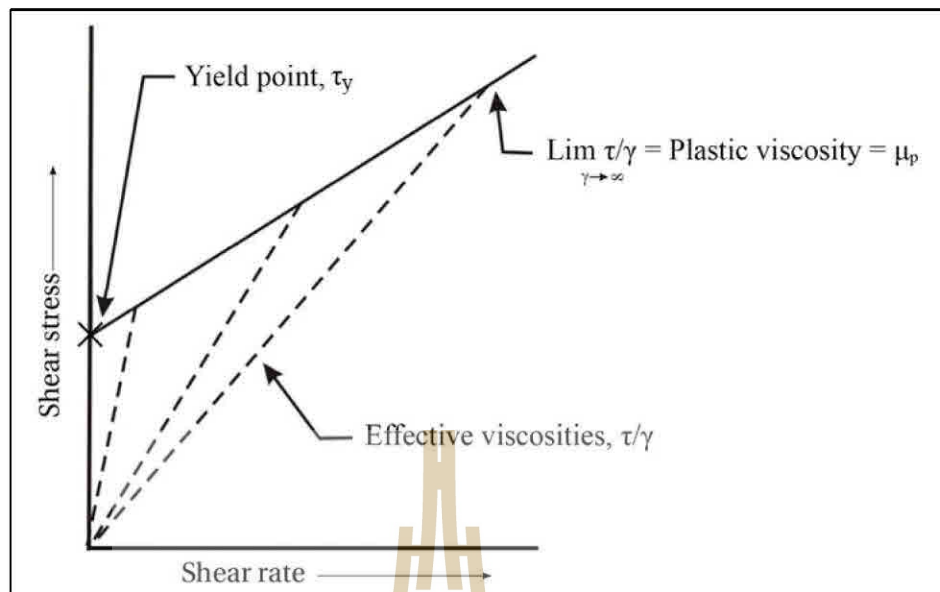


Figure 2.3 Flow curve for a Bingham plastic model (after Baker Hughes, 2006).

The PV and YP are two parameters of drilling mud that many in the industry still consider to be vitally important in the overall drilling operation. The YP is now considered an outdated concept that has no real meaning or application in drilling operations. The following rheological models better describe the behavior of drilling mud. This can clearly be seen when the viscometer readings are plotted on a graph and the resulting line is a curve and not a straight line. The Bingham model uses a straight line relationship.

2.7.2.2 Power law model

Most drilling mud exhibit behavior that falls between the behaviors described by the Newtonian model and the Bingham plastic model. This behavior is classified as pseudoplastic. The relationship between shear stress and shear rate for pseudoplastic fluids are defined by the Power law mathematical model. Figure 2.4 illustrates the flow curve for a pseudoplastic fluid.

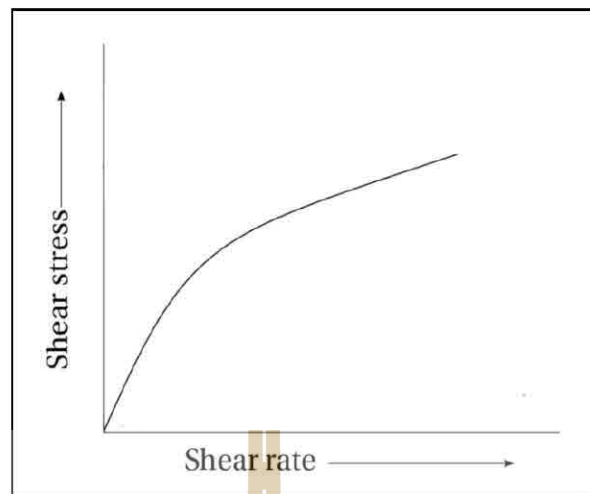


Figure 2.4 Flow curve for a Power law model (after Baker Hughes, 2006).

$$\tau = K\gamma^n \quad (2.3)$$

where

$$\tau = \text{shear stress, lb}_f/\text{100 ft}^2$$

$$K = \text{fluid consistency index}$$

$$\gamma = \text{shear rate, sec}^{-1}$$

$$n = \text{flow behavior index}$$

The two terms K and n are constants in the Power law model. Generally, K is called the consistency index and describes the thickness of the fluid and is thus somewhat analogous to effective viscosity. If the drilling mud becomes more viscous, then the constant K must increase to adequately describe the shear stress/shear rate relationship. Additionally, n is called the flow behavior index and indicates the degree of non-Newtonian behavior. A special fluid exists when

$n = 1$, Newtonian; where shear rate and shear stress are directly proportional.

$n > 1$, Dilatant or shear thickening; where the effective viscosity increases as shear rate increases.

$n < 1$, Pseudoplastic or shear thinning; where the effective viscosity decreases as the shear rate increases just like the Bingham plastic model.

Figure 2.5 shows the flow curves for these values of n .

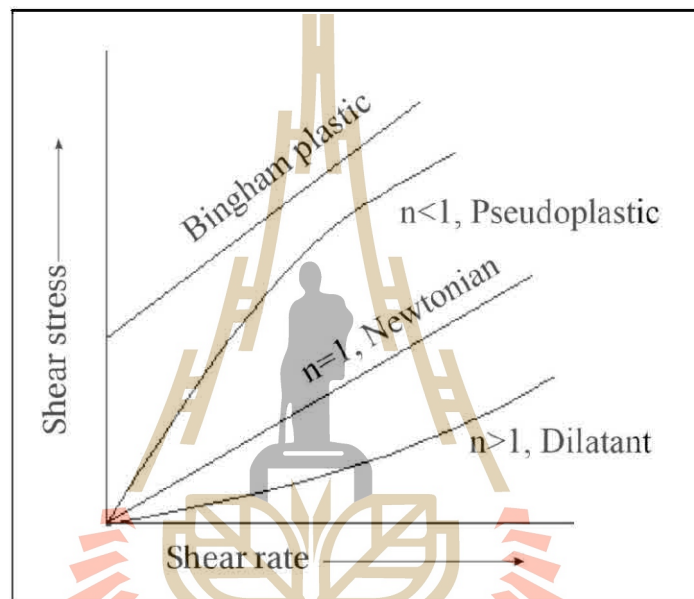


Figure 2.5 Flow Behavior for Power law model (after Baker Hughes, 2006).

Similar to the Bingham plastic model, the Power law model does not describe the behavior of drilling mud exactly. However, the Power law constants n and K are used in hydraulic calculations that provide a reasonable degree of accuracy.

From Figure 2.1, compares the flow curve of a typical drilling mud to the flow curves of Newtonian, Bingham plastic and Power law models. A typical drilling mud exhibits a yield stress and is shear thinning. At high rates of shear,

all models represent typical drilling mud reasonably well. Differences between the models are most pronounced at low rates of shear, typically the shear rate range most critical for hole cleaning and the suspension of weight material.

The Bingham plastic model includes a simple yield stress, but does not accurately describe the fluid behavior at low shear rates. The Power law model more accurately describes the behavior at low shear rates, but does not include a yield stress and therefore can give poor results at extremely low shear rates. A typical drilling mud actually exhibits behavior between the Bingham plastic model and the Power law model. This sort of behavior approximates the Herschel-Bulkley model.

2.7.2.3 Herschel-Bulkley model

The Herschel-Bulkley model is also referred to as the modified Power law model, which is a Power law model with the addition of yield stress to the model. The Herschel-Bulkley model gives mathematical expressions which are solvable with the use of computers. This model is one of the complex models which has three parameters and defines the behavior of the drilling mud better than the simpler Power law and Bingham models. The behavior of a Herschel-Bulkley fluid is described as

$$\tau = \tau_0 + K \gamma^n \quad (2.4)$$

where

τ	=	shear stress, lb _f /100 ft ²
τ_0	=	yield stress or stress to initiate flow
K	=	fluid consistency index
γ	=	shear rate

n = flow behavior index

The Herschel-Bulkley model is a general model that can be reduced to the Bingham and Power law model. If n is equal to 1, then the Herschel-Bulkley reduces to the Bingham plastic model. The concept of the τ_0 and τ_y are very different. τ_y in the Bingham plastic model is determined at high shear rate (300 to 600 RPM) while τ_0 is determined at low shear rates (3 to 6 RPM) to estimate fluid behavior more accurately.

2.8 API recommended practices

The American Petroleum Institute (API) has set forth numerous recommended practices designed to standardize various procedures associated with the petroleum industry. The practices are subject to revision from time-to-time to keep pace with current accepted technology. One such standard is API RP 13B-1, "Recommended Practice Standard Procedure for Field Testing Water-Based". This Bulletin describes the following drilling mud measurements as necessary to describe the primary characteristics of a drilling mud (Baker Hughes, 2006). This research focuses on the section on

- Density - for the control of formation pressures.
- Viscosity and Gel Strength - measurements that relate to a mud flow properties.
- Filtration - measurement of the mud loss of liquid phase to expose, permeable formations.
- Resistivity - measurement the resistivity of drilling mud and their mud filter cakes.

- pH - measurement of the alkaline and acid relationship in the mud.
- Chemical Analysis - qualitative and quantitative measurement of the reactive chemical components of the mud.



CHAPTER III

METHODOLOGY

3.1 Introduction

The objective of the experiments in this research is to evaluate the effects of POFA and SCBA concentration, temperature and mixing ratio on chemical properties, rheological properties and physical properties of water based drilling mud. This chapter includes the research methodology, sample collection, sample preparation, testing instruments and experimental methods. The tests are divided into two groups; chemical properties tests and physical properties tests.

3.2 Research methodology

The research methodology comprises 5 steps, as shown in Figure 3.1, including literature review, collecting the samples of POFA and SCBA, preparing and analysis of POFA and SCBA (physical and chemical properties tested), collection data and testing results, discussions and conclusions, and thesis writing. Each step is described as follows:

3.2.1 Literature review

A literature review was carried out to improve understanding of the drilling mud properties. It's composed of reviewing and studying water based drilling mud and applications, POFA and SCBA properties and testing procedure. The sources of information were from journals, researches, dissertation and books concerned.

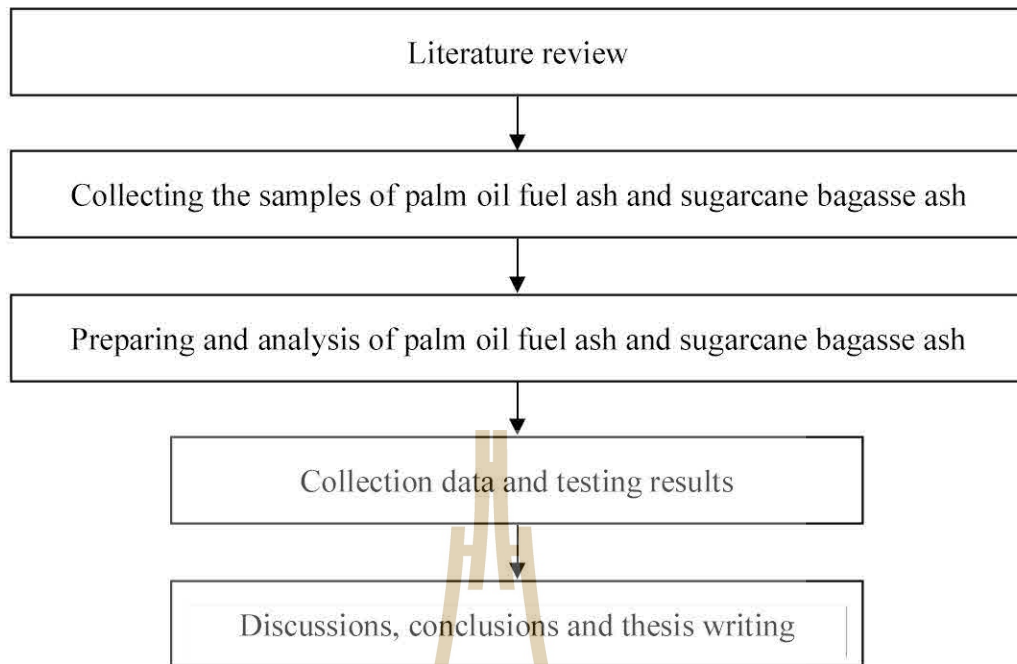


Figure 3.1 Research methodology.

3.2.2 Collecting the samples of POFA and SCBA

POFA was collected from Chumporn Palm Oil Industry Public Company Limited, Chumporn province. SCBA was collected from Prachuap Sugar Industry Company Limited, Kanchanaburi province.

3.2.3 Preparing and analysis of POFA and SCBA

The sample was prepared and tested in the laboratory of Suranaree University of Technology. The POFA and SCBA were sieved a size less than $75\ \mu\text{m}$ (mesh No.200) before storing in zip lock bags. These samples were divided into two parts for chemical properties tests and physical properties tests before and after mixed with drilling mud. A water based drilling mud suspension was prepared using 60 grams of bentonite per 1,000 milliliter of water and 100 grams of barite was added to control density. Various concentrations of POFA and SCBA were added to test

divided into two groups; chemical and physical properties tests. The properties testing were determined in the laboratory under the temperature at 25, 50 and 80°C. These samples were tested for each condition. The test methods were followed the relevant API standard practice.

3.2.3.1 Chemical properties tests

The objective of chemical properties was to measurement, chemical composition in samples by using X-ray Fluorescence (XRF) and mineral composition by using X-ray Diffraction (XRD).

3.2.3.2 Physical properties tests

The objective of physical properties was to measure rheological characteristics of drilling mud with the study of the deformation of fluids, flow of matter and filtration loss that invaded to the permeable formation while drilling mud was circulating and mud filter cake building. The test procedures followed API RP 13B-1 (1997). Besides rheological other tests such as density, filtration, hydrogen ion, resistivity and solid content. The test was performed by mud balance, direct-indicated viscometers, Baroid standard filter press, analytical pH meter, Baroid resistivity meter and Baroid oil and water retort kit. These drilling mud samples were prepared and tested under each designed condition. Consequently, the drilling mud rheological parameters were observed and recorded. In addition, morphology (texture), crystalline structure and orientation are measured by using Scanning Electron Microscope (SEM) and Field Emission Scanning Electron Microscope (FE-SEM).

3.2.4 Collection data and testing results

The results from analysis of POFA, SCBA and drilling mud with mixed were compared between before and after of additive addition follows these

topics (1) components and properties of POFA and SCBA were additive in drilling mud, (2) appropriate concentration of additives for increasing efficiency of drilling mud and (3) efficiency of drilling mud which varies in temperatures and concentration of additives between before and after of additive addition.

3.2.5 Discussions, conclusions and thesis writing

The results from laboratory measurements in terms of density, plastic viscosity, apparent viscosity, yield point, gel strength, filtrate volume, mud filter cake thickness, hydrogen ion, resistivity and solid defined as the percentage by volume were compared between those results from base mud and base mud mixed additives. Similarity and discrepancy of results have been discussed. The effect of temperature on drilling mud properties was described and the feasibility of using water based mud mixed additives in petroleum industry was also considered. All research activities, methods, and results are documented and completed in the thesis.

3.3 Sample collection

The materials used in this work are barite, bentonite, POFA and SCBA. Barite was assisted by Golden Lime Public Company Limited, Thailand. Bentonite was supported from Thai Nippon Chemical Industry Company Limited, Thailand. POFA was obtained from Chumporn Palm Oil Industry Public Company Limited at Chumporn province, Thailand. SCBA was collected during the cleaning operation of a boiler operating in Prachuap Sugar Industry Company Limited, located in the city of Kanchanaburi province, Thailand.

3.4 Sample preparation

The POFA and SCBA were prepared and tested in the laboratory of Suranaree University of Technology. The POFA and SCBA were air dried and then crushed to fine particles. The ensuring ash was then sieved via using sieve shakers (Figure 3.2) sizes to less than 75 μm (mesh No.200) before storing in zip lock bags. These samples were divided into two parts for chemical properties tests and physical properties tests before and after mixed with drilling mud.

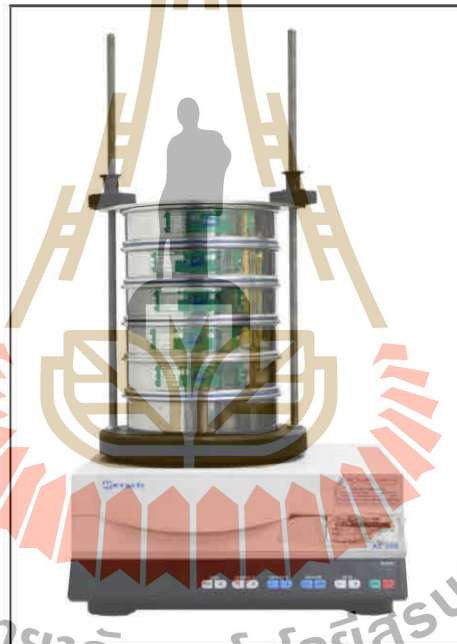


Figure 3.2 Retsch sieve shakers.

The range of drilling mud density of typical well drilling is 1.5 to 8.5% bentonite weights by volume. Mud weight varied around 8.85 to 18 lb/gal depends on graded bentonite and drilled formations (MI-Swaco, 1998). Figure 3.3 demonstrates the composition and nature of common drilling muds. The curves show the increasing of viscosity with a percentage of bentonite solids.

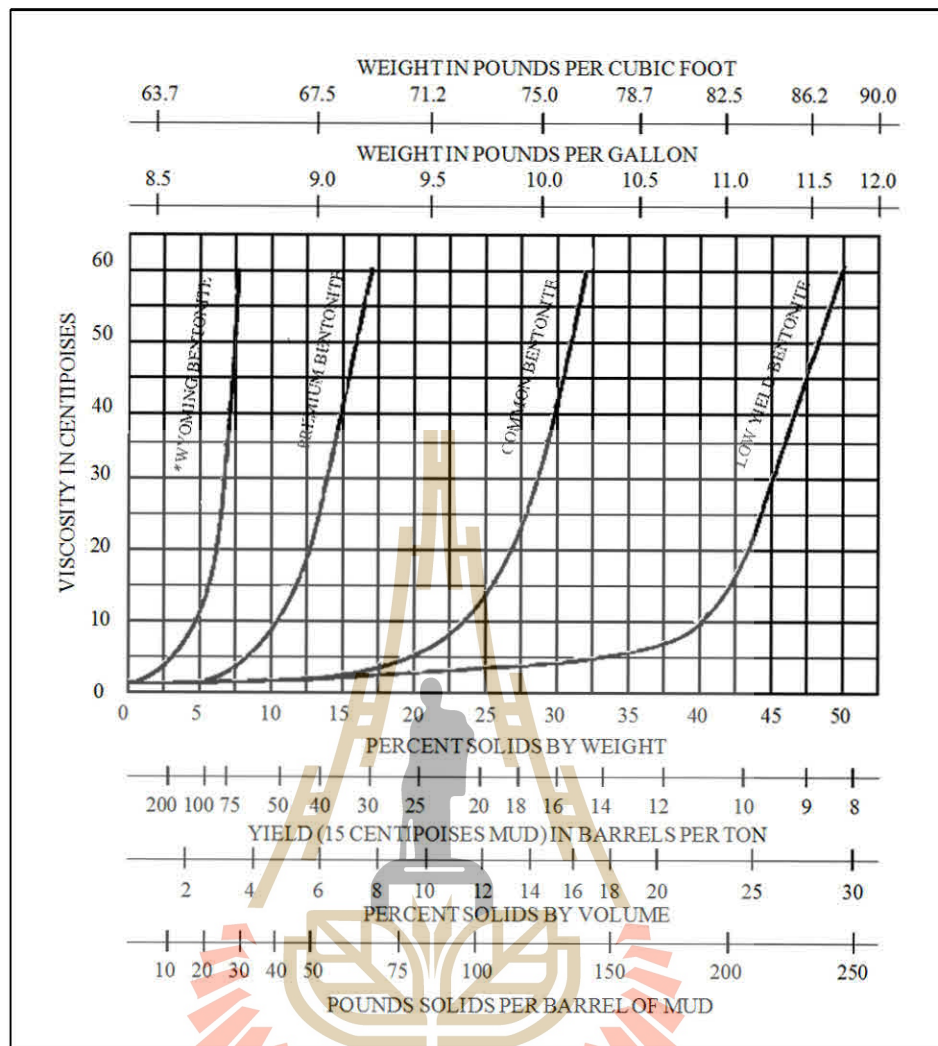


Figure 3.3 Yield curve for typical clays (after Gatlin, 1960).

Since the grade of bentonite clay that uses in the experiment is not Wyoming grade. It is necessary to find the appropriate amount of bentonite that meet the viscosity requirement for typical well drilling. Table 3.1 shows bentonite water based suspension at 2, 4, 6 and 8% of bentonite weights by volume, it shows that bentonite mud suspension at 6% of bentonite weight by volume meets a minimum required viscosity for typical well drilling. Therefore, the experiment had selected 6% of bentonite weight by volume as a base composition.

Table 3.1 Bentonite water based suspension.

Bentonite (%weight by volume)	Average apparent viscosity (cP)
2	6.0
4	12.5
6	21.5
8	39.0

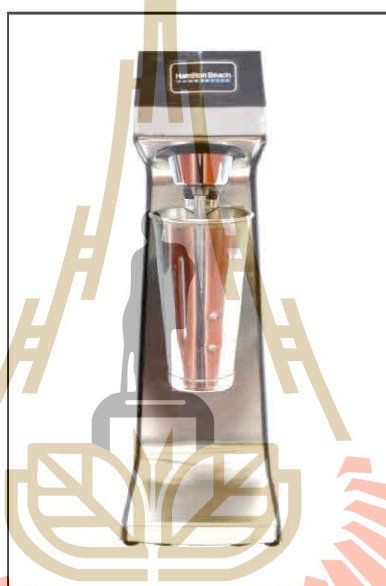
A water based drilling mud sample suspension was prepared to use 60 grams of bentonite per 1,000 milliliters of water, 100 grams of barite was added to control density. This mud sample was named “base mud”. The mixing ratio was maintained constant for all subsequent mud samples used in this work. A single spindle Hamilton Beach commercial mixer was utilized for preparing drilling mud samples (Figure 3.4). The mud components are mixed for 15 minutes using a high-speed mixture. During mixing, the POFA and SCBA were added slowly to agitate base mud to avoid a lump occurring within the mud system. Mud samples with various concentrations of POFA and SCBA were added to perform as a mud additive. These systems were prepared to compare the properties of the mud. Table 3.2 and Table 3.3 summarize the compositions of the various mud samples.

Table 3.2 Composition of POFA mud samples.

Mud composition	Water (ml)	Barite (g)	Bentonite (g)	POFA(g)
Base mud	1,000	100	60	-
Base+ 1% POFA	1,000	100	60	11.60
Base+ 3% POFA	1,000	100	60	34.80
Base+ 5% POFA	1,000	100	60	58.00

Table 3.3 Composition of SCBA mud samples.

Mud composition	Water (ml)	Barite (g)	Bentonite (g)	SCBA (g)
Base mud	1,000	100	60	-
Base+ 1% SCBA	1,000	100	60	11.60
Base+ 3% SCBA	1,000	100	60	34.80
Base+ 5% SCBA	1,000	100	60	58.00

**Figure 3.4** Hamilton Beach Commercial mixer 3 speed mixers with 1 spindle.

3.5 Chemical properties tests

The objective of chemical properties was to measure the chemical composition in samples by using X-ray Fluorescence (XRF) and mineral compositions by using X-ray Diffraction (XRD).

3.5.1 X-ray Fluorescence

X-ray Fluorescence analysis using Horiba XGT-5200 spectrometers was a commonly used technique for the identification and quantification of the

element in a substance (Figure 3.5). Place the sample approximately 0.5 to 1.0 grams in the sample holder. Load the sample holder into the ED-XRF, analysis probe is set with vacuum, making it possible to analyze the sample at normal atmospheric pressure. The X-ray excitation sources used in wavelength and energy-dispersive XRF provides adequate analytical sensitivity for quantitative analysis across the element sodium to uranium. Typically, all elements from sodium through to uranium can be detected simultaneously, with good quality spectra obtained in 100 seconds per sample. Results are analyzed in the spectrum, including Rayleigh and Compton scattered characteristic line from the X-ray generator, a peak caused by X-ray diffraction, and sum/escape peak. The quantitative XRF analysis of unknown samples is usually performed using calibrations with matrix-matched standards. The XRF results are presented as the percentage of major elements.



Figure 3.5 Horiba XGT-5200 X-ray Fluorescence.

3.5.2 X-ray Diffraction

X-ray Diffraction analysis using Bruker-D2 Phaser was an essential technique in the material characterization analysis to obtain qualitative and quantitative mineralogical characterization (Figure 3.6). Load the prepared samples approximately 0.5 to 1.0 grams into the sample holder. Pull down the spherical handle of the stage and place onto sample holder into the sample position of the stage. Lift the sample back into the sample measurement position by pulling up the spherical handle of the stage and slide down the instrument door and spent time 10 minutes per sample. The X-ray beam is diffracted by innumerable crystallites in specific 2θ directions and the intensity of diffracted X-rays is continuously recorded as the sample. Data is recorded the exact 2θ positions a narrow slit in front of a point detector is required. A peak in intensity occurs when the mineral contains lattice planes with d-spacings appropriate to diffract X-rays at that value of θ . Conditions of analysis include a Cu standard ceramic sealed tube (0.4x12 mm), X-ray generation (30 kV, 10 mA), angular range analysis (2θ , 5° to 80°) and accuracy ($\pm 0.02^\circ$ throughout the entire measuring range). Results are presented as peak positions at 2θ and X-ray counts (intensity) in the form of a table or an x-y plot and calculated relative intensity, divide the absolute intensity of every peak by the absolute intensity of the most intense peak, and then convert to a percentage by software TOPAS.



Figure 3.6 Bruker-D2 Phaser X-ray Diffraction.

3.6 Physical properties tests

The physical properties tests consist of density, rheology, filtration, hydrogen ion, resistivity and solid content. They are determined following API standard. Moreover, the physical tests involve morphology (texture), crystalline structure and orientation by using Scanning Electron Microscope (SEM) and Field Emission Scanning Electron Microscope (FE-SEM).

3.6.1 Density

The mud density was measured by mud balance (Fann model 140 mud balance) which was one of the most sensitive and accurate field instruments available for determining the density means the weight per unit volume (specific gravity) and was measured by weighing the mud (Figure 3.7). The density of the drilling mud is important to maintain well control. The weight of a mud cup attached to one end of

the beam is balanced on the other end by a fixed counterweight and a rider free to move along a graduated scale. The density of the fluid is a direct reading from the scales located on both sides of the mud balance. The density may be expressed as pounds per gallon (lb/gal), pounds per cubic foot (lb/ft³), grams per cubic centimeter (g/cm³), specific gravity (SG) or hydrostatic pressure gradient (psi/ft). The density is measured with a mud balance of sufficient accuracy to measure within ± 0.1 lb/gal (± 0.5 lb/ft³ or 5 psi/ 1,000 ft of depth).

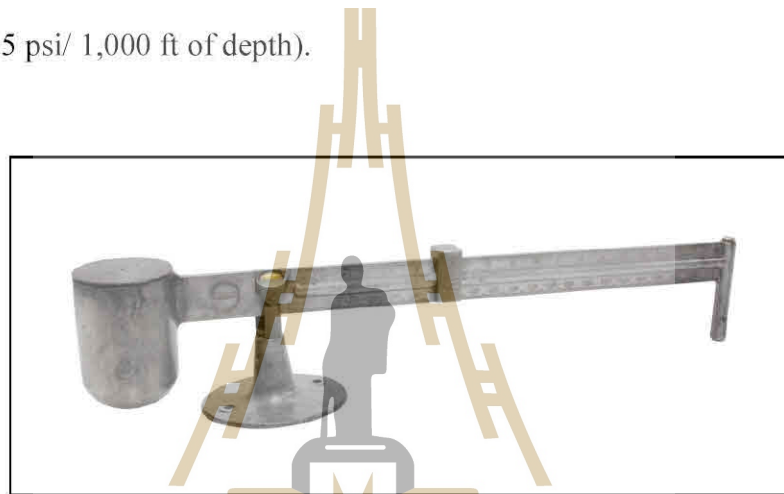


Figure 3.7 Fann model 140 mud balance.

3.6.2 Rheology

The rheology of drilling mud, was conducted by rotational viscometer (Fann model 35SA viscometer) was used to directly measure the viscosity of the drilling mud (Figure 3.8). Rheology is the study of how matter deformation and flows. It is primarily concerned with the relationship between shear stress and shear rate, temperature and the impact these have on flow characteristics inside tubular and annular spaces. The rheological property was monitored to assist in optimizing the drilling process. The rheological parameters of water base drilling mud were investigated and calculated.



Figure 3.8 Fann model 35SA viscometer.

Direct indicated viscometers are rotational types of instruments powered by an electric motor. Drilling mud is contained in the annular space between two concentric cylinders. The outer cylinder or rotor sleeve is driven at a constant RPM (rotational velocity); its rotation of the rotor sleeve in the drilling mud produces a torque on the inner cylinder or bob. A torsion spring restrains the movement of the bob and a dial attached to the bob indicates its displacement on a direct reading scale. For the instrument is powered by two speed synchronous motors to obtain rotational speeds of 3, 6, 100, 200, 300 and 600 rpm. The rheological calculation, it is appropriate to discuss some basic drilling mud flow properties, determination of rheological parameters that describe the flow behavior of a fluid.

The effective viscosity is sometimes referred to as the apparent viscosity (AV). Apparent viscosity is a rheological property calculated from rheometer readings. It measures the shear rate of drilling mud specified by API. Apparent viscosity is expressed in centipoises (cP), it indicates the amount of force required to move one layer of fluid in relation to another. The apparent viscosity is reported as either the mud viscometer reading at 300 RPM (θ_{300}) or one-half of the meter reading at 600 RPM (θ_{600}). It should be noted that both of these apparent viscosity values are consistent with the viscosity formula:

$$AV \text{ or } \mu_a \text{ (cP)} = \frac{300 \times \theta}{\omega} \quad (3.1)$$

Plastic viscosity (PV) in centipoise (cP) is the shearing stress in excess of yield point that will induce a unit rate of shear. Plastic viscosity is usually described as that part of the resistance to flow caused by mechanical friction. Primarily, it is affected by (1) solids concentration, (2) size and shape of solids, (3) viscosity of the fluid phase, (4) the presence of some long chain polymers, (5) the oil-to-water (O/W) or synthetic-to-water (S/W) ratio in invert emulsion fluids, (6) type of emulsifiers in invert emulsion fluids. The 600 dial reading (θ_{600}) minus the 300 dial reading (θ_{300}) gives the slope of the shear stress/shear rate curve. This is the plastic viscosity (Figure 3.9) and its range value used in well drilling is shown in Figure 3.10.

$$PV \text{ or } \mu_p \text{ (cP)} = \theta_{600} - \theta_{300} \quad (3.2)$$

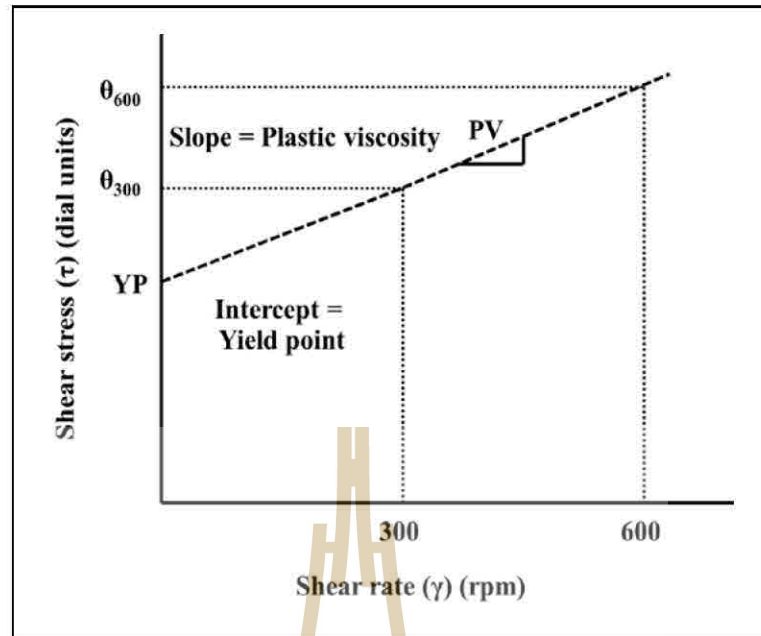


Figure 3.9 Plastic viscosity and yield point values from two measurements

(after Baker Hughes, 2006).

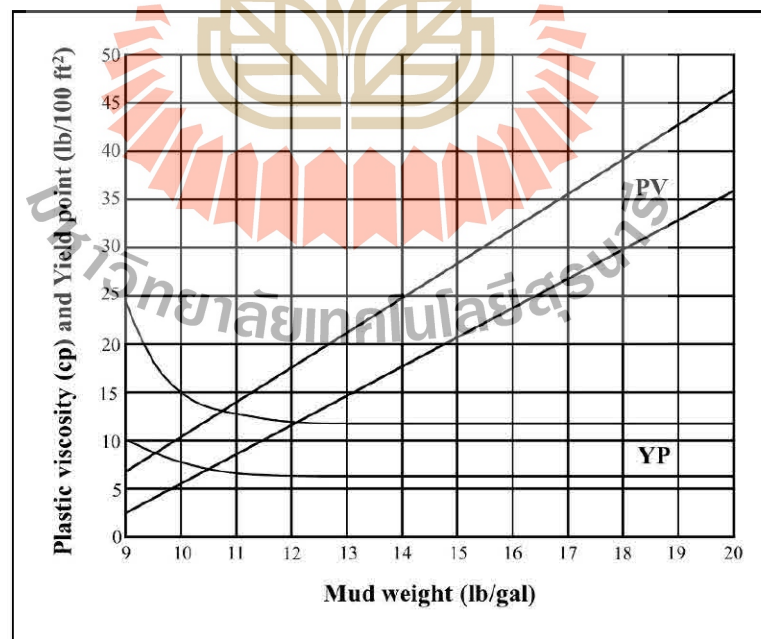


Figure 3.10 Plastic viscosity and yield point ranges for water base drilling mud

(after MI-Swaco, 1998).

Yield point, the second component of resistance to flow in drilling mud. This parameter is also obtained from the viscometer. It is a measurement of the electro-chemical or attractive forces. These forces are a result of negative and positive charges located on or near the particle surfaces. Yield point is a measure of these forces under flow conditions and is dependent upon: (1) the surface properties of the mud solids, (2) the volume concentration of the solids and (3) the electrical environment of these solids (concentration and types of ions in the fluid phase of the fluid). Yield point is that part of the resistance to flow that may be controlled by proper chemical treatment. The yield point will decrease as the attractive forces are reduced by chemical treatment. Reduction of yield point will also decrease the apparent viscosity. The yield point in pounds per 100 square feet ($\text{lb}_f/100 \text{ ft}^2$) equals the 300 rpm reading minus the plastic viscosity, is the shear stress at zero shear rate (see Figure 3.9) and its range value that used in well drilling is also shown in Figure 3.10.

$$\text{YP or } \gamma_p (\text{lb}_f/100 \text{ ft}^2) = 2 \times \theta_{300} - \theta_{600} \quad (3.3)$$

or

$$\text{YP or } \gamma_p (\text{lb}_f/100 \text{ ft}^2) = \theta_{300} - \text{PV} \quad (3.4)$$

Gel strength is a measure of the inter-particle forces and indicates the gelling that will occur when circulation is stopped. This property prevents the cuttings from setting in the hole. Similar to the yield point, gel strength is a measure of the electro-chemical attractive forces between solid particles. Gel strength is measured in units of $\text{lb}_f/100 \text{ ft}^2$. This reading is obtained by noting the maximum dial deflection when the rotational viscometer turned at a low rotor speed (3 rpm) after the mud has

remained static for some period of time (10 seconds and 10 minutes). If the mud is allowed to remain static in the viscometer for a period of 10 seconds, the maximum dial deflection obtained when the viscometer is turned on is reported as the initial gel on the API mud report form. If the mud is allowed to remain static for 10 minutes, the maximum dial deflection is reported as the 10 min gel. The strength of the gel formed is a function of the amount and type of solids in suspension, time, temperature and chemical treatment. In other words, anything promoting or preventing the linking of the particles will increase or decrease the gelation tendency of a fluid.

The other terms of viscosity can be described in terms of the ratio of the shear stress to the shear rate. By definition:

$$\mu = \frac{\tau}{\dot{\gamma}} \quad (3.5)$$

where

$$\begin{aligned} \mu &= \text{viscosity, cP} \\ \tau &= \text{shear stress, lb}_f\text{/100 ft}^2 \\ \dot{\gamma} &= \text{shear rate, sec}^{-1} \end{aligned}$$

The drilling mud, was characterized by their shear rate and shear stress relationships. The shear rate and shear stress were calculated using the viscometer dial readings. The shear stress and shear rate equations are as follows:

$$\tau = 1.0678 \times \theta \quad (3.6)$$

$$\dot{\gamma} = 1.703 \times \omega \quad (3.7)$$

where

$$\begin{aligned} \tau &= \text{shear stress, lb}_f\text{/100 ft}^2 \\ \theta &= \text{mud viscometer dial readings} \end{aligned}$$

γ = shear rate, sec^{-1}

ω = mud viscometer RPM

The power law model parameter constants in term of flow behavior index (n) and consistency index (K) can be determined from any two sets of shear stress to shear rate data. Plotted on a log-log graph, a power law fluid shear stress to shear rate relationship forms a straight line, as shown in Figure 3.11. The “slope” of this line is “n.” “K” is the intercept of this line were calculated from viscometer readings using following equations.

$$n = \frac{\log\left(\frac{\theta_{600}}{\theta_{300}}\right)}{\log\left(\frac{\omega_{600}}{\omega_{300}}\right)} \quad (3.8)$$

$$K = \frac{\theta_{300}}{\omega_{300}^n} \quad (3.9)$$

where

n = flow behavior index

K = fluid consistency index

θ_{600} = mud viscometer dial readings at 600 rpm

θ_{300} = mud viscometer dial readings at 300 rpm

ω_{600} = mud viscometer RPM at 600 rpm

ω_{300} = mud viscometer RPM at 300 rpm

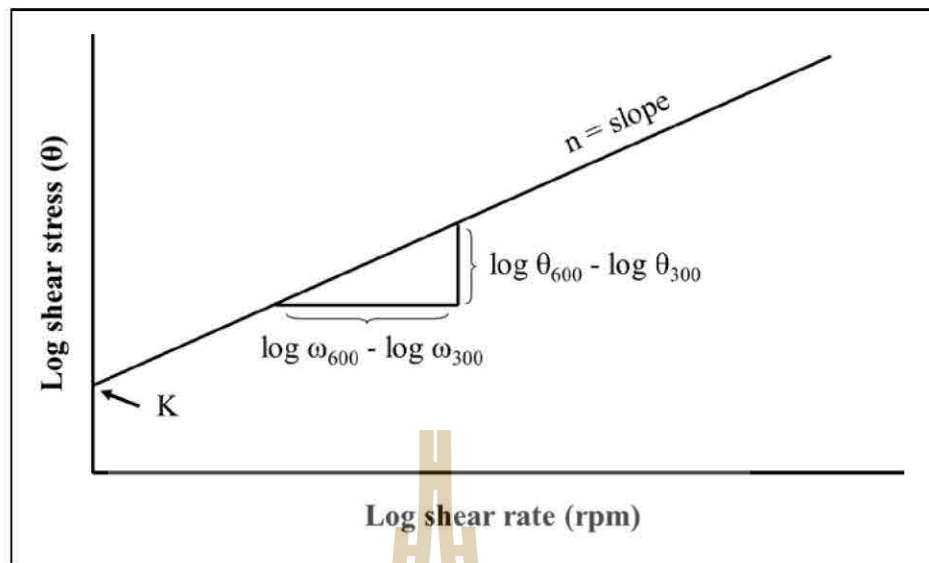


Figure 3.11 Log plot of Power law models (after Baker Hughes, 2006).

3.6.3 Filtration

The filtration experiment was conducted by filter press API low pressure, low temperature (Fann series 300 API filter press) which used to determine the filtration loss of a drilling mud through standard filter paper and the mud filter cake building characteristics under static conditions (Figure 3.12). The filter press consists of a cylindrical mud chamber made of materials resistant to strongly alkaline solutions. A filter paper is placed on the bottom of the chamber just above a suitable support. Below the support is a drain tube for discharging the filtrate into a graduated cylinder. The entire assembly is supported by a pressurized nitrogen gas cylinder and stand so 100 psi (6.9 bars) pressure can be applied to the mud sample in the chamber. At the end of the 30 minute filtration time, the volume of filtrate is reported as API filtration in cubic centimeters (cm^3). The thickness of the residue deposited upon the filter paper washes the cake gently to remove excess mud. Measure the thickness of the mud filter cake and reported in millimeters (mm) by using a vernier caliper. The

properties of the mud filter cake were visually examined, and its consistency was recorded using such notations as texture, color, hardness, or flexibility.



Figure 3.12 Fann series 300 API filter press.

3.6.4 Hydrogen ion concentration

The hydrogen ion concentration (pH) was conducted by using a glass electrode pH meter (Oakton pH 700 benchtop meters) to measure of drilling mud or mud filtrate pH and adjustments to the pH are fundamental to drilling mud control (Figure 3.13). Two methods are used for measurements the pH of water based drilling mud: a modified colorimetric method, using plastic backed test strips (sticks); and the potentiometric method, employing the glass electrode electronic pH meter. In this work used glass electrode pH meter, consists of a glass electrode, an electronic amplifier and a meter calibrated in pH units. The electrode is composed of (1) the glass electrode, a thinly walled bulb made of special glass within which is sealed a suitable electrolyte and an electrode and (2) the reference electrode, which is a

saturated calomel cell. Electrical connection with the mud is established through a saturated solution of potassium chloride contained in a tube surrounding the calomel cell. The electrical potential generated by the glass electrode system by the hydrogen ions in the drilling mud is amplified and operates the calibrated pH meter. Measurement and adjustments of pH are the fundament of drilling mud control. Clay interactions, a solubility of various components and effectiveness of additives are all dependent on pH, as in the control of acidic and sulfide corrosion processes.



Figure 3.13 Oakton pH 700 benchtop meters.

3.6.5 Resistivity

The resistivity of drilling mud, mud filtrate and mud filter cake are measured by resistivity meter (Fann model 88c resistivity meter) to control of the resistivity of the drilling mud and mud filtrate while drilling may be desirable to permit enhanced evaluation of the formation characteristics from electric logs (Figure 3.14). The determination of resistivity is essentially the measurement of the resistance

to electrical current flow through a known sample configuration. Measured resistance is converted to resistivity by use of a cell constant. The cell constant is fixed by the configuration of the sample in the cell and is determined by calibration with standard solutions of known resistivity. Fill the clean, dry resistivity cell with freshly stirred drilling mud, mud filtrate or mud filter cake and fill the cell to the correct volume according to the manufacturer's procedure. Connect the cell to the meter and measure the resistance in ohm-meters and temperature. The resistivity meter provides a direct digital readout of resistivity in three ranges; 2, 20 and 200 ohm-meters/meters². Instrument calibration is using salt solution and calculated the correction factor for accurate data.



Figure 3.14 Fann model 88c resistivity meter.

3.6.6 Solid content

The liquid and solid content was measured by retort kit (Fann retort oil and water 50 ml kit) which was a direct-reading method for measuring volumes of water and solids contained in drilling mud (Figure 3.15). Disassemble retort assembly

and lubricate sample cup threads with high-temperature grease. Fill sample cup almost level full of the mud to be tested. Put the sample cup cover in place by rotating firmly, squeezing out excess fluid to obtain the exact volume 50 ml required. Clean spills from cover and threads. Pack fine steel wool into the upper expansion chamber, then screw sample cup into the expansion chamber and heated at high temperature until the liquid components have been distilled off and vaporized. These vapors passed through a condenser and collected in a graduated cylinder that usually is graduated in percentage. Water volumes are read directly in percentage from the graduated cylinder. The solids, both suspended and dissolved, are determined by subtracting from 100% or by reading the void space at the top. Drilling mud retorts are generally designed to distill 50 ml sample volumes.

The percentage by volume solids analysis, weight method (calculated by weight difference using conventional retort) was calculated following formulas from API standard, four measurements are taken:

- A. Mud weight.
- B. Weight of retort (including steel wool and cup).
- C. Weight of retort with whole mud.
- D. Weight of retort with mud solids.

Compute volume percentage solids:

$$\text{Fraction of solids} = \frac{(C - B) - SG_{\text{MUD}} \times (C - D)}{C - B} \quad (3.10)$$

$$\% \text{ solids} = 100 \times \text{volume fraction solids} \quad (3.11)$$

where $\text{Mud density (g/cm}^3\text{)}; \text{SG}_{\text{MUD}} = \text{mud weight (lb/gal)} \times 0.11994.$

Grams of mud in retort: grams of mud = Value C - Value B.

Grams or cm^3 water distilled: Value C - Value D.



Figure 3.15 Fann retort oil and water 50 ml kit.

3.6.7 Scanning Electron Microscope

Scanning Electron Microscope analysis using JEOL JSM-6010LV was utilized in imaging and chemical analysis and forms the subject of scanning electron microscopy (Figure 3.16). The sample was mounted on a sample holder using conductive carbon tapes and applies a thin gold film conductive coating to the sample that is effective in eliminating charging of non-conductive materials. Load sample holder on the bottom that fits over the raised circle in the center of the stage. Press and hold the EVAC button on the vacuum control until it starts flashing. It will take about 1 minute to evacuate to a pressure that is safe for the beam. The electrons are generated using the electron Gun. The electrons pass through the electromagnetic lenses (condenser lens) to make the electrons into an electron beam. The electron

beam is adjusted by the objective lens to focus on the sample surface, make interaction with the sample reflected from the surface of the sample and to cause secondary electrons. The resulting electrons emitted from the sample are attracted and collected by a secondary electron detector and secondary electron signal translated into electronic signals into images in the three-dimensional display on the screen. Imaging in an SEM can be done using secondary electrons to obtain fine surface topographical features or with backscattered electrons which give contrast based on atomic number. Images are typically resolved in 5-3,000 \times magnification with a spot size of 20-30 and beam strength of 5-10 kV.

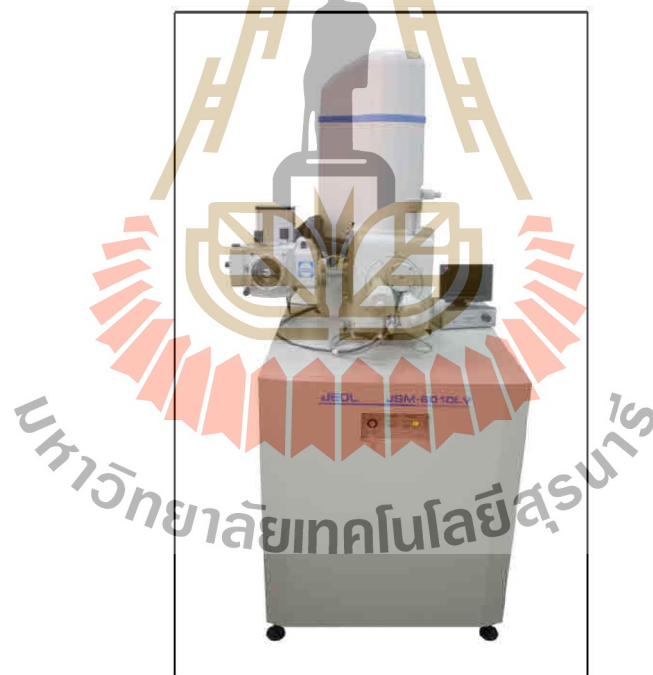


Figure 3.16 JEOL JSM-6010LV Scanning Electron Microscope.

3.6.8 Field Emission Scanning Electron Microscope

Field emission scanning electron microscope analysis using Carl Zeiss Auriga was allowed to examine subsurface structures, sample porosity, grain orientation, layered materials, cell structures and membranes and many other features (Figure 3.17). Prior to analysis, the sample was mounted on a sample holder using conductive carbon tapes and was coated with thin gold. The sample is prepared and mounted on the SEM sample mount, to vent the SEM to load it. The stage usually vents in about 1 minute. When it arrives at atmospheric pressure, gently pull the SEM chamber door open. Carefully slide the sample holder over this disk until it docks against the cross bar on top of the SEM stage table. The pump down sequence will take several minutes to achieve sufficient vacuum in the chamber in the system to open the column valve and establish a beam. As the vacuum level in the chamber drops below 7.5×10^{-5} Torr, the column valve will open and the gun EHT (High Voltage) was "Run Up". If the electron beam has been on and at high voltage, the system will automatically bring it back on after proper vacuum levels have been reached. The beam is established, the substrate needs to be positioned under the column, so the beam can see it. This requires moving the stage from its default loading position to the inspection location which may depend on the sample and its size and shape. The standard SEM image is generated by secondary electron emission from the substrate. These are low energy electrons produced both by the primary electron beam and the high energy backscattered electrons. Images are typically resolved in 5-30,000 \times magnification with a spot size of 20-30 and beam strength of 5-10 kV. However, while the primary electron beam can penetrate the substrate by

several or many microns, the escape depth for the secondary electrons was only on the order of tens or hundreds of angstroms.



Figure 3.17 Carl Zeiss Auriga Field Emission Scanning Electron Microscope.

CHAPTER IV

RESULTS AND DISCUSSIONS

4.1 Introduction

This chapter exhibits the results of laboratory experiments, including data analyzed and discusses the results of the experiments. Drilling mud samples were tested and analyzed to determinate their chemical properties, physical properties, radical properties and the cost of newly invented mud were discussed and compared to a common mud system that used in well drilling. The results of the experiment and analysis are revealed below.

4.2 Chemical properties

The objectives of these tests were to determine the chemical composition and mineral composition of drilling mud both before and after mixed with palm oil fuel ash (POFA) and sugarcane bagasse ash (SCBA). The step of methods was the rheological properties and physical properties. These results lead to the determination that the most suitable mixing ratios and temperature of drilling mud mixed with these additives.

4.2.1 Chemical composition

The chemical composition was measured by X-ray Fluorescence (XRF). Table 4.1 and Table 4.2 show the major chemical composition of various materials before mixed and drilling mud after mixed with POFA and SCBA additives by varying mixing ratio and temperature.

A base mud sample suspension was prepared to use 60 grams of bentonite per 1,000 milliliter of water and 100 grams of barite. X-ray fluorometry analysis revealed that drilling mud contains a high composition of silica (65.774% to 67.560%), followed by aluminium oxide (14.694% to 15.278%), iron oxide (4.774% to 5.951%), magnesium oxide (4.651% to 5.5248%) and barium oxide (2.029% to 5.773%).

POFA most contains of silica (57.583%), potassium oxide (18.278%), calcium oxide (8.534%), chloride (7.911%) and magnesium oxide (5.247%). The percentage of chemical compositions of drilling mud after mixed with POFA comprise silica (60.383% to 68.726%), aluminium oxide (9.761% to 13.727%), barium oxide (3.848% to 9.835%), magnesium oxide (4.767% to 6.895%) and iron oxide (4.274% to 6.107%). From Table 4.2, the drilling mud after mixed POFA was found to have an increase in magnesium oxide from base mud. The relatively high magnesium oxide content was also one of the favorable points considered in terms of swelling and viscosity features (Karagüzel et al., 2010). This will result in base mud mixed POFA having a higher viscosity.

The chemical composition of SCBA has a high percentage of silica (88.379%), potassium oxide (3.712%), iron oxide (2.848%) and calcium oxide (2.034%). After SCBA containing drilling mud, the major oxide observed has silica (65.607% to 71.460%), aluminium oxide (11.572% to 14.614%), iron oxide (4.249% to 5.732%), magnesium oxide (3.288% to 5.715%) and barium oxide (3.225% to 5.982%).

However, the chemical compositions of drilling mud depend on the amount of bentonite, barite and concentrations of POFA and SCBA.

Table 4.1 Chemical compositions of various materials.

Compounds	Materials			
	Chemical compositions (weight %)			
	Barite	Bentonite	POFA	SCBA
MgO	-	4.941	5.247	1.283
Al ₂ O ₃	1.305	16.276	-	-
SiO ₂	1.902	55.619	57.583	88.379
SO ₃	8.888	0.088	-	-
K ₂ O	0.209	0.634	18.278	3.712
CaO	0.186	4.485	8.534	2.034
Fe ₂ O ₃	1.454	14.195	1.779	2.848
SrO	0.831	0.049	0.107	-
ZrO ₂	-	0.033	-	-
Rh ₂ O ₃	2.795	0.111	0.114	0.103
BaO	82.430	-	-	-
Cl	-	0.076	7.911	0.647
TiO ₂	-	2.653	0.090	0.795
MnO ₂	-	0.164	0.201	0.157
CuO	-	-	0.067	0.026
ZnO	-	0.017	0.089	0.016
P ₂ O ₅	-	0.628	-	-
Ta ₂ O ₅	-	0.031	-	-
Total	100	100	100	100

Table 4.2 Chemical compositions of drilling mud mixed with additives.

No.	Chemical compositions (weight %)									Total
	MgO	Al ₂ O ₃	SiO ₂	K ₂ O	CaO	Fe ₂ O ₃	SrO	Rh ₂ O ₃	BaO	
1	4.941	14.694	66.527	0.526	2.852	4.774	0.343	0.262	5.773	100
2	4.651	15.278	65.774	0.526	3.740	5.951	0.457	0.370	3.253	100
3	5.248	14.992	67.560	0.514	3.064	5.931	0.370	0.292	2.029	100
4	5.182	13.686	61.521	2.160	3.406	5.435	0.182	0.522	7.906	100
5	5.163	13.428	68.726	1.135	2.183	4.676	0.130	0.362	4.197	100
6	5.929	10.232	63.868	4.719	4.961	4.744	0.137	0.390	5.020	100
7	5.305	13.415	60.536	1.992	2.941	5.776	0.189	0.582	9.264	100
8	5.203	11.800	63.618	4.283	5.153	4.993	0.143	0.380	4.427	100
9	6.895	9.761	62.971	4.759	6.729	4.274	0.122	0.350	4.139	100
10	4.767	13.727	60.383	2.222	3.376	6.107	0.177	0.509	8.732	100
11	5.043	10.813	60.601	3.885	4.073	5.093	0.158	0.499	9.835	100
12	5.955	9.779	64.975	4.805	5.848	4.322	0.125	0.343	3.848	100
13	4.650	14.407	65.607	0.947	2.875	5.732	0.167	0.442	5.173	100
14	5.715	14.614	65.734	2.311	2.516	4.637	0.115	0.317	4.041	100
15	4.750	12.380	69.874	1.447	2.671	4.711	0.123	0.326	3.718	100
16	4.123	13.226	68.697	0.815	2.661	5.034	0.121	0.350	4.973	100
17	4.566	14.077	69.078	2.022	2.179	4.442	0.113	0.298	3.225	100
18	3.965	11.572	70.429	1.362	1.937	4.249	0.123	0.381	5.982	100
19	3.819	12.593	69.804	0.803	2.628	4.912	0.115	0.346	4.980	100
20	4.549	13.402	68.499	2.153	2.251	4.652	0.121	0.331	4.042	100
21	3.288	12.228	71.460	1.425	2.586	4.474	0.121	0.343	4.075	100

4.2.2 Mineral composition

The mineral compositions were measured by X-ray Diffraction (XRD). Table 4.3 and Table 4.4 show the mineral compositions of various materials before mixed and drilling mud after mixed with POFA and SCBA additives by varying mixing ratio and temperature.

The mineral compositions of base mud in three temperatures have likewise of main components. It was found that there was a maximum of barite (48.6% to 55.4%), followed by talc (14.3% to 20.5%), quartz (8.9% to 14.5%), calcite (1.7% to 5.6%), kaolinite (2.7% to 4.7%) and microcline (3.1% to 5.1%).

The XRD pattern of POFA (Figure 4.1), it can be noted that the main mineral was sylvite (35.479%). Peaks of XRD analysis belonging to the quartz (29.942%), anorthite (13.753%), kaolinite (3.735%), gypsum (3.507%) and calcite (2.493%) were also identified. The percentage of mineral composition of drilling mud after mixed with POFA comprise barite (22.81% to 39.98%), quartz (21.06% to 33.05%), calcite (1.74% to 10.26%), nacrite (3.40% to 10.95%) and tobermorite (2.39% to 9.19%). From Table 4.1 and Table 4.3, the chemical components were founded in POFA to show a relationship with the main mineral as follows silica (SiO_2) in the form of quartz, montmorillonite, anorthite, kaolinite, tobermorite and mullet. Potassium oxide (K_2O) in the form of sylvite. Calcium oxide (CaO) in the form of calcite, anorthite, gypsum and tobermorite. Chlorine oxide (Cl) in the form of sylvite.

The XRD pattern of the SCBA was shown in Figure 4.2, presents the major minerals of SCBA. The following crystalline phases were found: barite (0.299%), quartz (73.123%), calcite (1.851%), anorthite (6.005%), kaolinite (13.038%) and gypsum (5.684%) with a predominance of quartz (SiO_2). The analysis of the

SCBA shows the amorphous silica formation with traces of low quartz (Hussein et al., 2014). The SCBA samples chemical compositions provided in Table 4.1. According to said data, the SCBA sample contains a large amount of silica (88.379%). This result is consistent with the X-ray Diffraction pattern Figure 4.2. The major minerals of drilling mud after mixed with SCBA included barite (45.00% to 49.22%), quartz (14.11% to 17.78%), tobermorite (12.01% to 13.03%), kaolinite (5.24% to 9.60%), calcite (2.63% to 3.92%) and nacrite (2.42% to 3.34%).

Clay is an important component of drilling mud. It was added to increase the fluid viscosity and to form a mud filter cake to protect the permeable zones (Hallenburg, 1997). Common examples include chlorite, illite, kaolinite, montmorillonite and smectite. Meanwhile, A significant amount of tobermorite was formed leading to a denser and more stable structure of the samples (Kolias et al., 2005). From Table 4.4, the drilling mud after mixed POFA and SCBA were found to have an increase in kaolinite and tobermorite from base mud. Thus, the amount of kaolinite and tobermorite advocate increasing strength of drilling mud, which effect to the rheology properties.

Table 4.3 Mineral compositions of various materials.

Compounds	Materials			
	Mineral content (weight %)			
	Barite	Bentonite	POFA	SCBA
Barite	45.364	-	0.393	0.299
Quartz	22.879	0.113	29.942	73.123
Calcite	-	18.627	2.493	1.851
Anorthite	-	1.651	13.753	6.005
Kaolinite (BISH)	2.062	14.726	3.735	13.038
Gypsum	3.602	0.962	3.507	5.684
Hematite	-	5.787	0.870	-
Tobermorite	-	-	2.056	-
Periclase	-	-	-	-
Rutile	-	-	1.202	-
Pyrolusite	7.479	-	1.335	-
Chromite	-	2.057	-	-
Silica LeBail	1.986	11.947	-	-
Talc	2.462	28.508	-	-
Nacrite	3.792	2.069	-	-
Microcline intermediate1	3.915	13.553	-	-
Galena	1.468	-	1.185	-
Mullite 3:2	-	-	1.972	-
Troilite	-	-	2.078	-
Sylvite	4.991	-	35.479	-
Total	100	100	100	100

Table 4.4 Mineral compositions of drilling mud mixed with additives.

No.	Mineral content (weight %)															Total
	Bar.	Qtz.	Cal.	Anor.	Kao.	Gyp.	Hem.	Tob.	Per.	Rut.	Chr.	Sili.	Tal.	Nac.	Mic.	
1	48.73	14.52	5.21	2.72	2.68	0.81	1.19	-	-	-	0.25	-	17.27	1.57	5.05	100
2	55.52	8.89	1.67	0.10	3.87	2.08	0.79	-	-	-	0.80	0.00	20.52	2.65	3.11	100
3	53.51	11.72	5.60	1.47	4.73	0.92	0.93	-	-	-	0.17	0.34	14.29	2.67	3.65	100
4	25.05	21.06	10.26	3.91	6.79	2.02	0.96	7.81	1.98	-	-	-	3.84	10.95	5.38	100
5	28.60	22.68	4.31	4.20	5.37	0.71	1.42	9.19	2.35	-	-	-	7.89	8.87	4.43	100
6	22.81	27.57	2.23	4.62	7.10	4.18	1.23	8.05	2.71	-	-	-	6.73	6.48	6.29	100
7	36.30	21.42	8.40	0.72	6.06	2.99	1.57	2.46	3.36	-	-	-	5.83	3.40	7.49	100
8	35.59	27.49	5.02	0.80	3.64	2.67	1.48	4.09	3.45	-	-	-	5.24	7.47	3.06	100
9	33.99	28.11	4.02	4.14	3.90	3.82	0.88	4.71	1.62	-	-	-	5.38	6.09	3.34	100
10	39.98	21.75	3.05	4.48	4.02	1.64	0.83	4.65	2.42	-	-	-	4.25	8.67	4.27	100
11	38.80	22.99	1.84	2.28	4.32	3.19	1.76	2.39	2.84	-	-	-	7.02	7.33	5.23	100
12	30.96	33.05	1.74	4.64	3.18	2.87	1.25	3.71	1.82	-	-	-	7.29	6.71	2.80	100
13	48.88	15.53	3.82	1.57	9.60	1.90	0.81	12.52	0.32	1.20	-	-	1.30	2.55	-	100

Table 4.4 Mineral compositions of drilling mud mixed with additives (continued).

No.	Mineral content (weight %)															Total
	Bar.	Qtz.	Cal.	Anor.	Kao.	Gyp.	Hem.	Tob.	Per.	Rut.	Chr.	Sili.	Tal.	Nac.	Mic.	
14	48.29	15.04	3.92	2.75	6.55	1.53	0.77	13.03	0.10	2.48	-	-	2.21	3.34	-	100
15	48.84	15.85	3.17	2.94	6.57	1.81	0.84	12.24	0.06	3.01	-	-	1.73	2.95	-	100
16	49.22	16.46	3.49	1.92	6.08	1.79	0.68	12.01	0.54	2.02	-	-	2.66	3.11	-	100
17	46.37	16.60	3.27	3.37	6.33	2.15	0.56	12.34	0.59	2.42	-	-	3.58	2.43	-	100
18	45.00	17.78	2.89	3.69	5.24	1.32	0.68	12.34	0.90	3.24	-	-	3.73	3.18	-	100
19	47.68	15.73	3.72	1.46	6.48	1.20	0.72	12.40	0.57	2.66	-	-	4.56	2.83	-	100
20	47.94	14.85	2.63	2.25	6.04	1.92	0.86	12.17	0.89	2.66	-	-	4.59	3.19	-	100
21	47.77	14.11	3.23	2.20	7.19	1.79	0.88	12.33	0.08	3.43	-	-	4.55	2.42	-	100

***Bar.** = Barite, **Qtz.** = Quartz, **Cal.** = Calcite, **Anor.** = Anorthite, **Kao.** = Kaolinite (BISH), **Gyp.** = Gypsum, **Hem.** = Hematite, **Tob.** = Tobermorite, **Per.** = Periclase, **Rut.** = Rutile, **Chr.** = Chromite, **Sili.** = Silica LeBail, **Tal.** = Talc, **Nac.** = Nacrite, **Mic.** = Microcline intermediate.

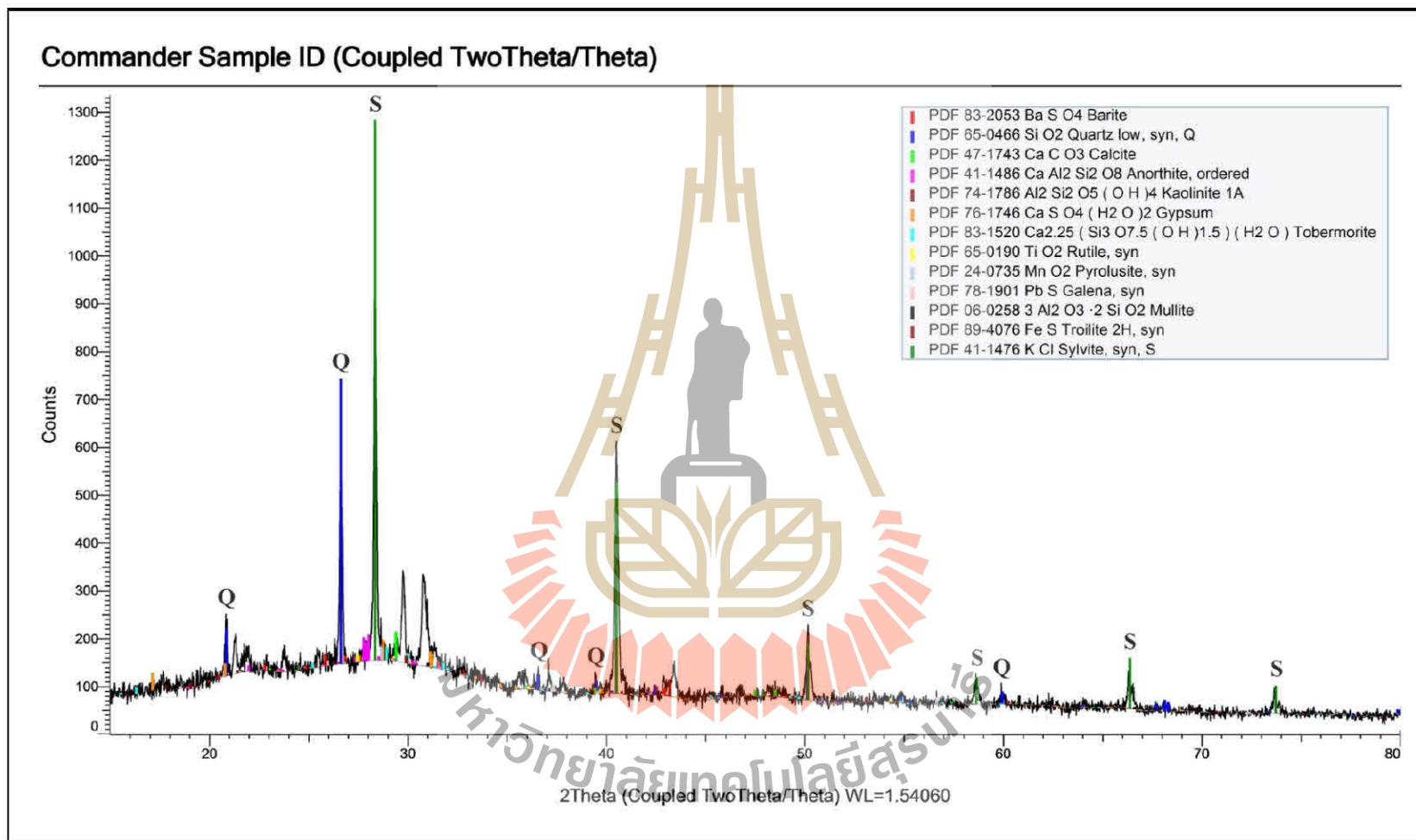


Figure 4.1 XRD pattern of POFA.

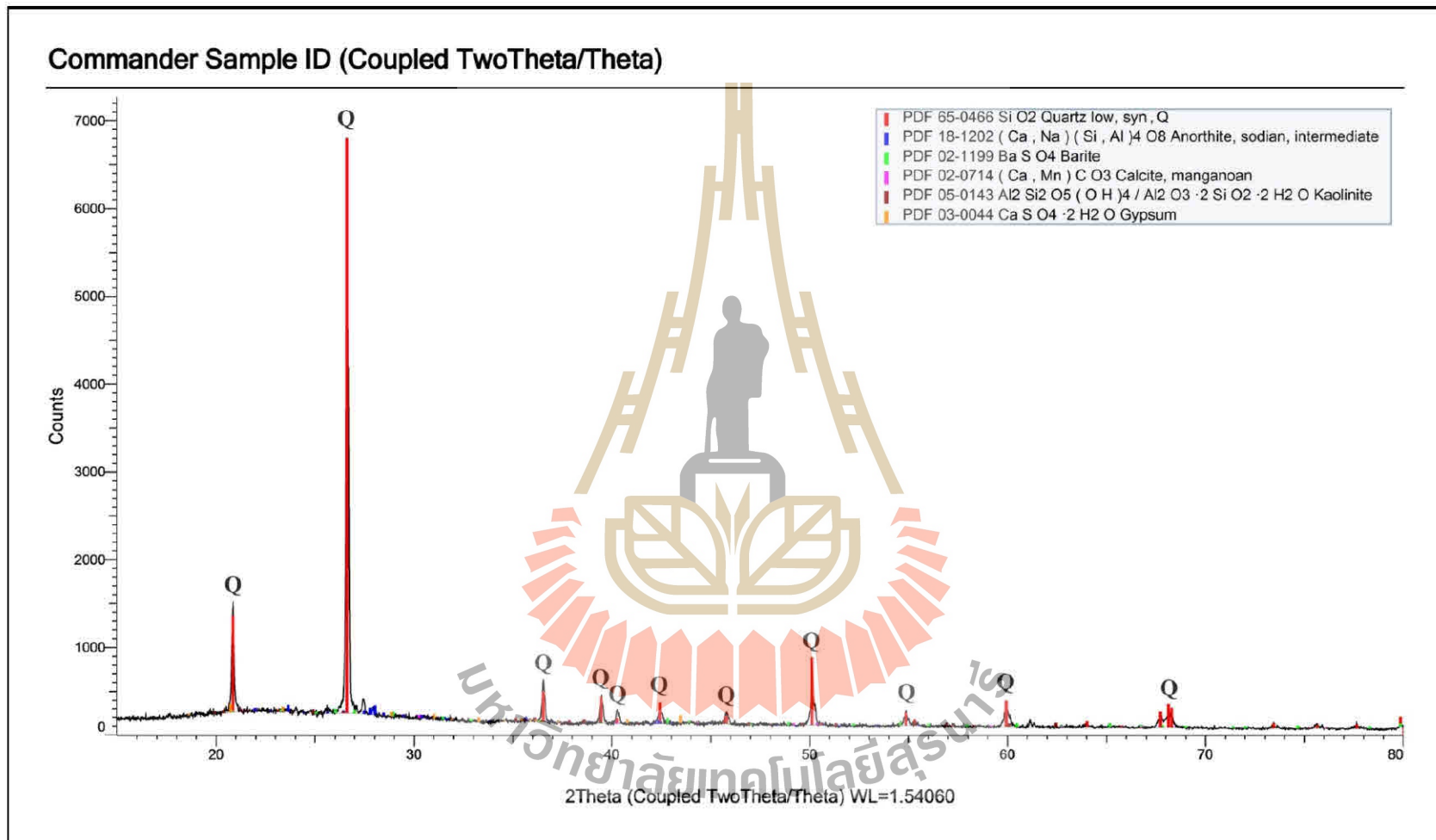


Figure 4.2 XRD pattern of SCBA.

4.3 Physical properties

The varied composition, mixing ratio and temperature of drilling mud mixed with POFA and SCBA was shown in Appendix A. A base mud sample suspension was prepared by using 60 grams of bentonite per 1,000 milliliters of water, 100 grams of barite were added to control density.

4.3.1 Density properties

The density of any fluid was directly related to the amount and average specific gravity of the solids in the system. The control of density has been criticized since the hydrostatic pressure exerted by the column of fluid was required to contain formation pressures and to aid in keeping the borehole open. The results of the density of drilling mud after mixing additives presents in Figures 4.3 to 4.5. A range of drilling mud mixed with these additives was 1.09 to 1.13 g/cm³ or 9.10 to 9.43 lbs/gallon. The density of drilling mud slightly decreased with increasing temperature, but the results obtained showed that adding POFA concentration (Figure 4.3) and SCBA concentration (Figure 4.4) produced a significantly higher density. Because a particle of POFA having a specific gravity to be in the range of 2.22-2.78 and as the specific gravity of SCBA between 2.20-2.52. The result demonstrates the ability of POFA and SCBA additives to provide weight to drilling mud. From Figure 4.5, the density of drilling mud using SCBA as additives in 1 and 3%w/w has the same value in all temperatures. However, the density of drilling mixed with POFA and SCBA at 25 and 50°C has similar value, but the temperature at 80°C the density of drilling mud mixed with POFA be greater than mixed with SCBA in all the concentration.

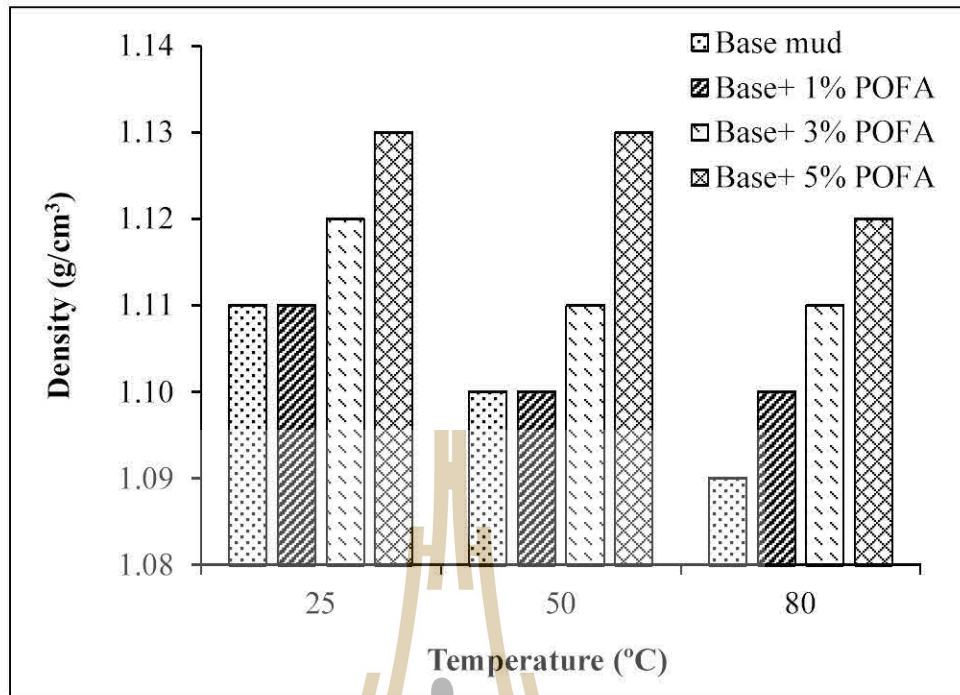


Figure 4.3 Density of base mud mixed with POFA versus temperature.

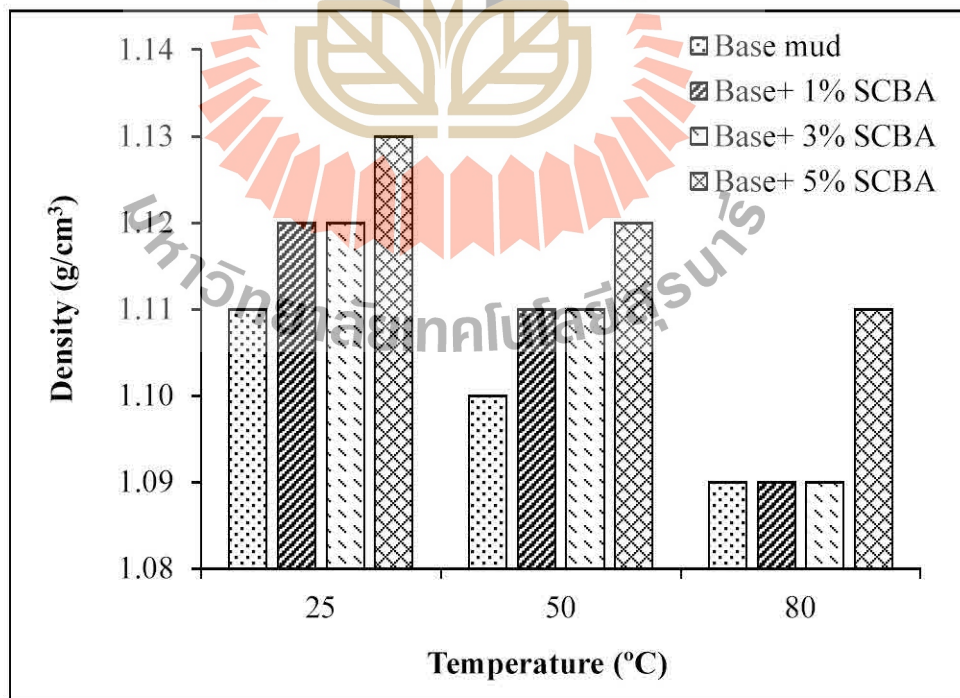


Figure 4.4 Density of base mud mixed with SCBA versus temperature.

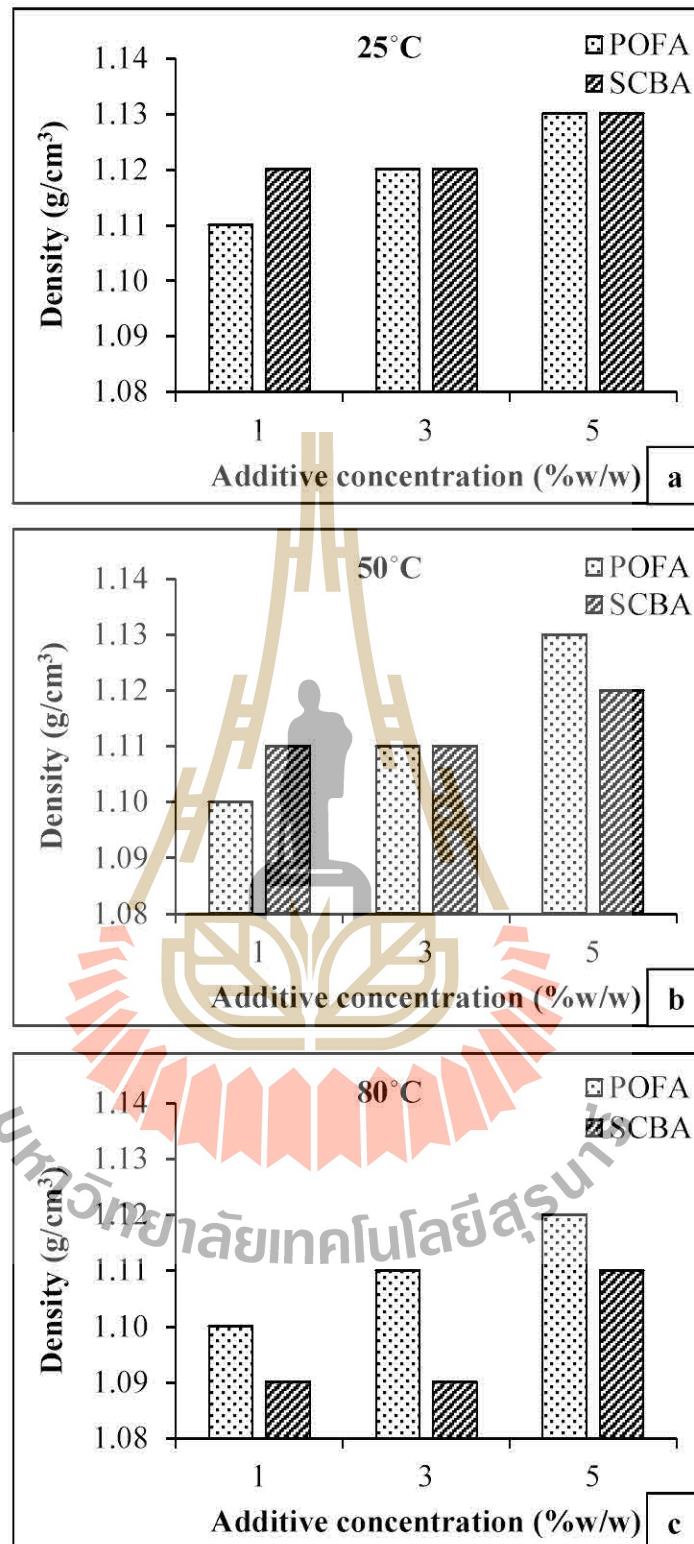


Figure 4.5 Density of drilling mud versus additive concentration at (a) 25°C, (b) 50°C and (c) 80°C.

4.3.2 Rheology properties and parameters

The shear stress and shear rate calculated from the average viscometer readings are following equations 3.6 and 3.7 in the previous chapter. Table 4.5 shows the values the shear stress and shear rate for all six viscometer readings of base mud under the temperature at 25°C. The calculated shear stresses were plotted against shear rates in order to choose the best-fit curve for the model. For example, Figure 4.6 shows the consistency plots for base mud under the temperature at 25°C, the Bingham plastic fluid plot curve was fitted with a linear correction and Figure 4.7 show the consistency plots for base mud under the temperature at 25°C, the Power law fluid plot curve was fitted with a power correlation. From the two plots, the Bingham plastic fluids were better fitted with a linear correlation represented in Figure 4.6. Thus, the model can be inferred that the fluid tends to be a Bingham plastic fluid.

Table 4.5 Results of shear stress and shear rate of base mud.

rpm	Average reading	γ (sec ⁻¹)	τ (lb _f /ft ²)
600	30	1021.8	32.034
300	21	510.9	22.424
200	17	340.6	18.153
100	13	170.3	13.881
6	9	10.2	9.610
3	7	5.1	7.475

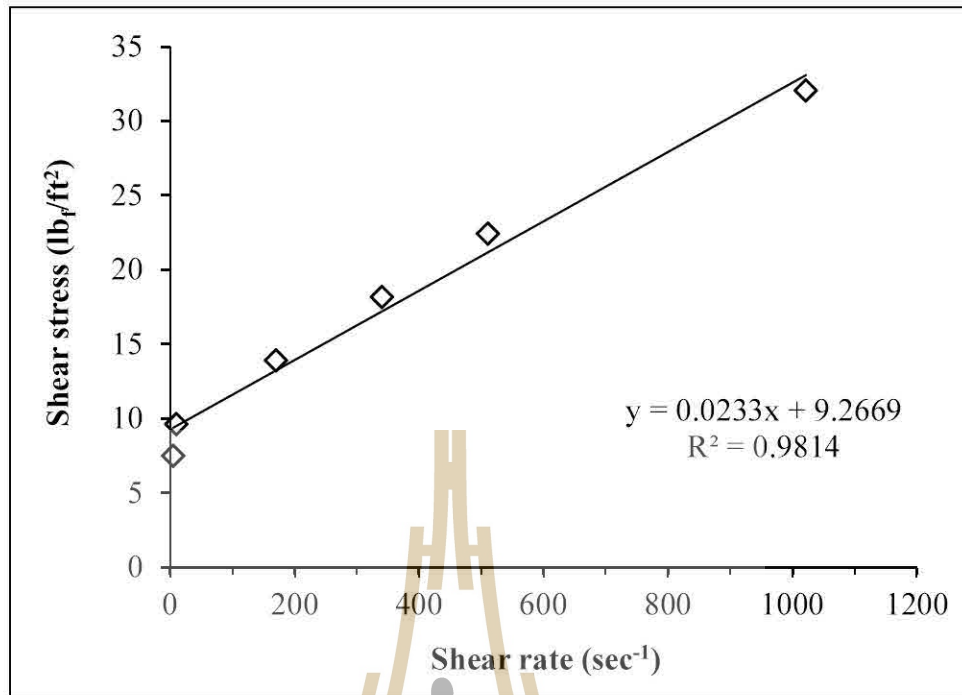


Figure 4.6 Consistency plot of base mud with a linear correction.

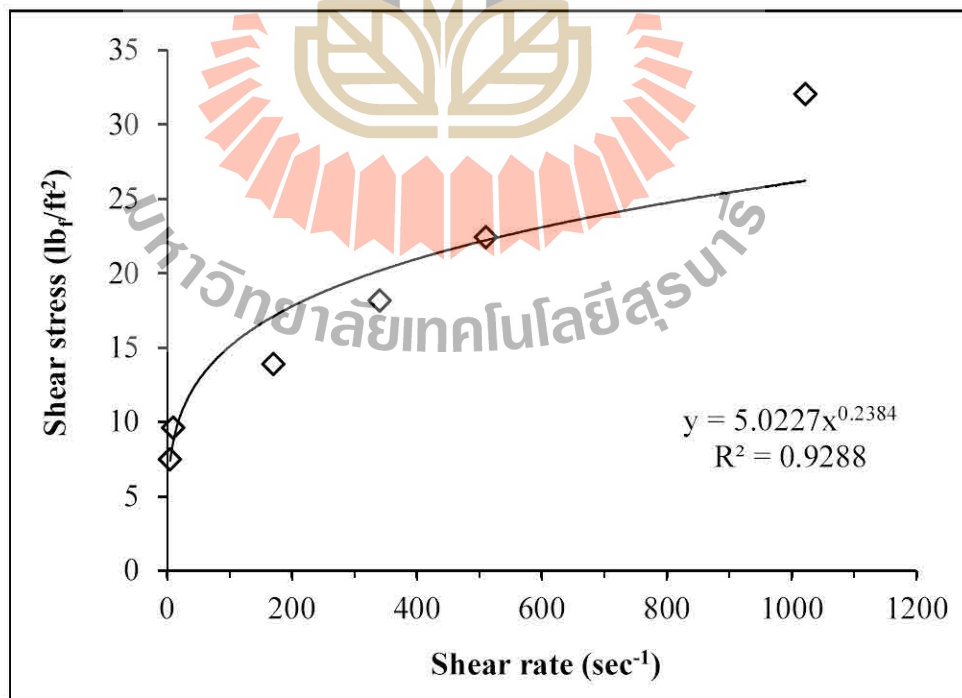


Figure 4.7 Consistency plot of base mud with a power correction.

The appropriate rheological model for other drilling mud samples was calculated in likewise. The base mud samples were categorized into six groups of testes temperature (25, 50 and 80°C) and different additives. Their consistency curves were plotted in Figure 4.8 to 4.16. Most of the base mud sample demonstrates the flow behavior in between the Bingham plastic model and the Power law model. The rheological properties of each sample were calculated for both models. Both models were used for each fluid just for comparison purposes. The results of a rheological calculation are shown in Table 4.6.

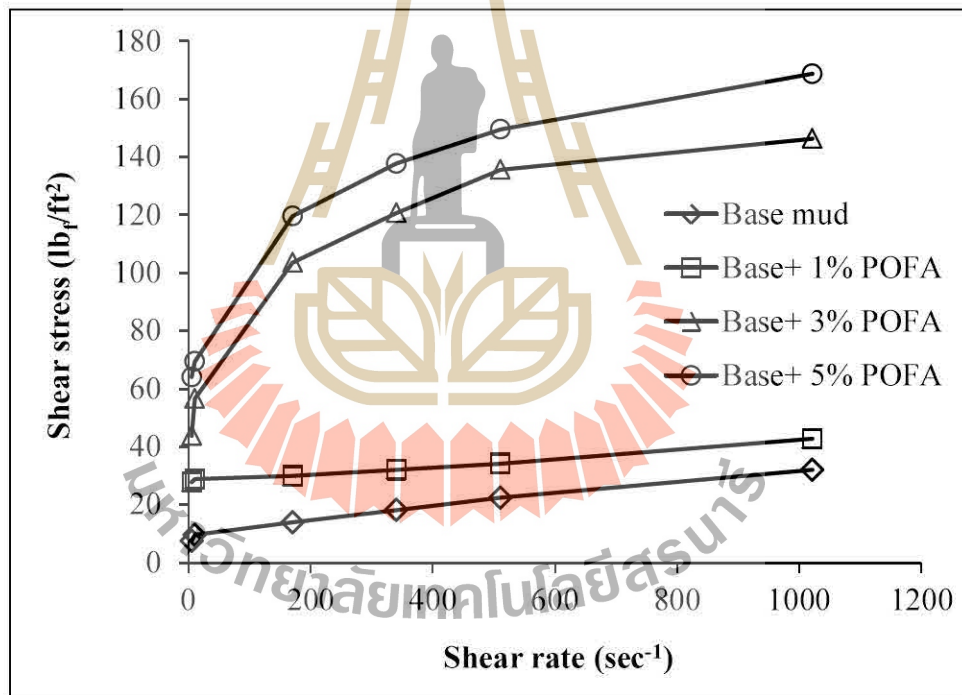


Figure 4.8 Consistency plot of base mud mixed with POFA at 25°C.

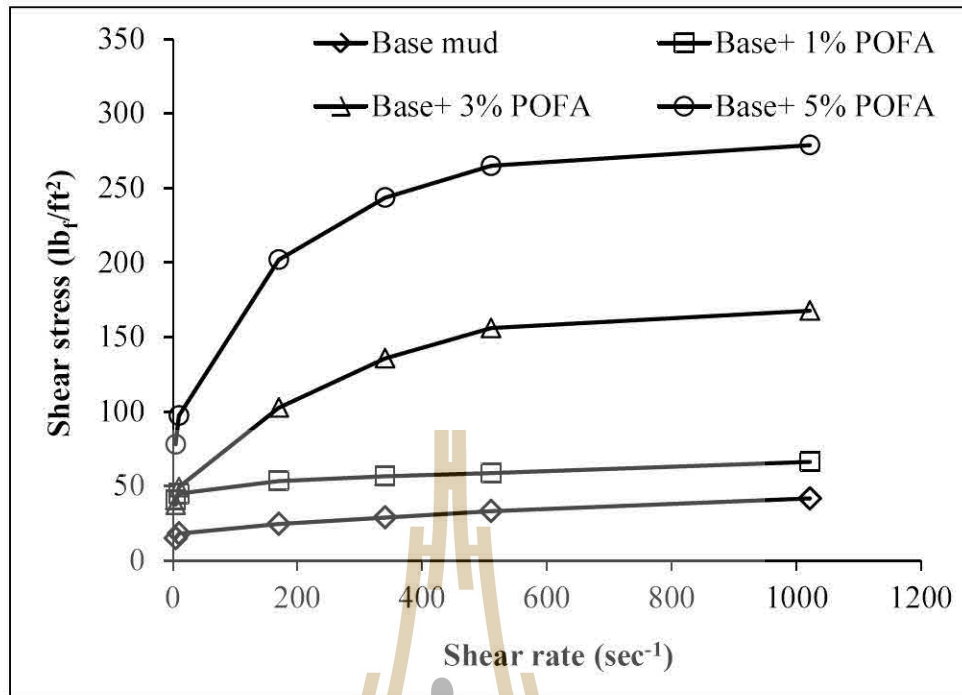


Figure 4.9 Consistency plot of base mud mixed with POFA at 50°C.

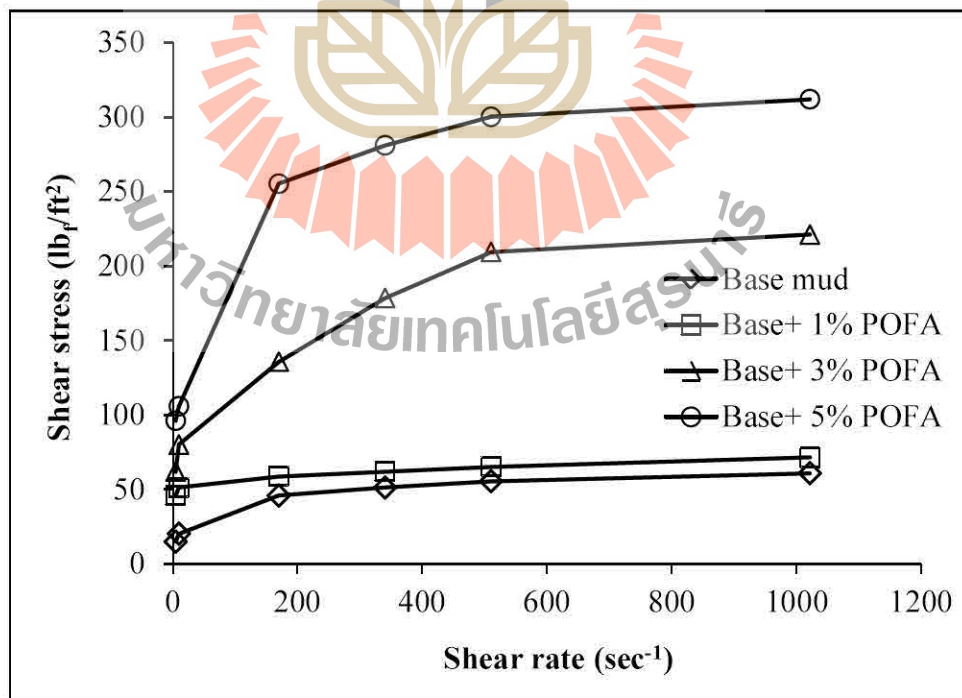


Figure 4.10 Consistency plot of base mud mixed with POFA at 80°C.

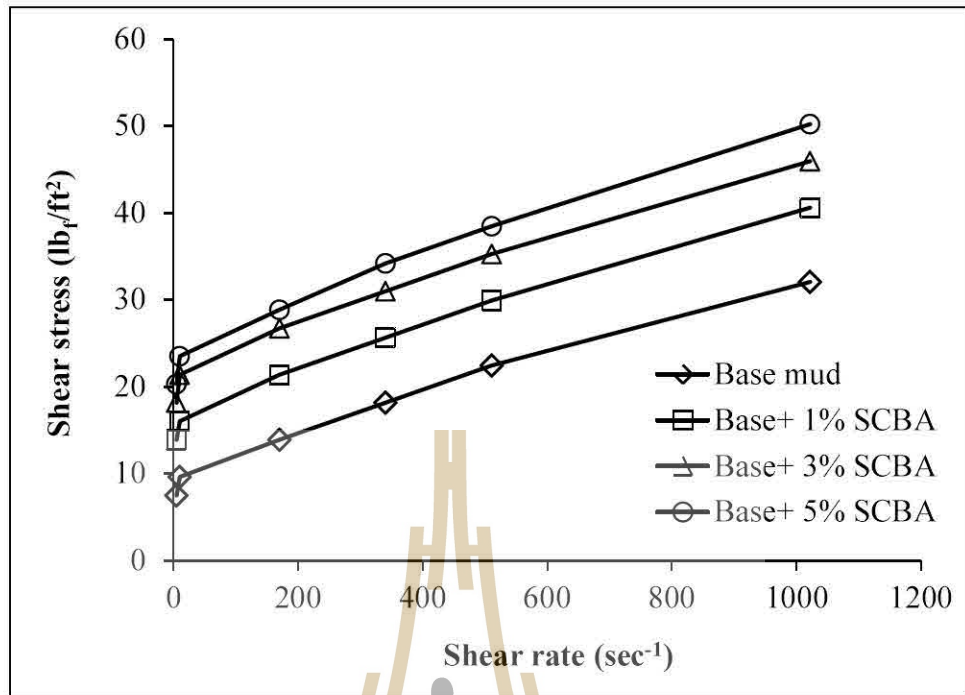


Figure 4.11 Consistency plot of base mud mixed with SCBA at 25°C.

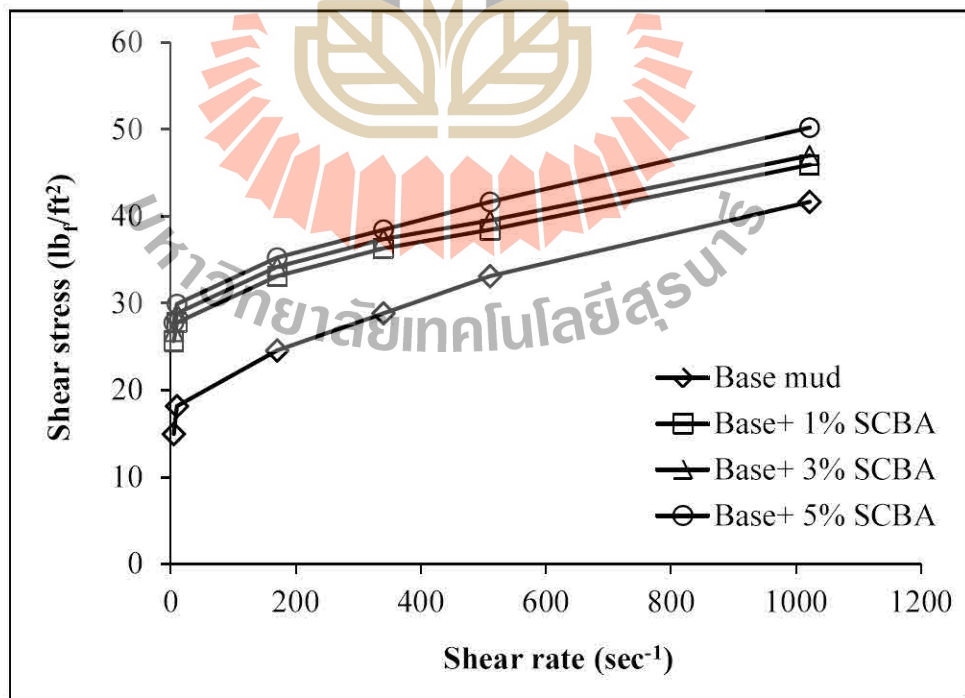


Figure 4.12 Consistency plot of base mud mixed with SCBA at 50°C.

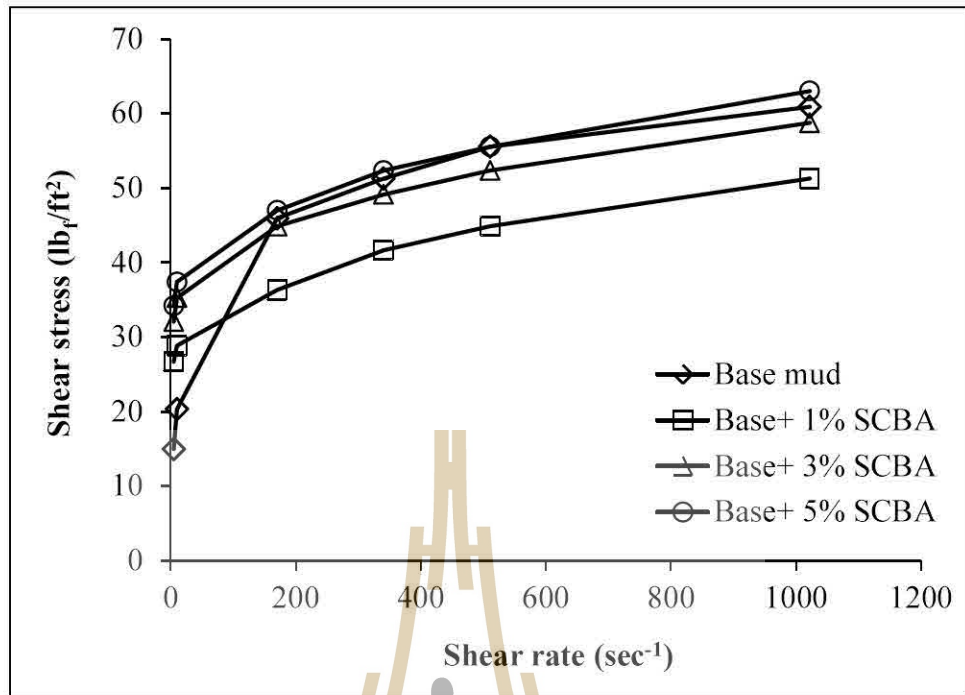


Figure 4.13 Consistency plot of base mud mixed with SCBA at 80°C.

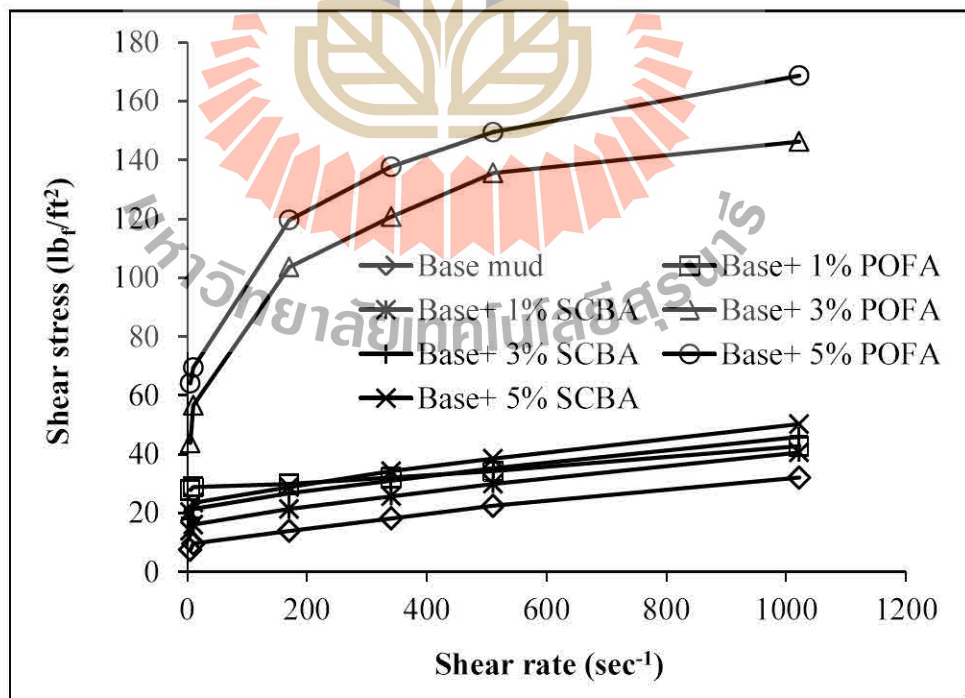


Figure 4.14 Consistency plot of drilling mud at 25°C.

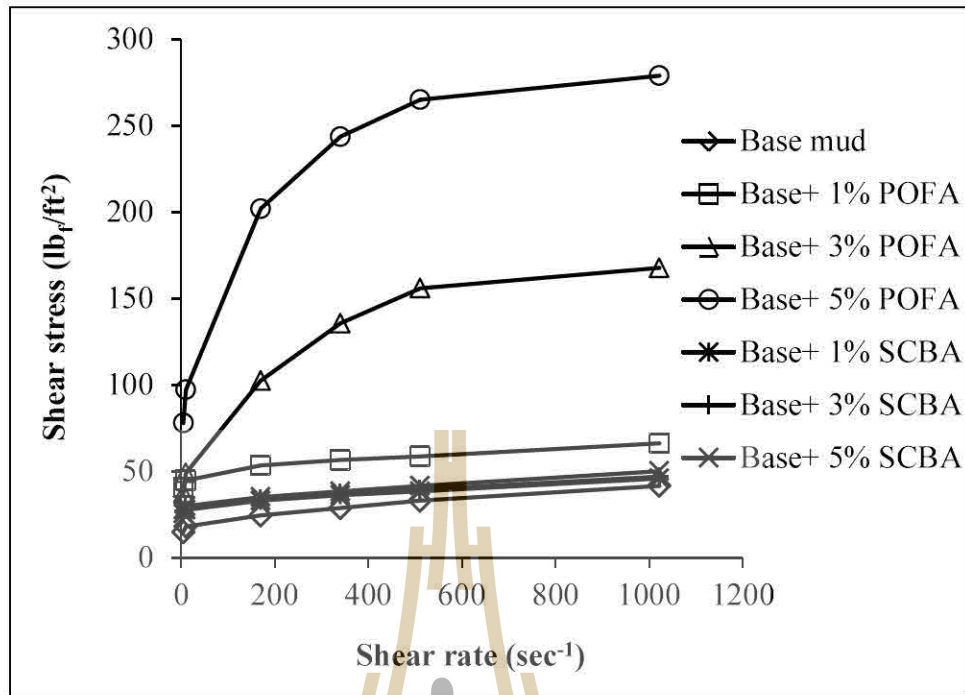


Figure 4.15 Consistency plot of drilling mud at 50°C.

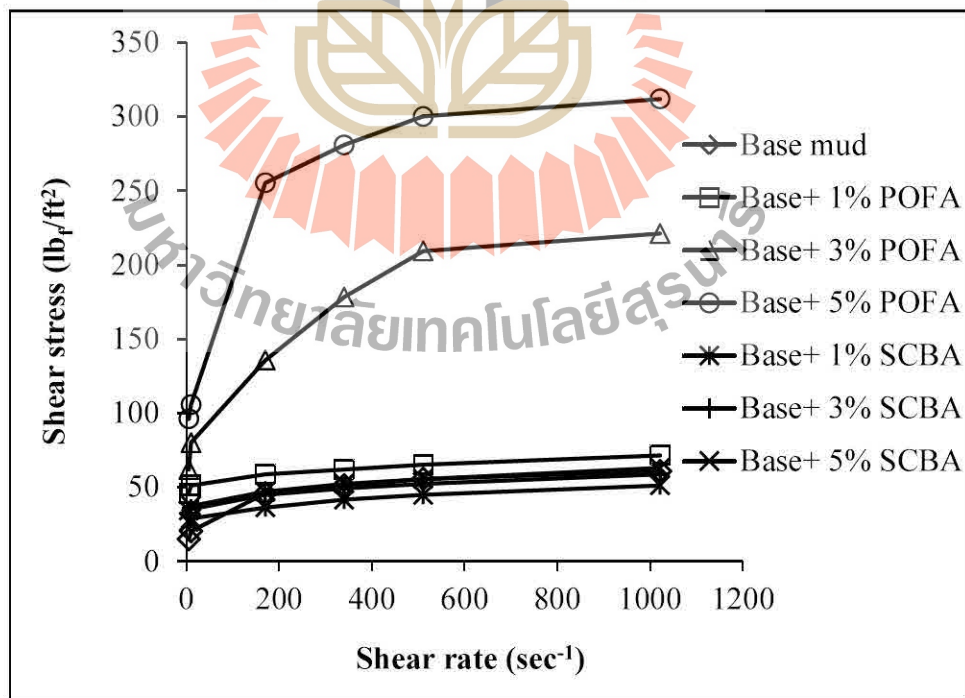


Figure 4.16 Consistency plot of drilling mud at 80°C.

Table 4.6 Rheological parameters of drilling mud.

Test Temp.	No.	Mud composition	Apparent viscosity (cP)	Bingham plastic model		Power law model		Gel _{in} * (lb _f /100 ft ²)	Gel ₁₀ ** (lb _f /100 ft ²)
				Plastic viscosity (cP)	Yield point (lb _f /100 ft ²)	n	K (lb·s ⁿ /100 ft ²)		
25°C	1	Base mud	15.0	8.8	12.5	0.5146	1.1157	8	9
50°C	2	Base mud	19.5	8.0	23.0	0.3312	4.6873	13	14
80°C	3	Base mud	28.6	5.3	46.8	0.1325	24.4291	14	15
25°C	4	Base+ 1% POFA	20.0	9.0	22.0	0.3219	5.1015	23	29
	5	Base+ 3% POFA	71.9	16.3	111.3	0.1712	47.8359	48	60
	6	Base+ 5% POFA	79.4	18.0	122.8	0.1745	51.7459	63	68
50°C	7	Base+ 1% POFA	31.3	6.8	49.0	0.1728	20.5223	39	40
	8	Base+ 3% POFA	78.8	11.0	135.5	0.1048	80.3082	53	62
	9	Base+ 5% POFA	130.6	13.3	234.8	0.0737	162.8785	67	80
80°C	10	Base+ 1% POFA	33.8	6.3	55.0	0.1354	28.1869	41	45
	11	Base+ 3% POFA	103.8	10.8	186.0	0.0788	125.0592	57	66
	12	Base+ 5% POFA	146.4	11.3	270.3	0.0554	204.8699	74	90

Table 4.6 Rheological parameters of drilling mud (continued).

Test Temp.	No.	Mud composition	Apparent viscosity (cP)	Bingham plastic model		Power law model		Gel _{in} * (lb _f /100 ft ²)	Gel ₁₀ ** (lb _f /100 ft ²)
				Plastic viscosity (cP)	Yield point (lb _f /100 ft ²)	n	K (lb·s ⁿ /100 ft ²)		
25°C	13	Base+ 1% SCBA	19.0	9.8	18.5	0.4406	2.2689	15	16
	14	Base+ 3% SCBA	21.6	10.3	22.8	0.3819	3.7374	20	21
	15	Base+ 5% SCBA	23.5	11.0	25.0	0.3847	4.0128	23	28
50°C	16	Base+ 1% SCBA	21.6	6.5	30.3	0.2563	8.3429	22	24
	17	Base+ 3% SCBA	22.1	6.8	30.9	0.2500	8.8915	27	31
	18	Base+ 5% SCBA	23.1	7.3	31.8	0.2382	10.0257	29	32
80°C	19	Base+ 1% SCBA	24.0	6.0	36.0	0.1926	13.9973	25	27
	20	Base+ 3% SCBA	27.9	6.3	43.4	0.1667	18.9402	27	29
	21	Base+ 5% SCBA	29.6	6.8	45.8	0.1822	18.3935	30	40

*Gel_{in} is initial gel strength and, **Gel₁₀ is 10 minutes gel strength of drilling mud.

4.3.3 Rheological behavior of drilling mud

The rheological parameters of base mud and base mud mixed with POFA and SCBA additives samples are summarized in Table 4.6 and the rheological data of the test are shown in Appendix A. The Power law model parameter constants in term of flow behavior index (n) and consistency index (K) can be calculated by equation 3.8 and 3.9 as shown in the previous chapter. The index “ n ” indicated that all drilling mud samples exhibited pseudoplastic flow with “ n ” less than 1. As mentioned above, the flow behavior of typical drilling mud usually acted between the Bingham plastic model and the Power law model, which was called pseudoplastic fluid. The consistency factor of drilling mud sample clearly increases as the increased of POFA and SCBA. The constant has resembled the apparent viscosity of the fluid that described the thickness of the fluid. The Power law model did not describe the behavior of drilling mud exactly, but the constant “ n ” and “ K ” normally described in the interest of hydraulic horsepower utilization which was used in hydraulic calculations (Baker Hughes, 2006).

Figure 4.17 to 4.32 was the plots of the rheological parameters obtained from the calculation with various POFA and SCBA concentrations.

The apparent viscosity was plotted with the change of POFA and SCBA concentration displays in Figure 4.17 and Figure 4.18. The results indicate a significant increase in the apparent viscosity as the POFA concentration increase and with the increase of SCBA concentration, the apparent viscosity shows a tendency to increase. However, the apparent viscosity of POFA concentration was greater than SCBA concentrations at all tested temperature. Because of the greater colloidal fraction of POFA and SCBA in the drilling mud sample, as a result, friction between

the particles increases and the shearing stress required to induce a unit rate of shear increases and hence apparent viscosity increase (Kumar et al., 2003). The change of the apparent viscosity at a different temperature was shown in Figure 4.19. For all the POFA and SCBA mixed with drilling, the apparent viscosity increase with increasing temperature. The consequence of temperature increase interaction energy of mud system. It induces more inter-particle attractive force between solid particles and so the clay particles come into contact with another and agglomerate which was known as flocculation (Luckham and Rossi, 1999).

The plastic viscosity was plotted with the change of POFA and SCBA concentration and temperature are shown in Figure 4.20 to 4.23. The results indicated for all tested temperature that the plastic viscosity of POFA and SCBA containing mud slightly increased with increasing POFA and SCBA concentration. While, the measured values for the plastic viscosity of POFA and SCBA mixed with drilling mud was shown slightly decreased as temperature increased. The trend of the line indicated that the mud behaved non-Newtonian and shear-thinning as temperature increased (up to 80°C), and displayed lower plastic viscosity and higher yield stress. The effect of temperature on bentonite suspension could be described as follows: heating up the bentonite suspension, increased the conductivity of the system, which indicated that more cations (Na^+) were dissolved from the surface of the particles. It was also suggested that this effect was responsible for the reduction of the normalized plastic viscosity and the observed of the yield stress, increasing the latter also due to thermally induced swelling (Luckham and Rossi, 1999).

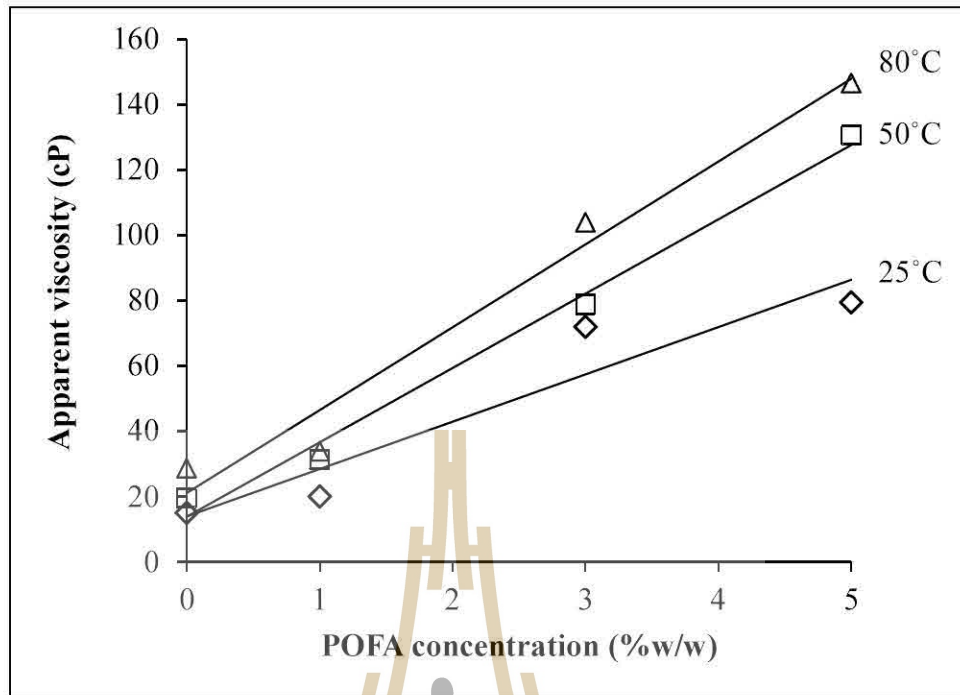


Figure 4.17 Apparent viscosity of drilling mud versus POFA concentration.

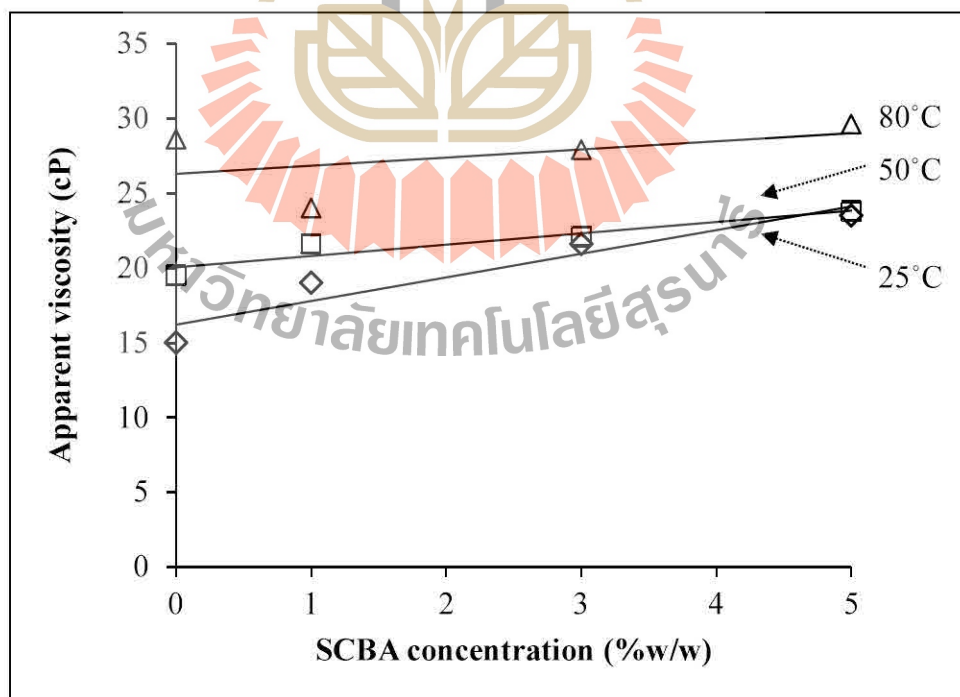


Figure 4.18 Apparent viscosity of drilling mud versus SCBA concentration.

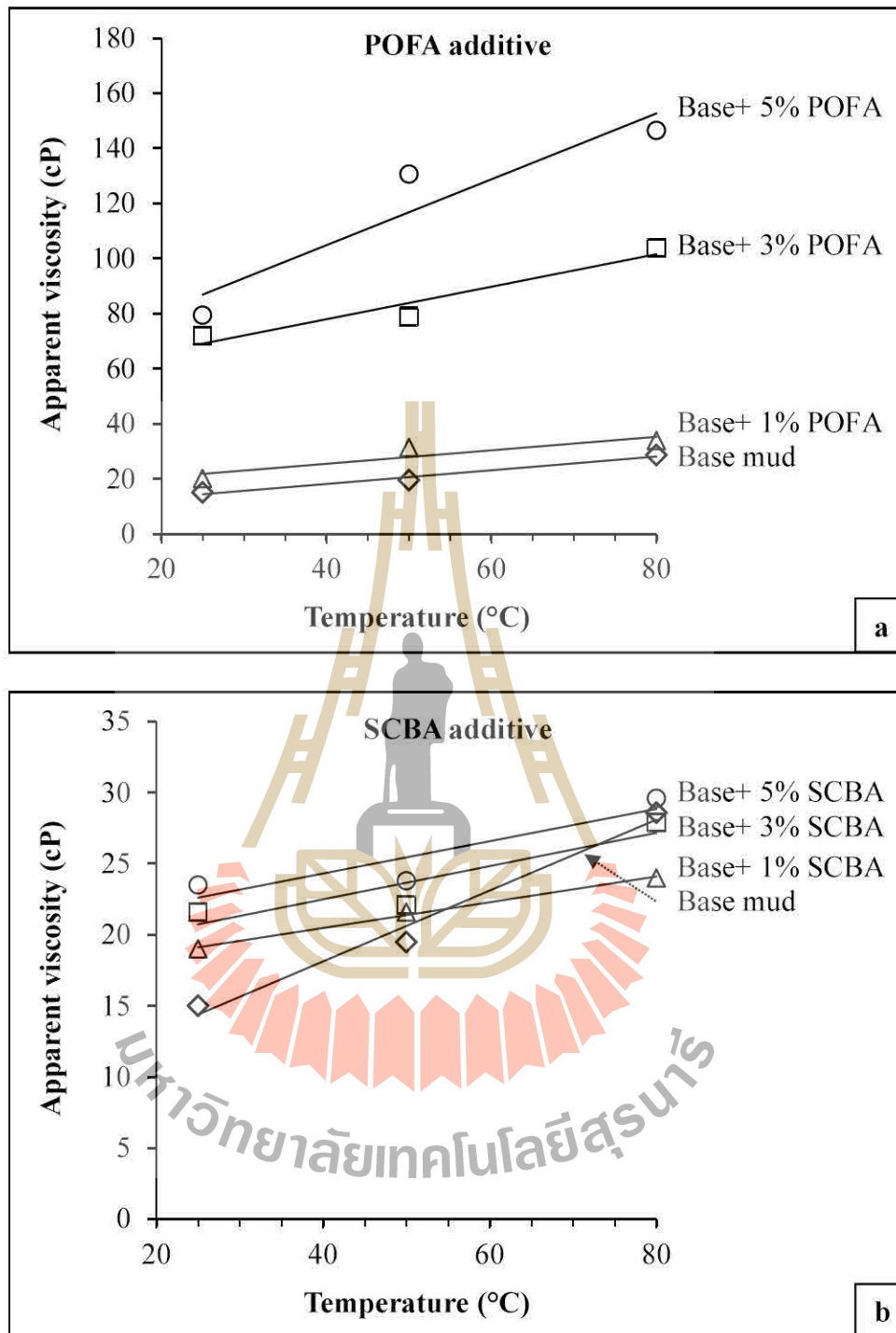


Figure 4.19 Apparent viscosity of base mud mixed with (a) POFA and (b) SCBA versus temperature.

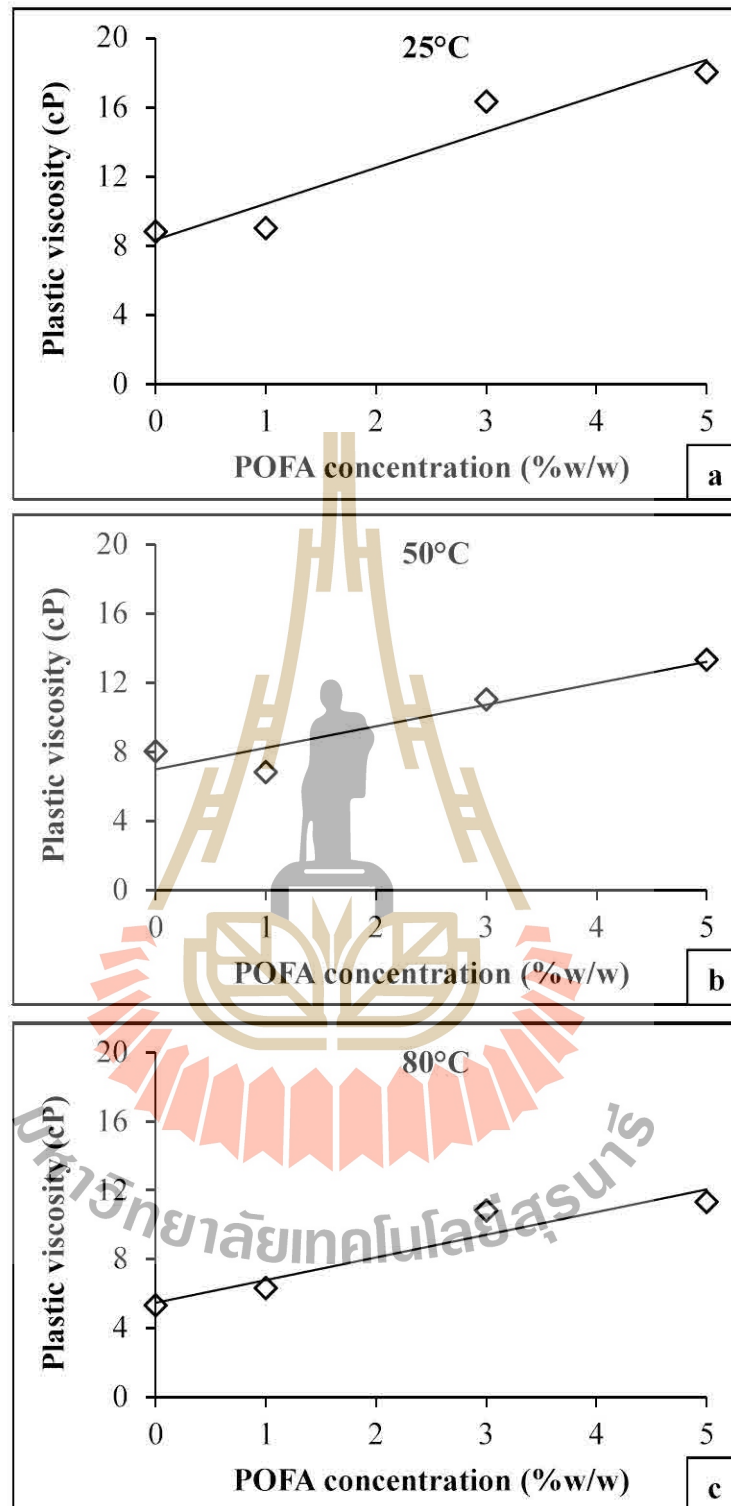


Figure 4.20 Plastic viscosity of drilling mud versus POFA concentration at (a) 25°C, (b) 50°C and (c) 80°C.

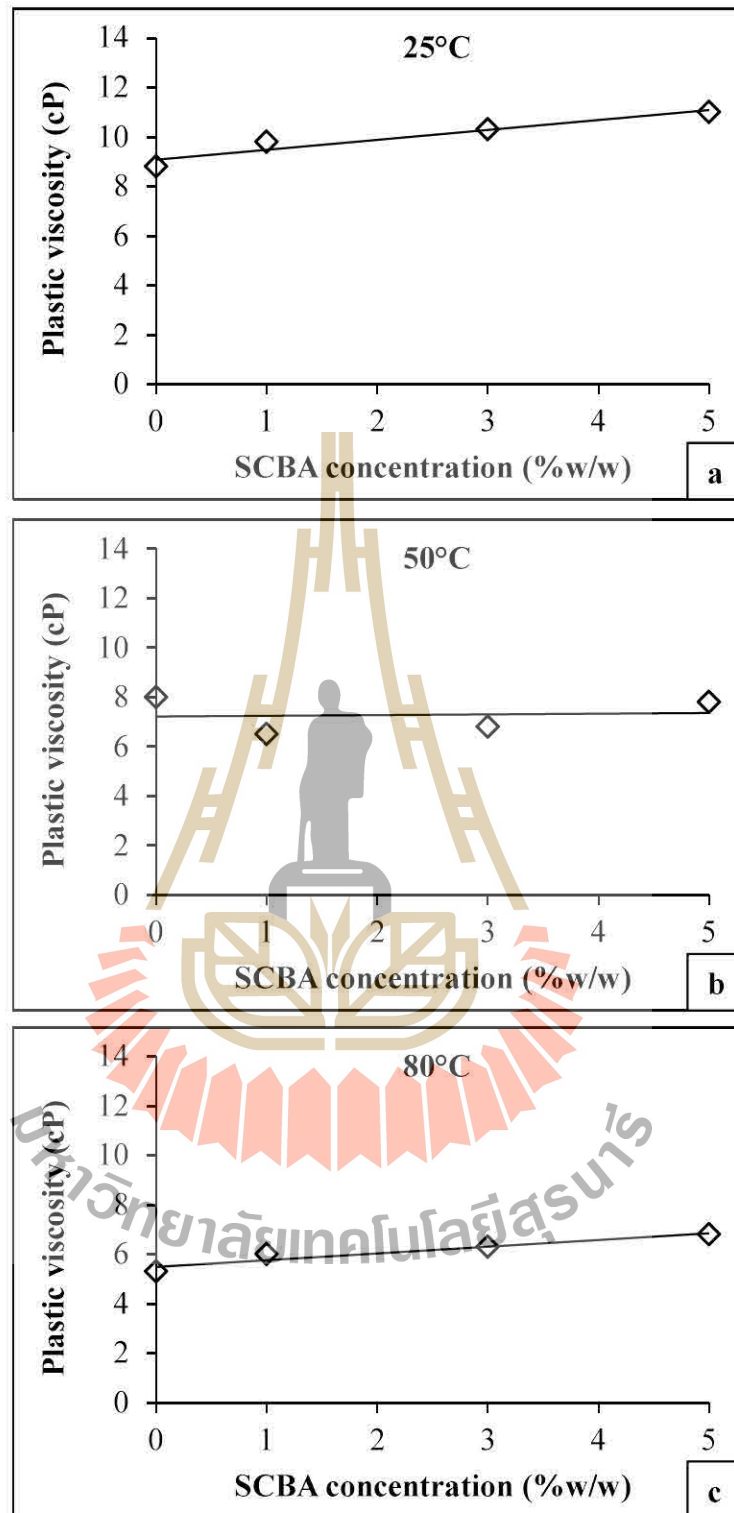


Figure 4.21 Plastic viscosity of drilling mud versus SCBA concentration at (a) 25°C, (b) 50°C and (c) 80°C.

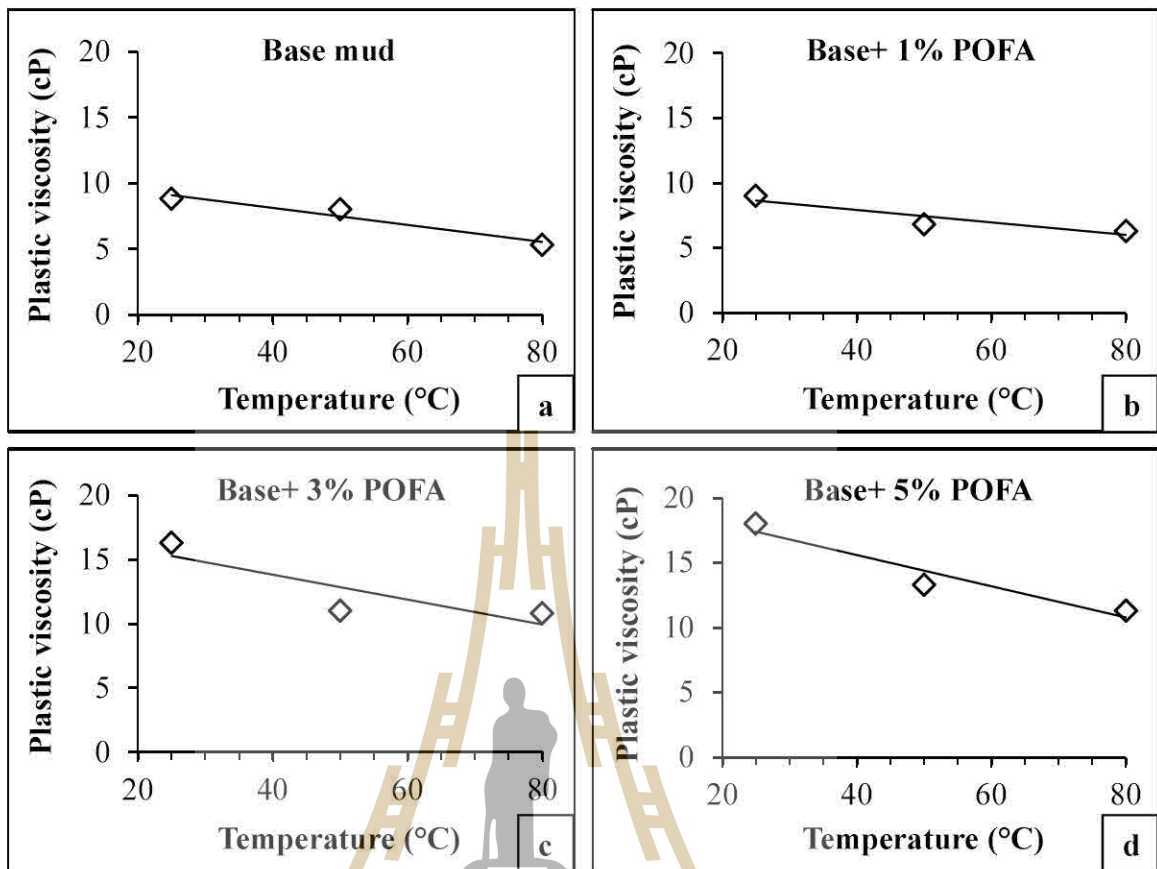


Figure 4.22 Plastic viscosity of base mud mixed with POFA versus temperature;

(a) base mud, (b) base+ 1% POFA, (c) base+ 3% POFA and
(d) base+ 5% POFA.

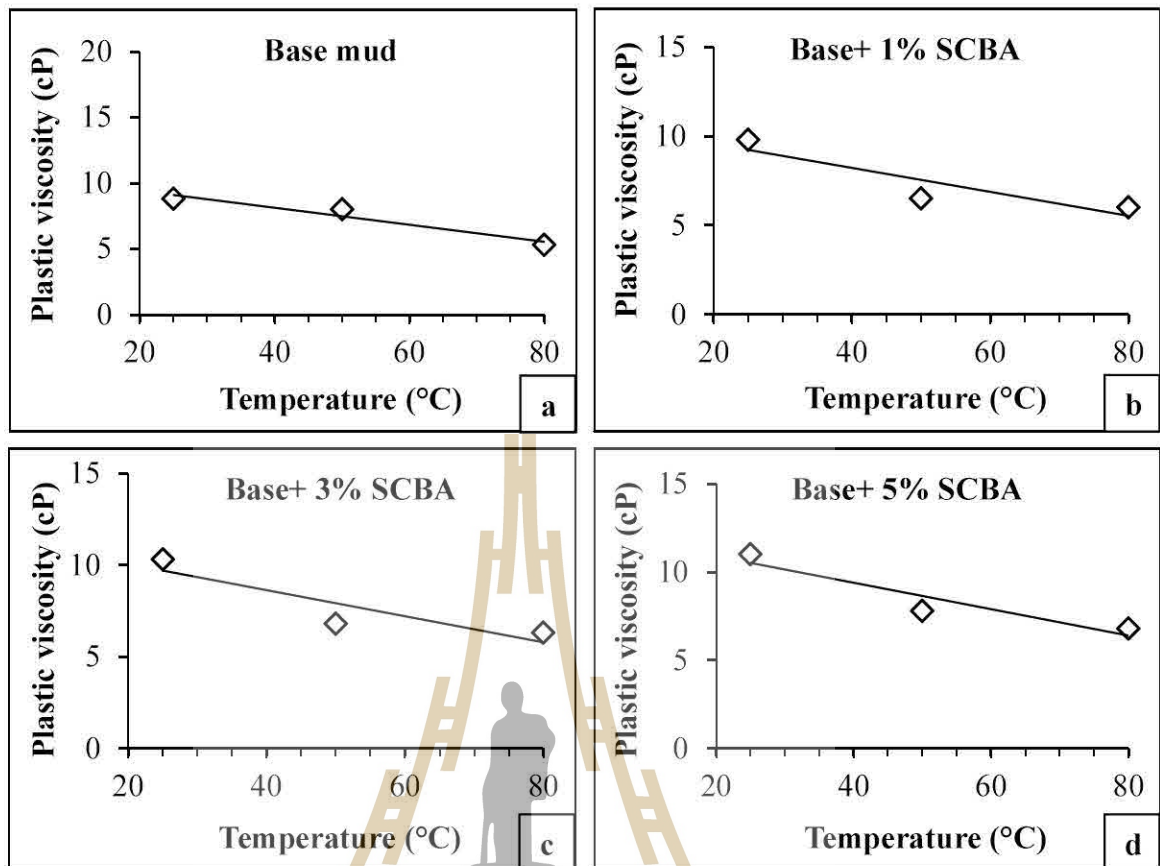


Figure 4.23 Plastic viscosity of base mud mixed with SCBA versus temperature;

(a) base mud, (b) base+ 1% SCBA, (c) base+ 3% SCBA and
(d) base+ 5% SCBA.

The yield point was plotted with the change of POFA and SCBA concentration was shown in Figure 4.24 and 4.25. The result indicates a significant increase in the yield stress as the POFA concentration increase and with the increase of SCBA concentration, the yield stress was showing a tendency to increase. However, the yield stress of POFA concentration was greater than SCBA concentrations at all tested temperature. Attributable a large amount of solid in drilling mud samples has a tendency to agglomerate and result in increasing yield

stress. The change of the yield point in different temperature was shown in Figure 4.26. For all the POFA and SCBA mixed with base mud, the yield stress increased with increasing temperature. The increase of temperature that the interaction energy of clay system that leads bentonite suspension becomes thickened. From the tested, can be summarized that the presence of POFA and SCBA increase yield strength of drilling mud which enhances carrying capacity of drilling mud while drilling circulation periods.

The initial and 10 minutes gel strength of POFA and SCBA containing drilling mud, was plotted as a function of POFA and SCBA concentration and temperature were shown in Figure 4.27 to 4.32. From the tested, It was found that the gel strength was increased with an increasing POFA and SCBA additive concentration and temperature. From Table 4.6, considering POFA and SCBA contain drilling mud in all tested temperatures. The 10 minutes gel strength was greater than the initial gel strength. Because of more undisturbed drilling mud, standing time would lead drilling mud to form a stronger gel structure compared to less undisturbed time. Meanwhile, the initial and 10 minutes gel strength of drilling mud mixed with POFA in all temperatures and concentration, was greater than the SCBA containing drilling mud. From the tested, can be summarized that the presence of POFA and SCBA increase gel strength of drilling mud which enhances hole cleaning efficiency of drilling mud by suspending cutting and weighting material when circulation was ceased.

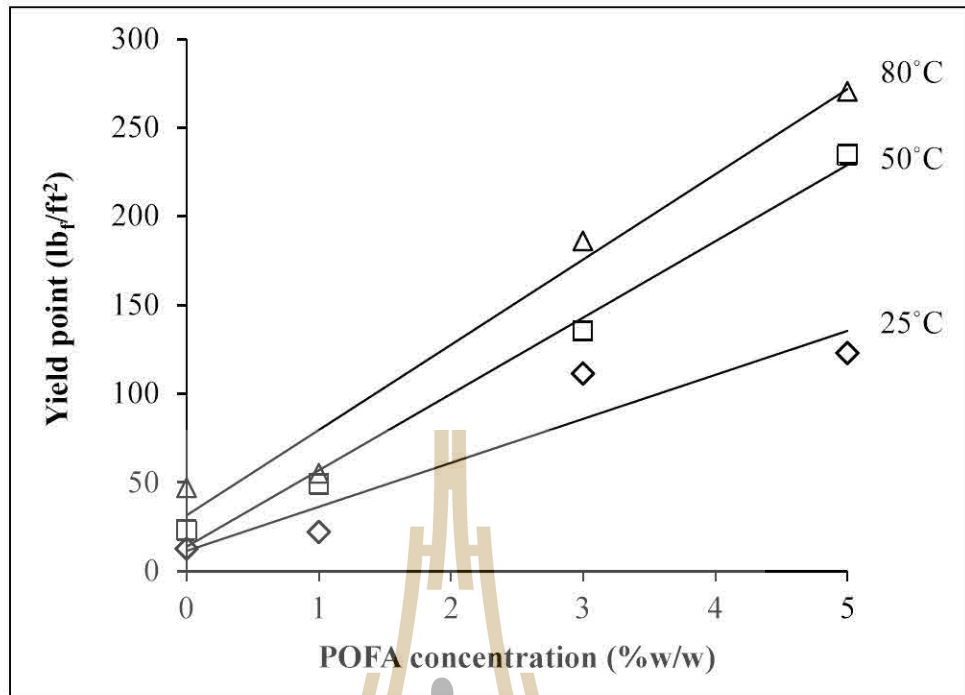


Figure 4.24 Yield point of drilling mud versus POFA concentration.

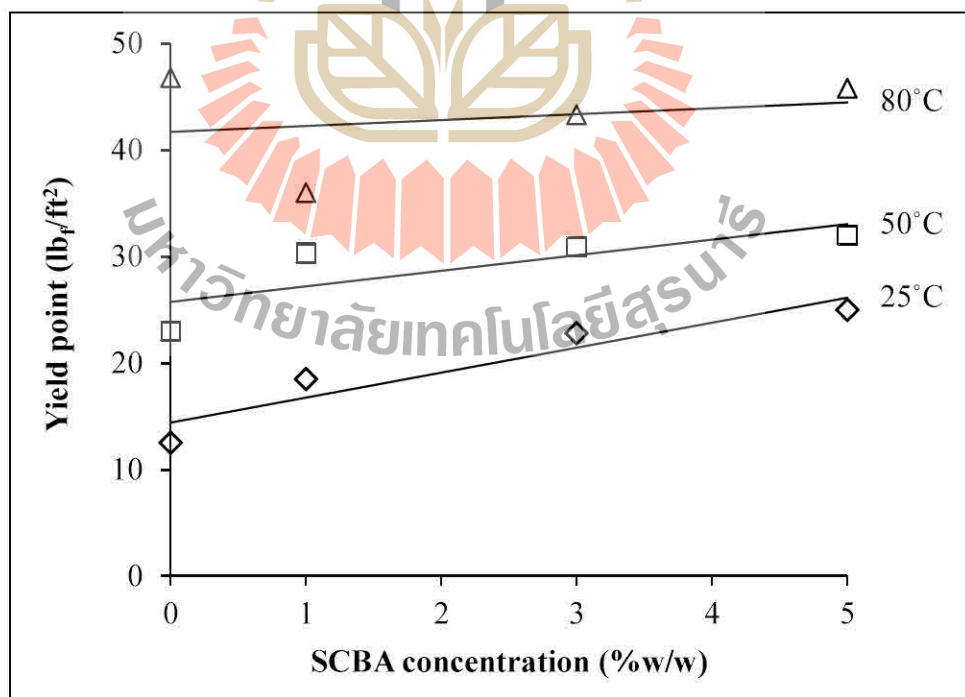


Figure 4.25 Yield point of drilling mud versus SCBA concentration.

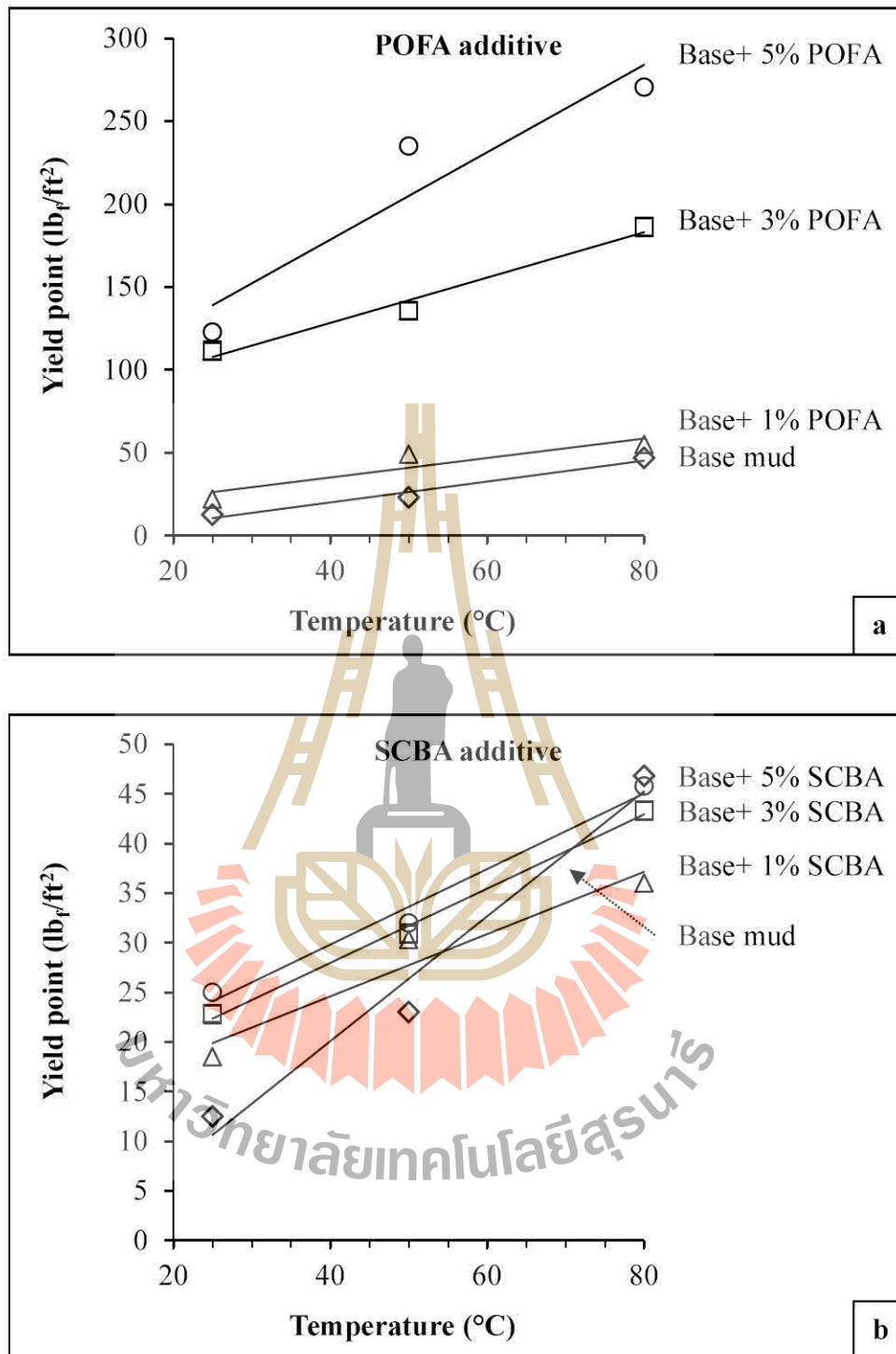


Figure 4.26 Yield point of base mud mixed with (a) POFA and (b) SCBA versus temperature.

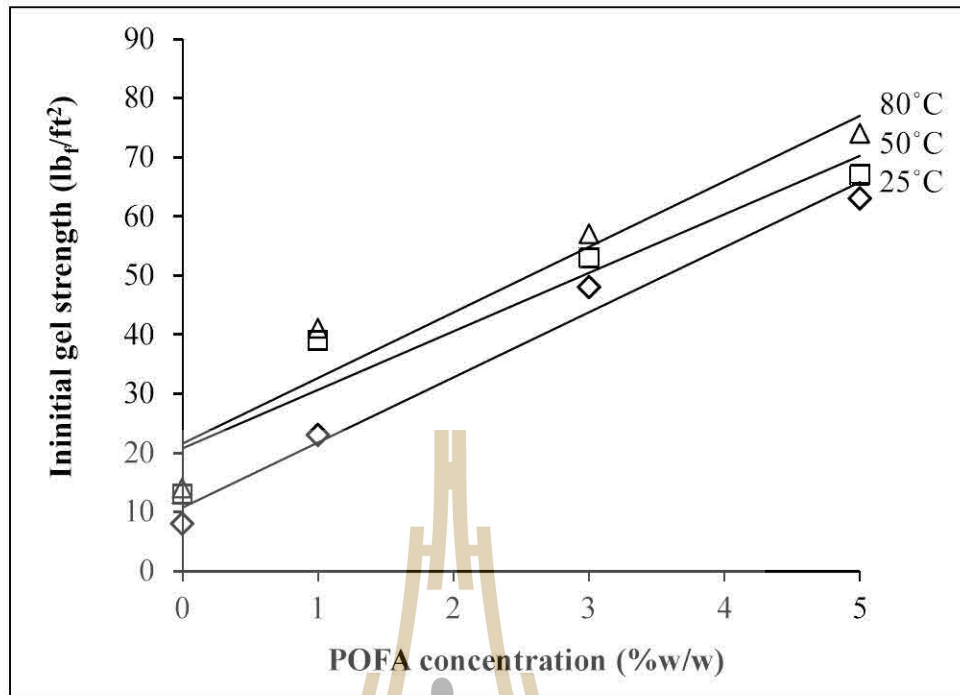


Figure 4.27 Initial gel strength of drilling mud versus POFA concentration.

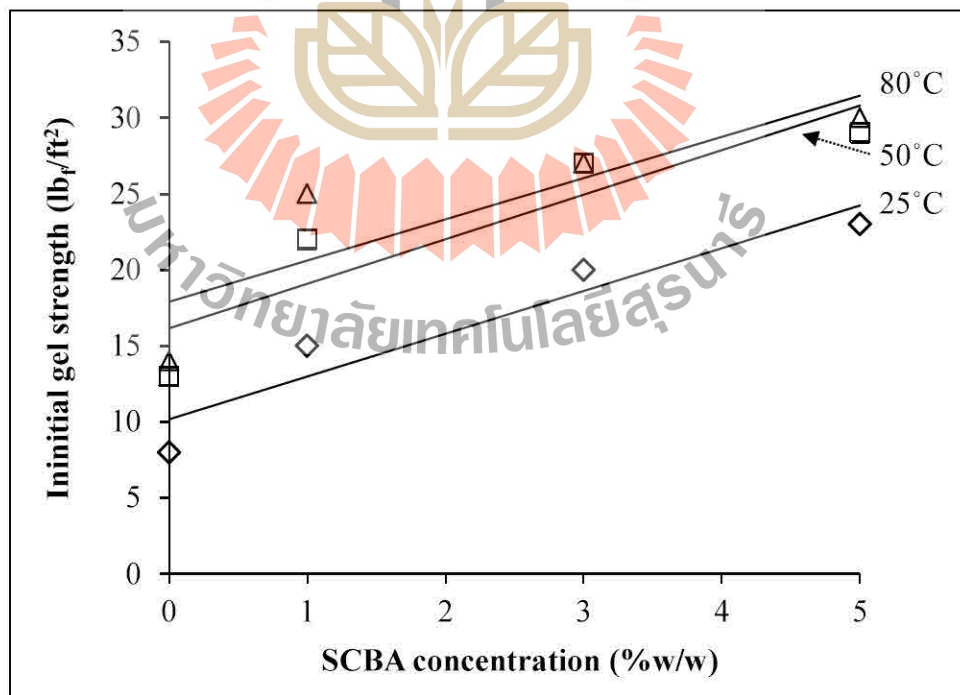


Figure 4.28 Initial gel strength of drilling mud versus SCBA concentration.

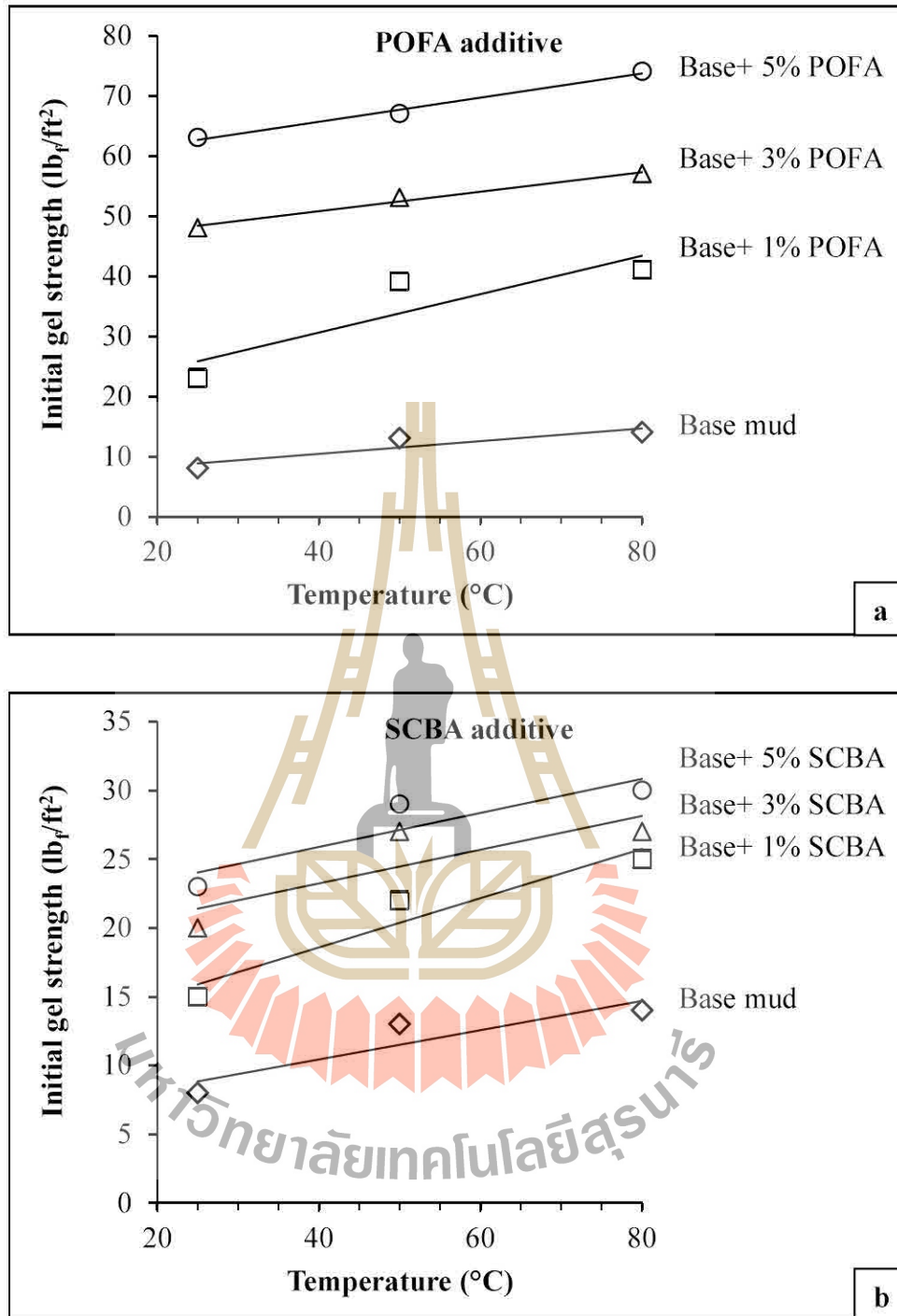


Figure 4.29 Initial gel strength of base mud mixed with (a) POFA and (b) SCBA versus temperature.

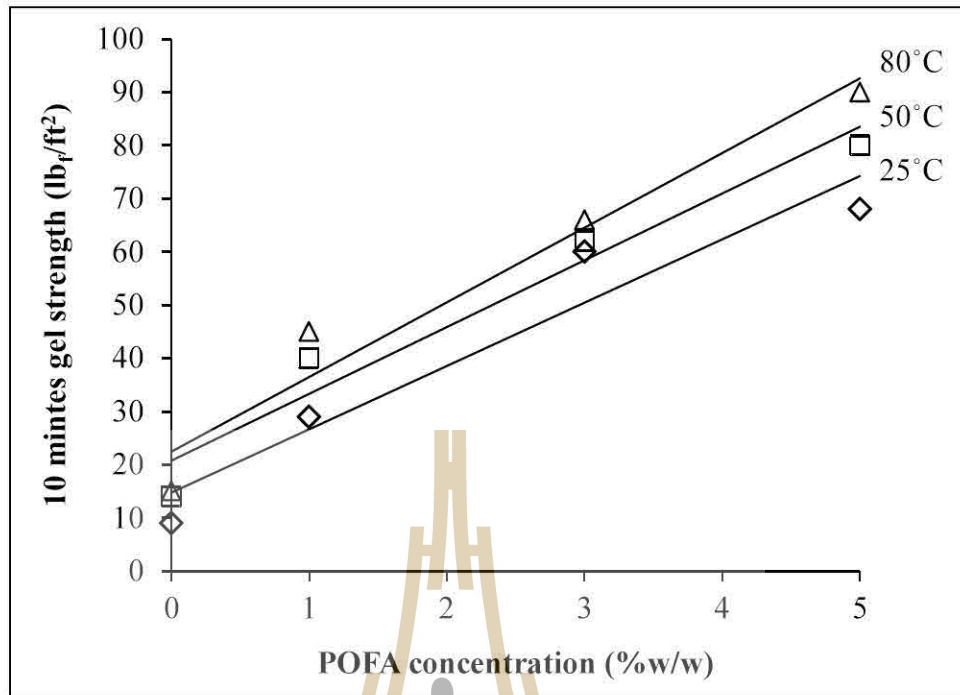


Figure 4.30 10 minutes gel strength of drilling mud versus POFA concentration.

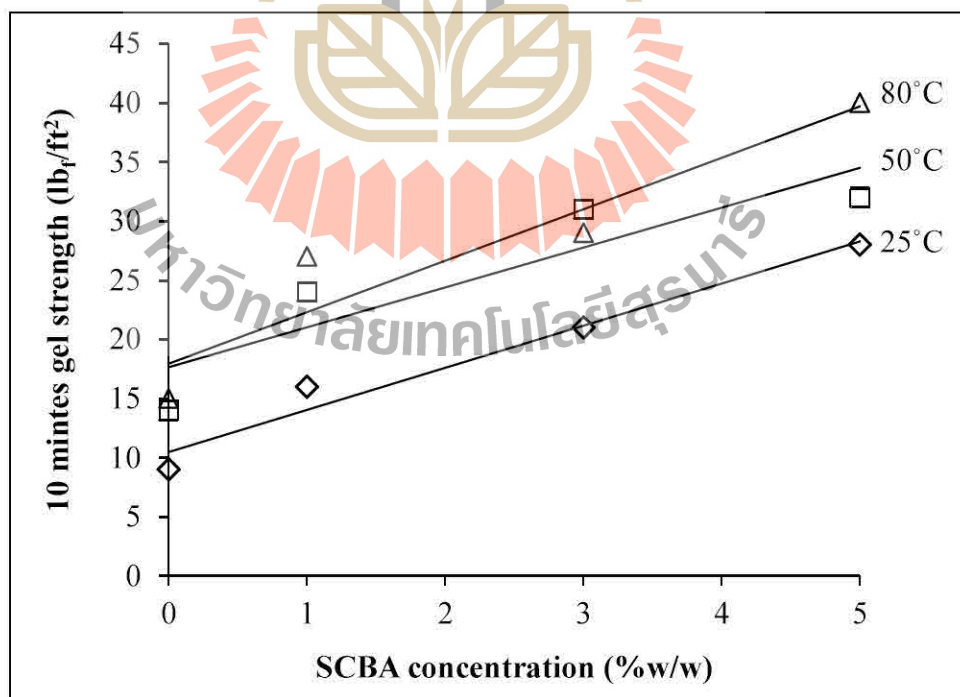


Figure 4.31 10 minutes gel strength of drilling mud versus SCBA concentration.

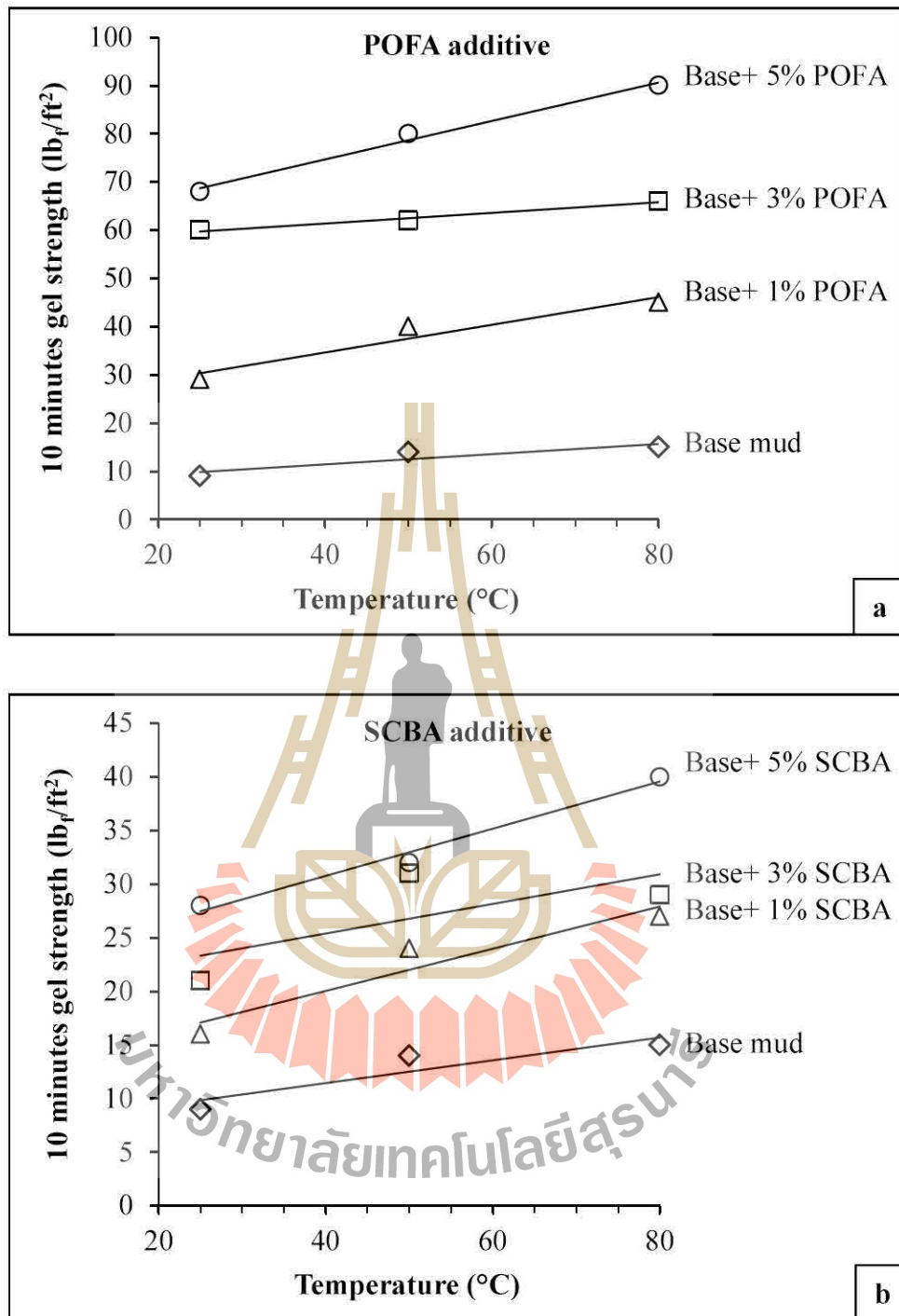


Figure 4.32 10 minutes gel strength of base mud mixed with (a) POFA and (b) SCBA versus temperature.

4.3.4 Filtration properties

The average API static filtrate loss within 30 minutes of base mud and base mud mixed with POFA and SCBA additives, the filtration properties and mud filter cake thickness data of the test was shown in Appendix A.

Figure 4.33 was the plot of filtration properties of base mud, was measured at 25, 50 and 80°C. Figure 4.34 to 4.39 was the plot of the filtration properties of base mud mixed with POFA and SCBA. These of graphs show time-dependent filtration behavior of drilling mud and physical examination of the filtrate volume indicates that filtrate volume increases as the time increase. The decreasing in filtration volume has resulted from continuous mud filter cake deposition and compaction until the formation of a constant thickness and stable mud filter cake had been formed completely.

The result of API static filtrate shows a significant increase in the static filtration volume of base mud samples as the temperature increasing (Figure 4.33). Because to adverse temperature effects on filtration that result in fluid phase viscosity decreasing and a colloidal fraction tends to flocculate which consequences of mud filter cake permeability increasing.

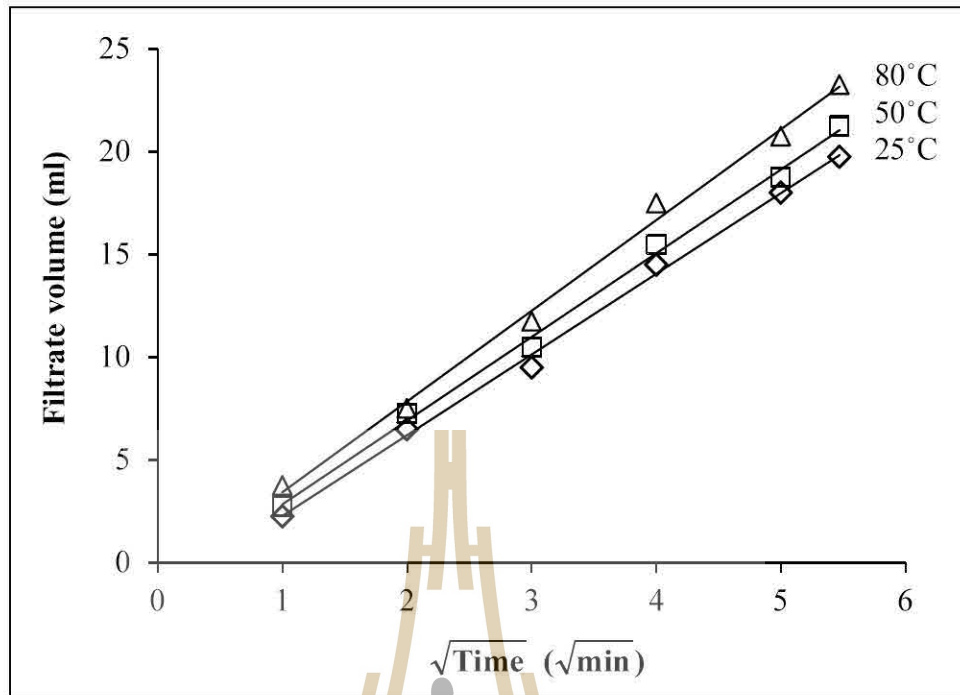


Figure 4.33 Static filtration and time of base mud.

Figure 4.34 to 4.36 was shown the effect of POFA concentration of the filtration properties at 25, 50 and 80°C. The static filtration curves indicate that at 1, 3 and 5%w/w of POFA concentration at all tested temperature, shown increasing of filtrate volume loss rate comparison with base mud. Because POFA particle not even have a porous texture and rough particle distributed on the surfaces affect and engender to small pores between particle. Also, it was observed that when the concentration of chloride increases in the drilling mud samples the fluid loss into the formation increases (Sami, 2016). From X-ray Fluorometer analysis revealed that POFA contains a chloride about 7.911%, this results in an increased of filtration loss. Thus, the POFA containing drilling mud has increased filtration loss.

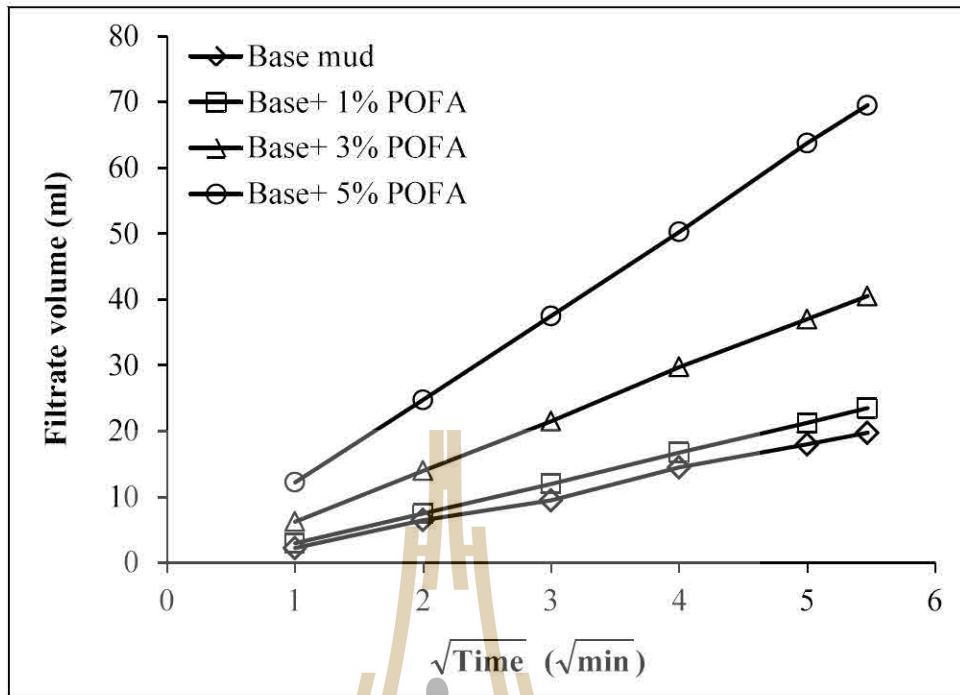


Figure 4.34 Static filtration of base mud mixed with POFA versus time at 25°C.

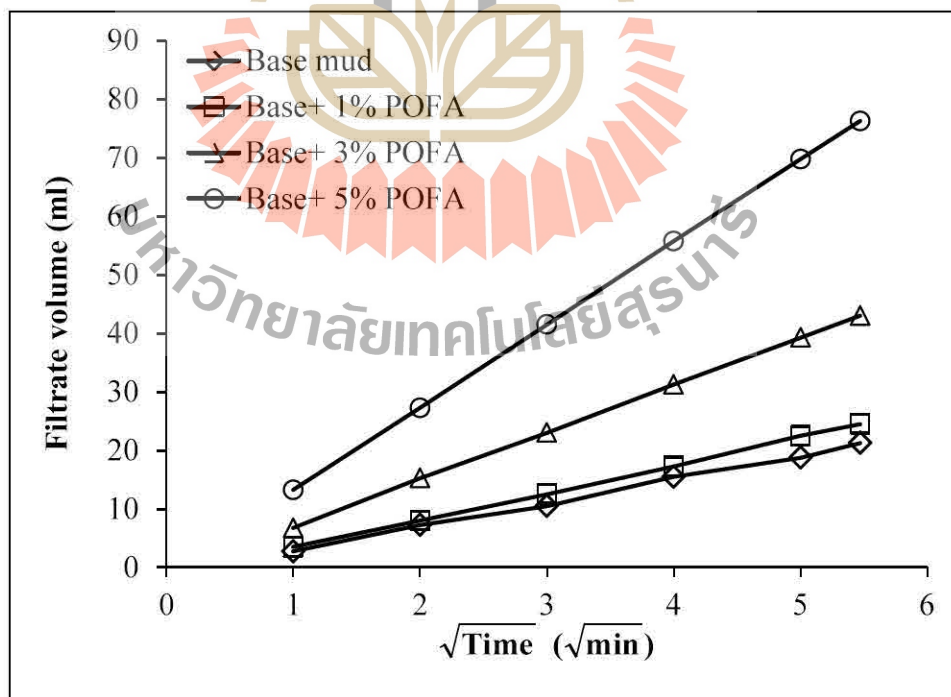


Figure 4.35 Static filtration of base mud mixed with POFA versus time at 50°C.

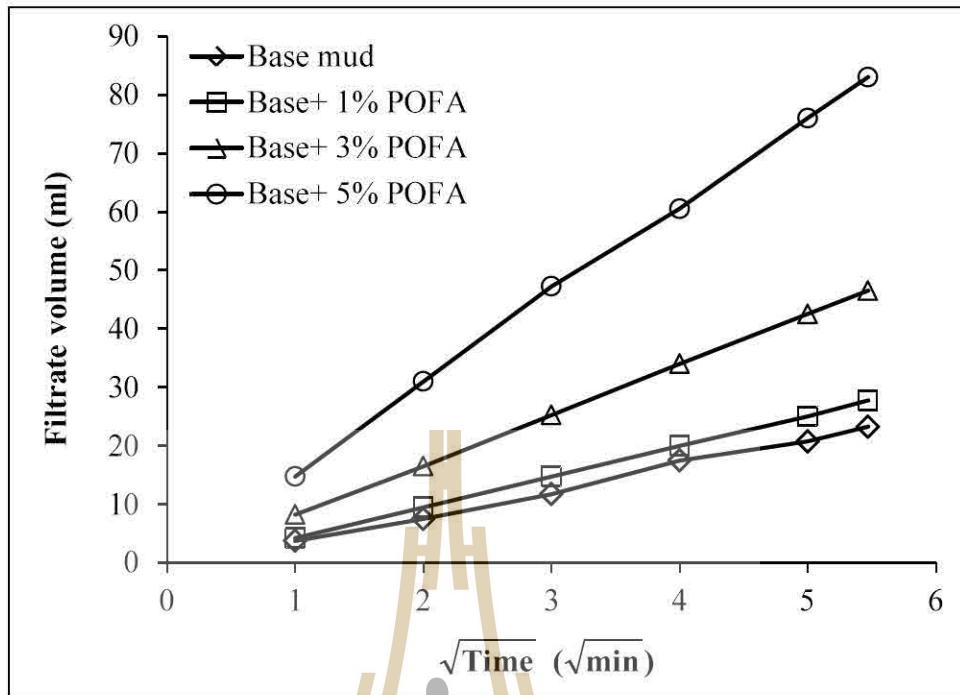


Figure 4.36 Static filtration of base mud mixed with POFA versus time at 80°C.

Figure 4.37 to 4.39 was shown the effect of SCBA concentration of the filtration properties at 25, 50 and 80°C. Comparison of 1, 3 and 5 the percentage of SCBA concentration at all temperatures, which produced the least filtrate volume, demonstrated better filtration control characteristics than base mud. Because, from FE-SEM image, Figure 4.64 the mud filter cake formed by base mud was of a poor, causing to form a high permeability mud filter cake. From Figure 4.68 shows the mud filter cake formed by base mud with SCBA additives are distributed of particles SCBA into pores of mud filter cakes in tight connection. It represents that adding a quantity particle SCBA reacts more effectively with base mud to result in seal a porous layer, lower filtration loss and prevents the filtrate in the drilling mud leaking to the formation.

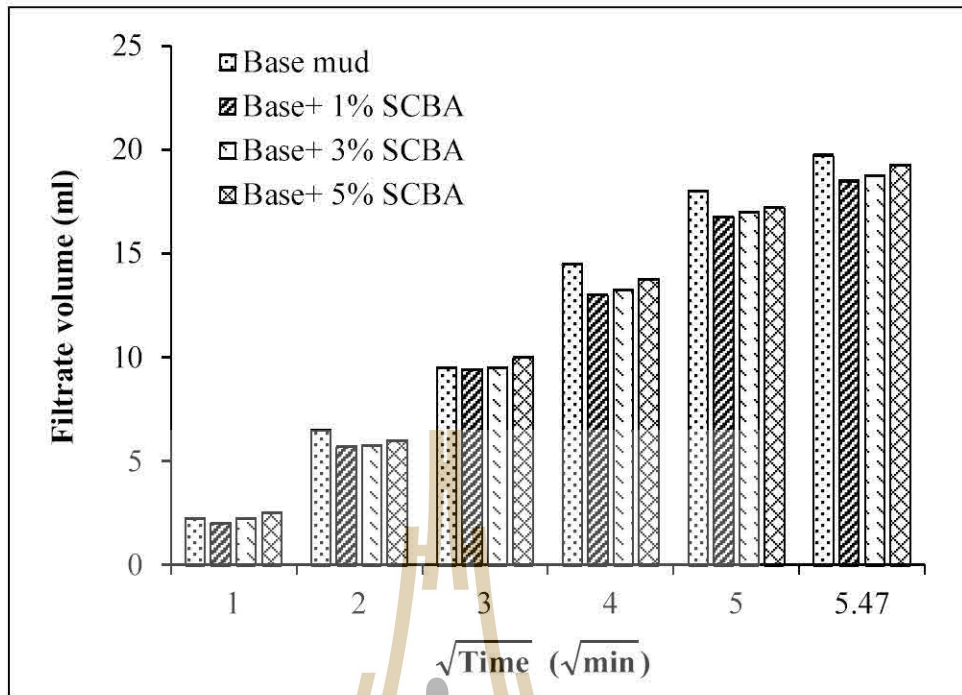


Figure 4.37 Static filtration of base mud mixed with SCBA versus time at 25°C.

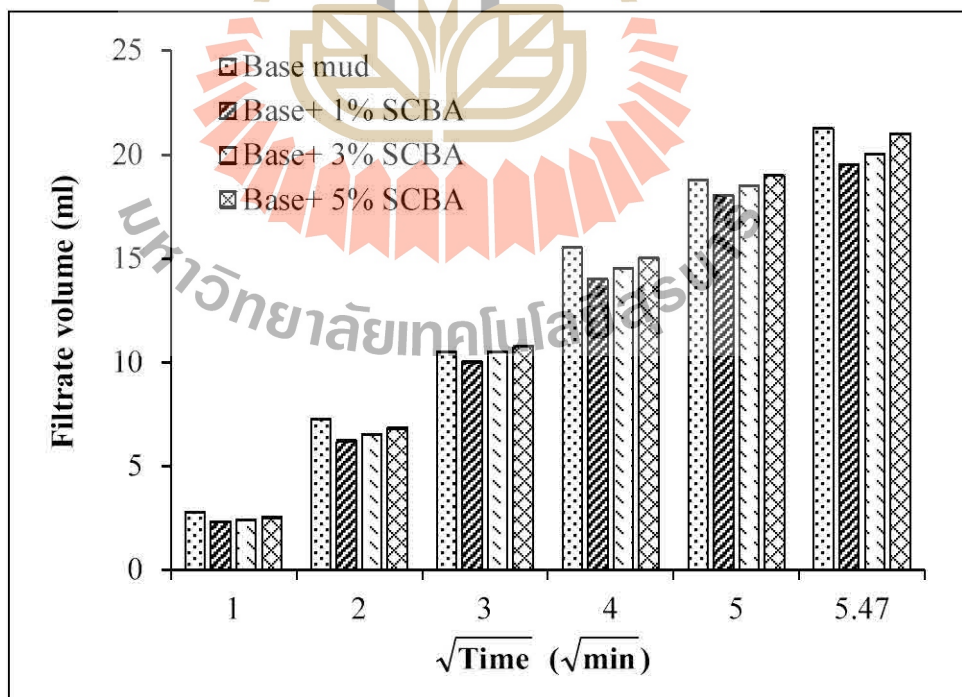


Figure 4.38 Static filtration of base mud mixed with SCBA versus time at 50°C.

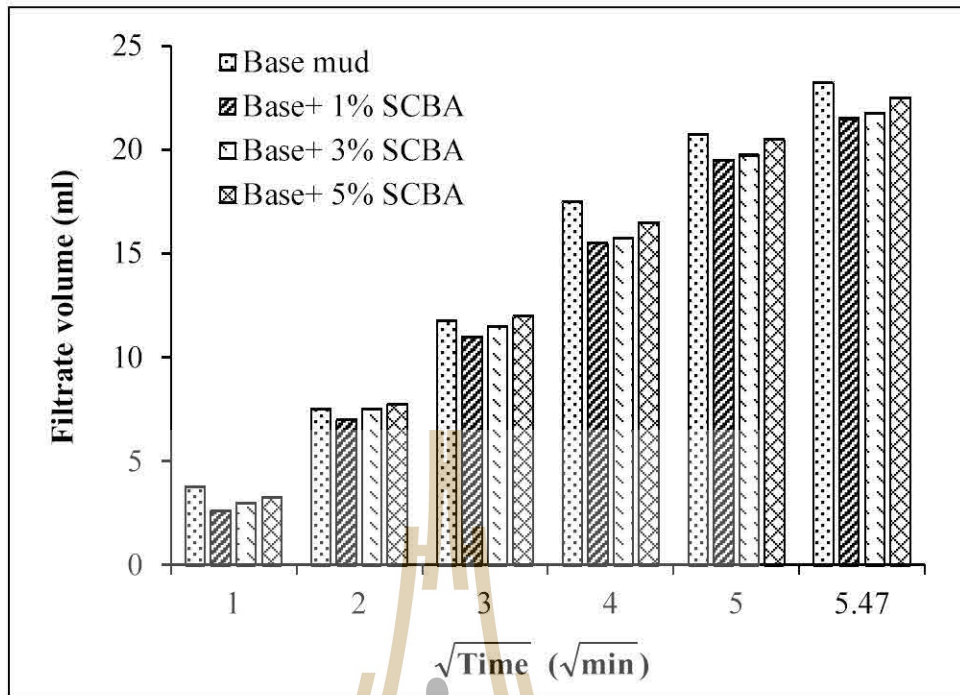


Figure 4.39 Static filtration of base mud mixed with SCBA versus time at 80°C.

Figure 4.40 and Figure 4.41 represents 30 minutes static filtrate volume loss values of base mud mixed POFA and SCBA. Physical examination of the filtrate volume indicates that filtrate volume increases as the additive concentration and temperature increase. The SCBA have proved to possess good filtration control properties which were major responsible for the minimal filtrate volume produced was base mud mixed with 1%w/w of SCBA can reduce the filtrate volume loss about 6 to 8%, but increasing the concentration of SCBA to 3 and 5%w/w did not result in better filtration characteristics. In the range of testing temperature from 25 to 80°C, there is no sign of temperature degradation of SCBA additive in drilling mud. Thus, The SCBA can be used mixed with drilling mud could be performed under this temperature range.

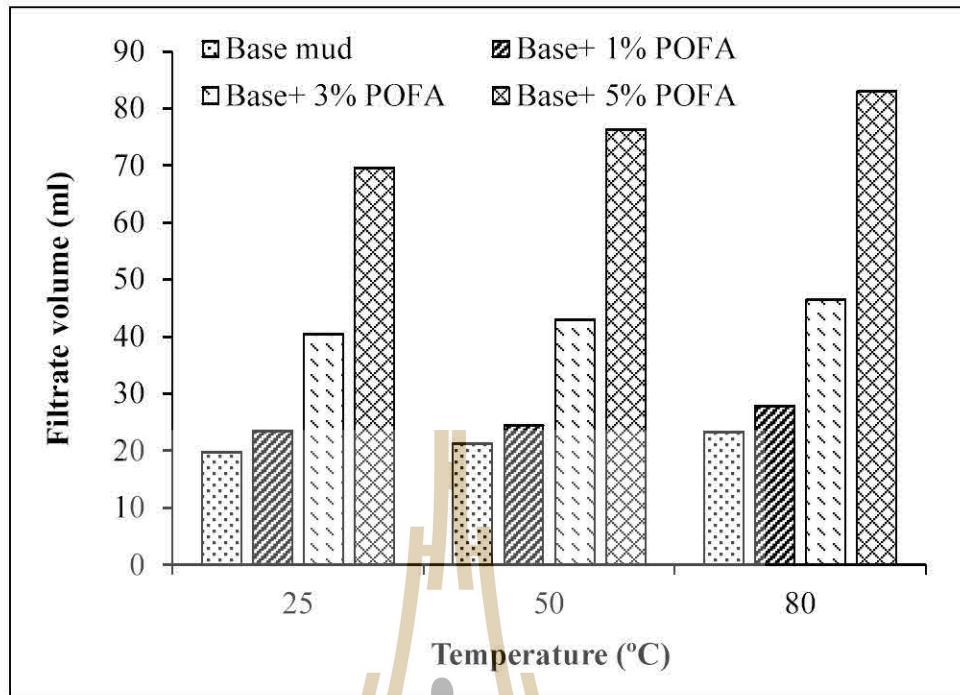


Figure 4.40 API filtrate volume at 30 minutes of base mud mixed with POFA.

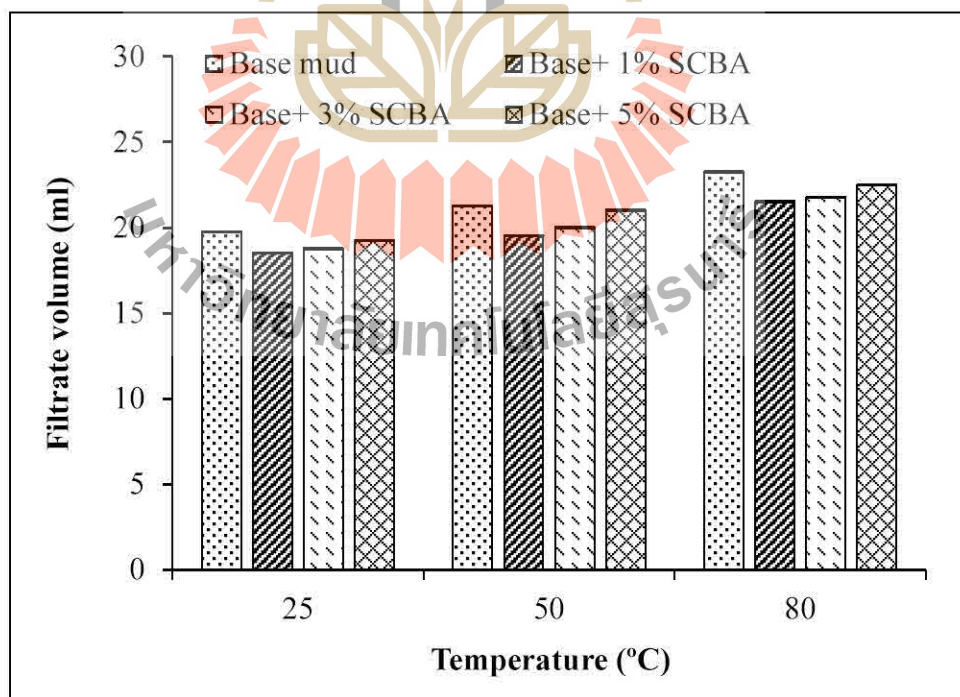


Figure 4.41 API filtrate volume at 30 minutes of base mud mixed with SCBA.

Figure 4.42 and Figure 4.43 shown mud filter cake thickness of the base mud mixed with these additives. The histograms show the thicker mud filter as the POFA and SCBA concentration and temperature increase. The qualities of mud filter cake deposited by mixed the additives containing mud were inspected. The slickness and toughness of POFA containing drilling mud were more than base mud and indicates the presence of mud filter cake stability and lubricity, but the SCBA was less than base mud. A good mud filter cake helps stabilize the wall of the hole, helping in reducing the formation damage and will reduce mud filtrate loss into the formation. This reduces the interstitial clays swelling and can cause permeability reductions (Azar and Samuel, 2007).

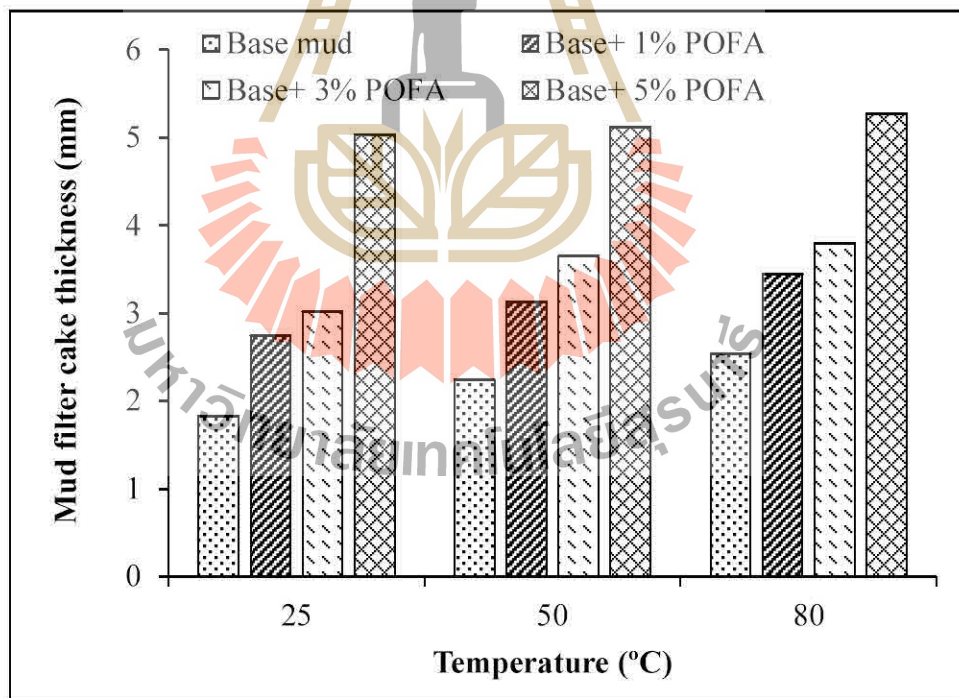


Figure 4.42 Mud filter cake of base mud mixed with POFA versus temperature.

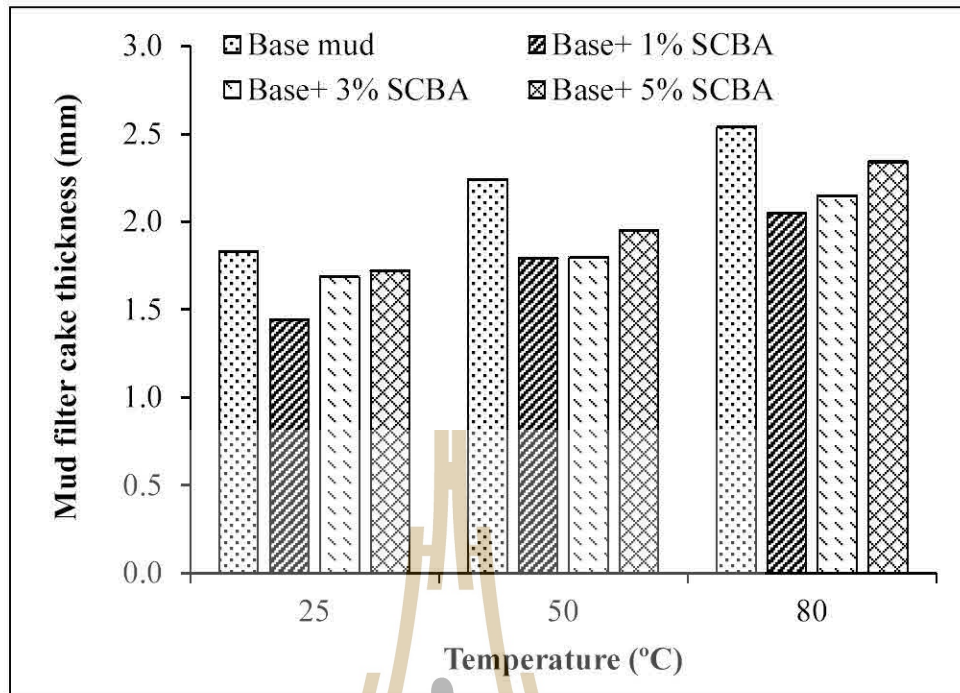


Figure 4.43 Mud filter cake of base mud mixed with SCBA versus temperature.

4.3.5 Hydrogen ion concentration properties

A data of the tested results of the hydrogen ion (pH) of drilling mud before and after mixed with POFA and SCBA additives in 25, 50 and 80°C are shown in Appendix A. The data of tested were averaged and plotted in Figure 4.44 to 4.50.

A pH was important because it affects the solubility of the organic thinners, contaminant removal, corrosion mitigation and the dispersion of clays presents in the drilling mud. Except for salt mud, the pH of drilling mud was seldom below 7. Generally, the pH of drilling mud falls between 8 and 11, depends on the type of drilling mud in use and the nature of the formation being drilled (Azar and Samuel, 2007). In the tested, the POFA and SCBA additives in drilling mud have a pH range of 10.11 to 10.74 (it's revealed that all drilling mud was in a very strongly

alkaline state, pH more than 9). The result indicated that the pH was slightly decreased as the POFA and SCBA concentration increased. However, the pH decreased as the effect of temperature increased. The pH of the drilling mud was more than the mud filtrate in all experiments tested and the pH of base mud mixed with these additives and mud filtrate was found to be higher than that of the base mud. Because POFA and SCBA (plant ash) were the powdery residues that remain after plants are burned; chemically the ash was alkaline (pH more than 10). In its natural state, plant ash can be applied as an amendment to acidic soils and as a substitute for limestone fertilizer (Johnson, 2011). Thus, the alkalinity of POFA and SCBA containing mud can minimize the corrosion problem of steel tubular and solids control devices.

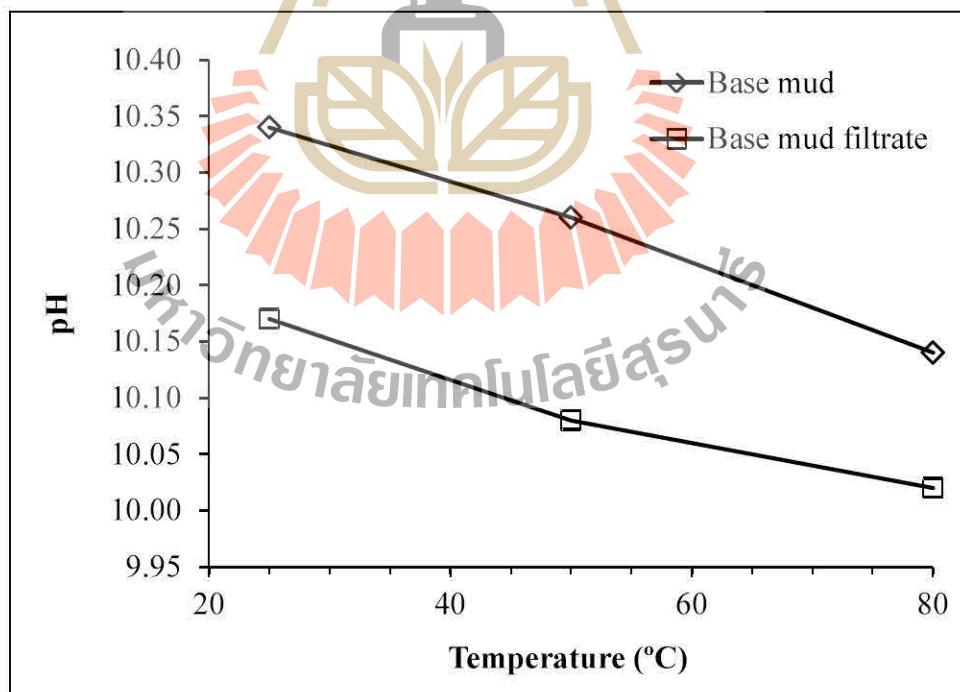


Figure 4.44 pH of base mud versus temperature.

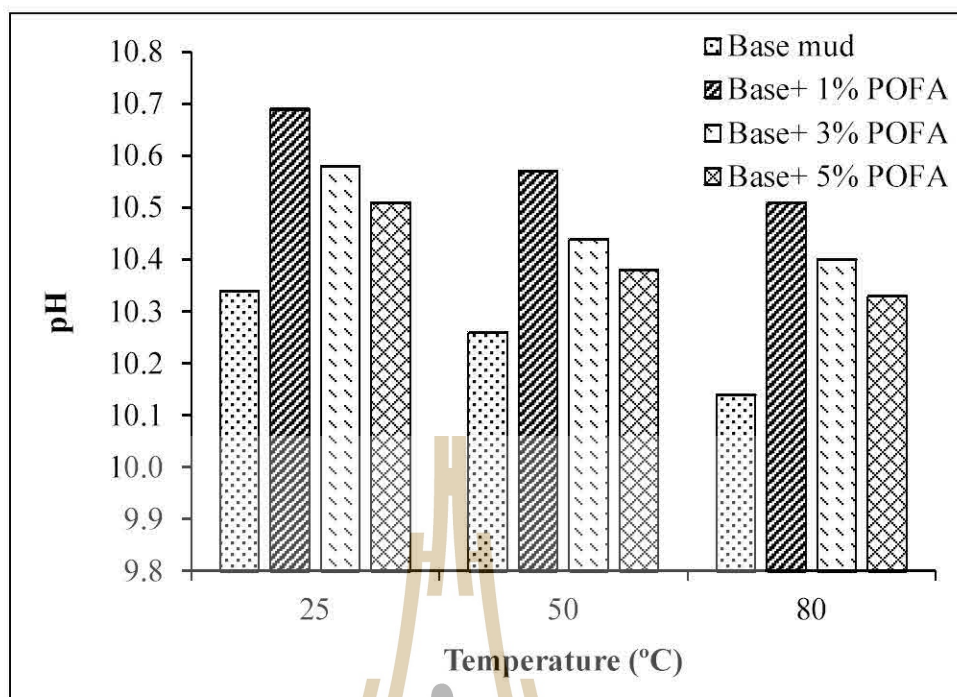


Figure 4.45 pH of base mud mixed with POFA versus temperature.

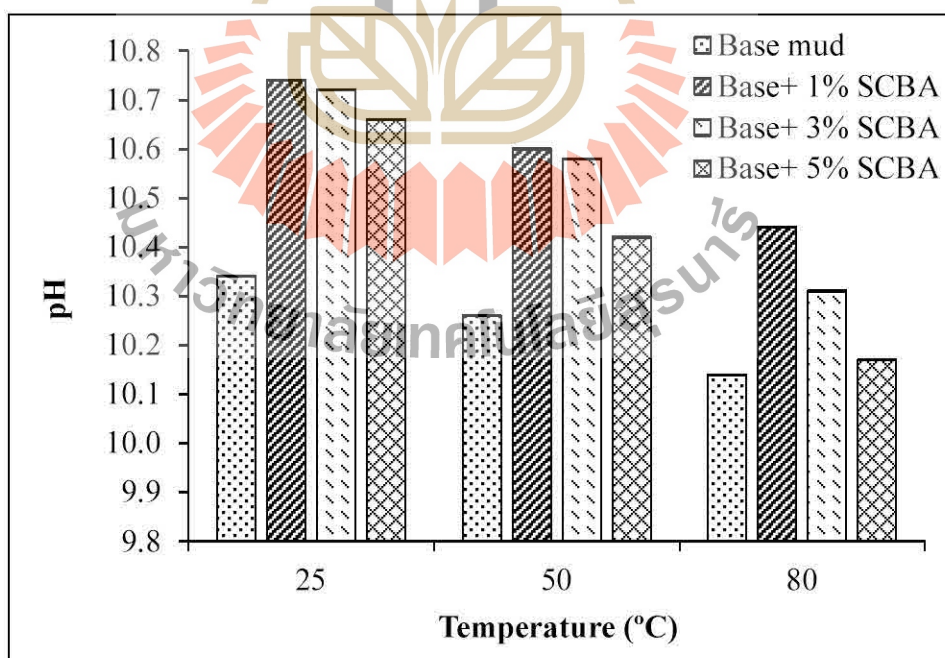


Figure 4.46 pH of base mud mixed with SCBA versus temperature.

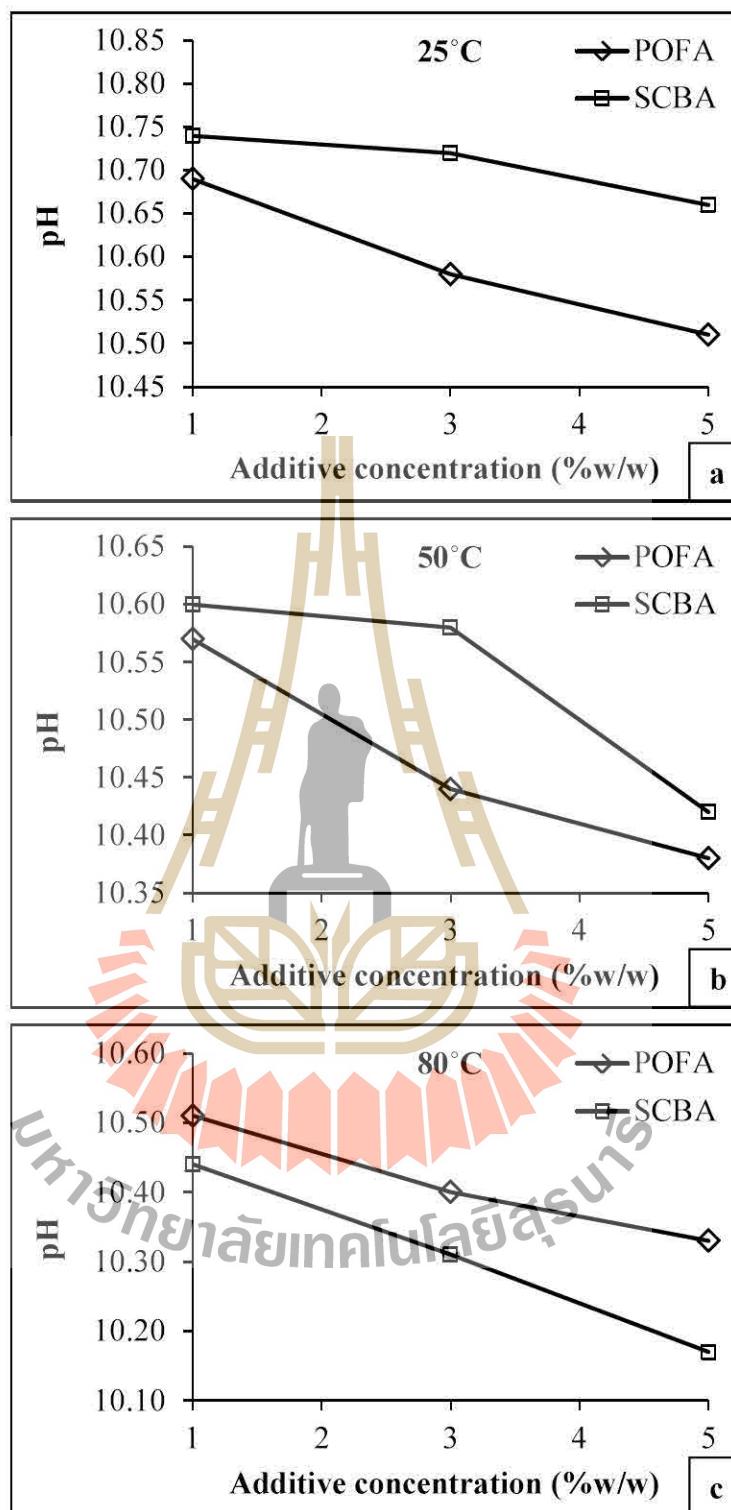


Figure 4.47 pH of drilling mud versus additive concentration at (a) 25°C, (b) 50°C and (c) 80°C.

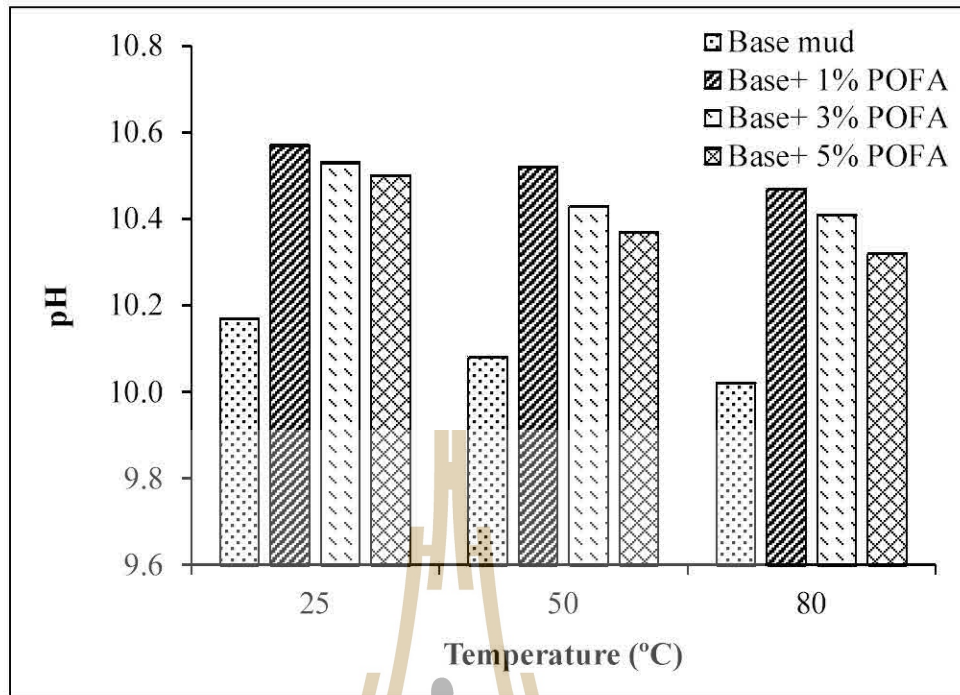


Figure 4.48 pH of mud filtrate of base mud mixed with POFA versus temperature.

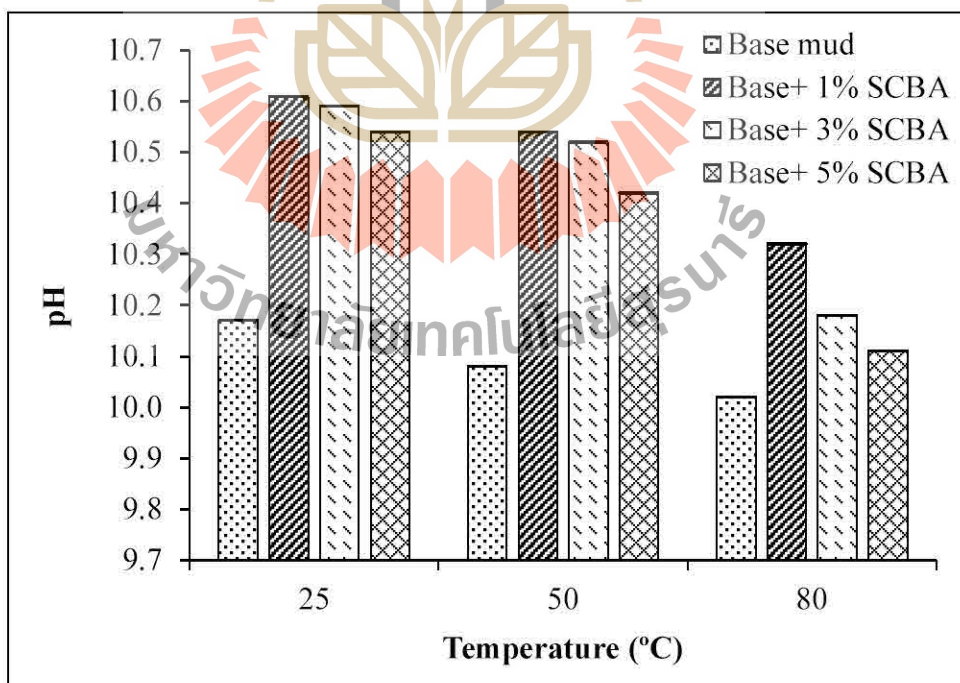


Figure 4.49 pH of mud filtrate of base mud mixed with SCBA versus temperature.

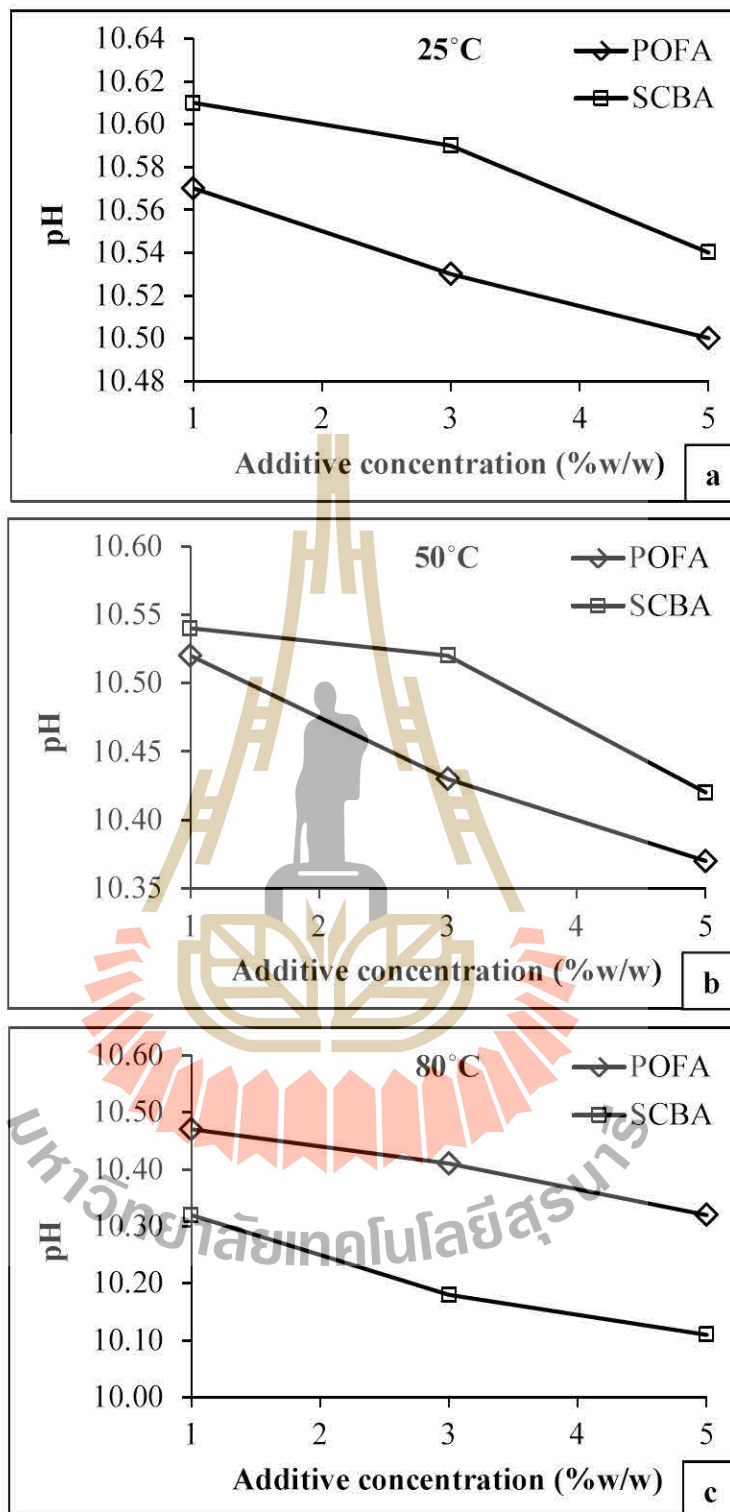


Figure 4.50 pH of mud filtrate versus additive concentration at (a) 25°C, (b) 50°C and (c) 80°C.

4.3.6 Resistivity properties

The results of resistivity are presented in Figure 4.51 to 4.60. Increasing the POFA content from 1 to 5%w/w in three temperatures tested, reduced the resistivity of drilling mud by about 50 percent. Meanwhile, the resistivity of SCBA containing mud decreased by about 8 percent when the temperature was increased from 25 to 80°C at 1, 3 and 5%w/w of additive concentration. This is a clear indication of the resistivity of drilling mud, mud filtrate and mud filter cake decreased as the additive concentration and temperature increased. The resistivity of mud filtrate was more than the drilling mud and mud filter cake, respectively. However, after mixed with POFA additives, it can be implied that the resistivity of drilling mud, mud filtrate and mud filter cake tended to become less than base mud and SCBA additive slightly decreased after SCBA containing mud. This is because chloride effects, the change in the resistivity of the drilling mud has decreased as the chloride content increased (Raheem and Vipulanandan, 2014). From the X-ray Fluorometer analysis revealed that POFA contains a chloride about 7.911%. Therefore, results in a decrease in the resistivity of the base mud mixed with POFA. Thus, it is necessary to control the resistivity of the drilling mud and mud filtrate while drilling may be desirable to permit enhanced evaluation of the formation characteristics from electric logs (Lyons et al., 2016).

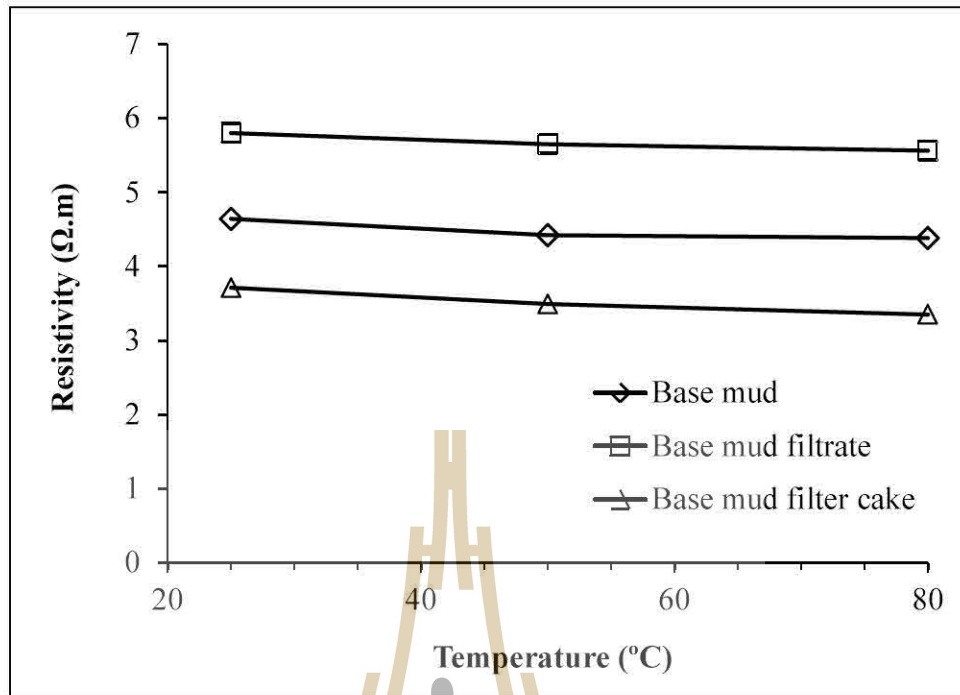


Figure 4.51 Resistivity of base mud versus temperature.

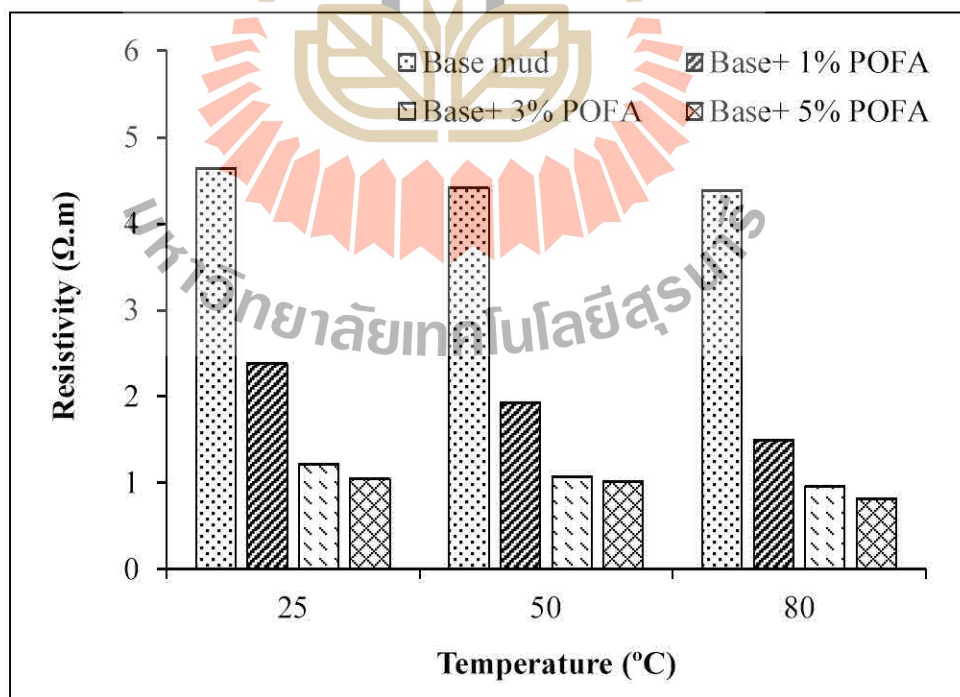


Figure 4.52 Resistivity of base mud mixed with POFA versus temperature.

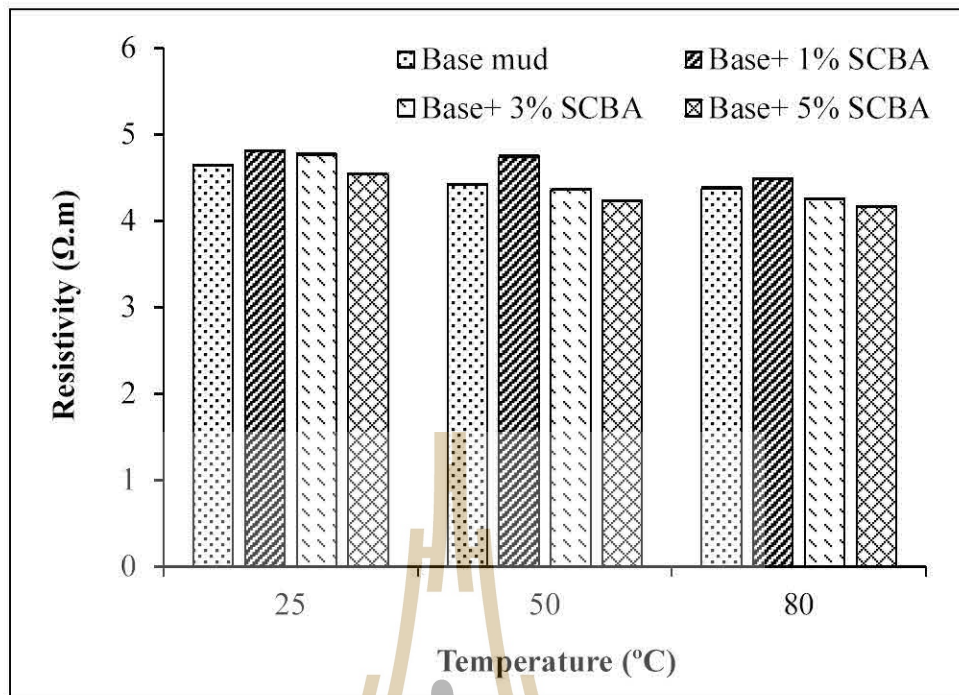


Figure 4.53 Resistivity of base mud mixed with SCBA versus temperature.



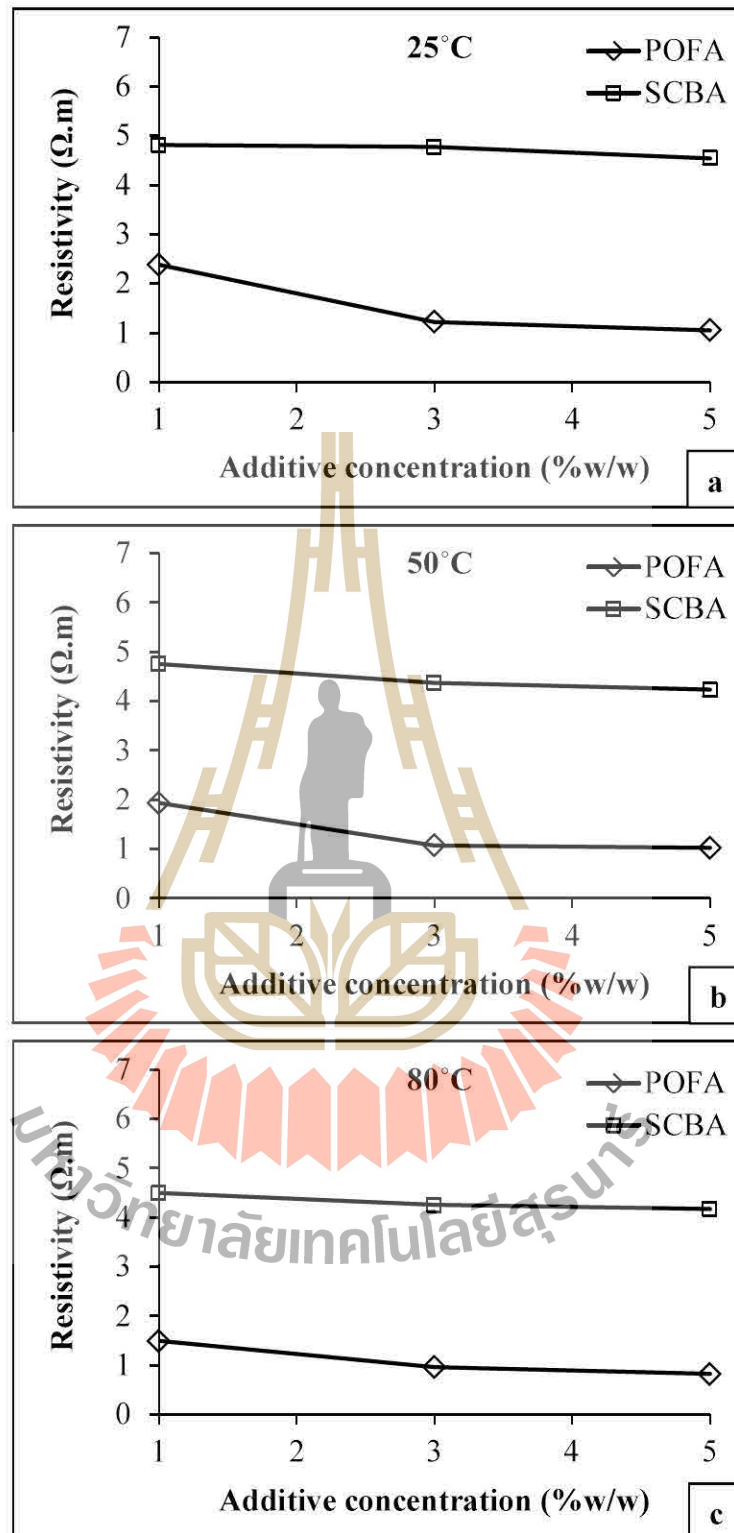


Figure 4.54 Resistivity of drilling mud versus additive concentration at (a) 25 $^{\circ}C$, (b) 50 $^{\circ}C$ and (c) 80 $^{\circ}C$.

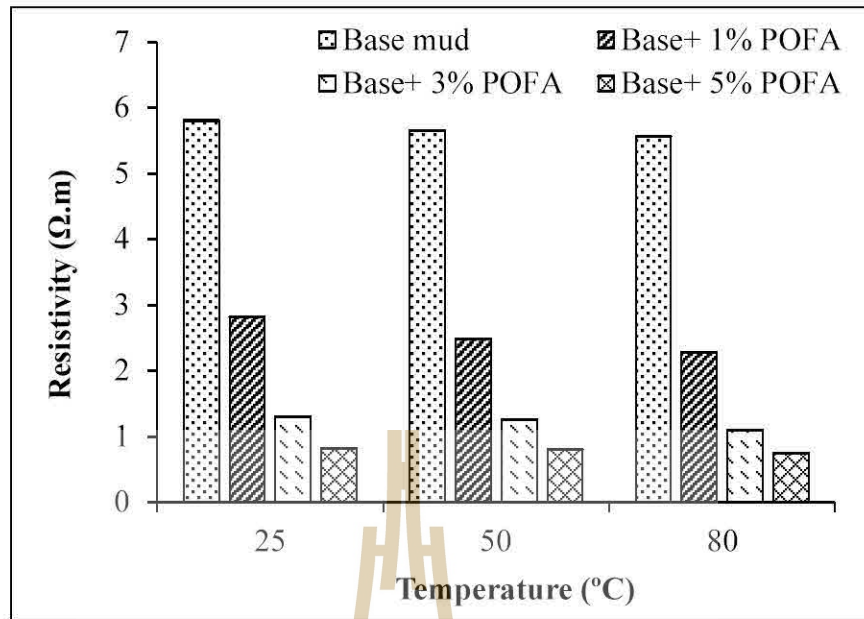


Figure 4.55 Resistivity of mud filtrate of base mud mixed with POFA versus temperature.

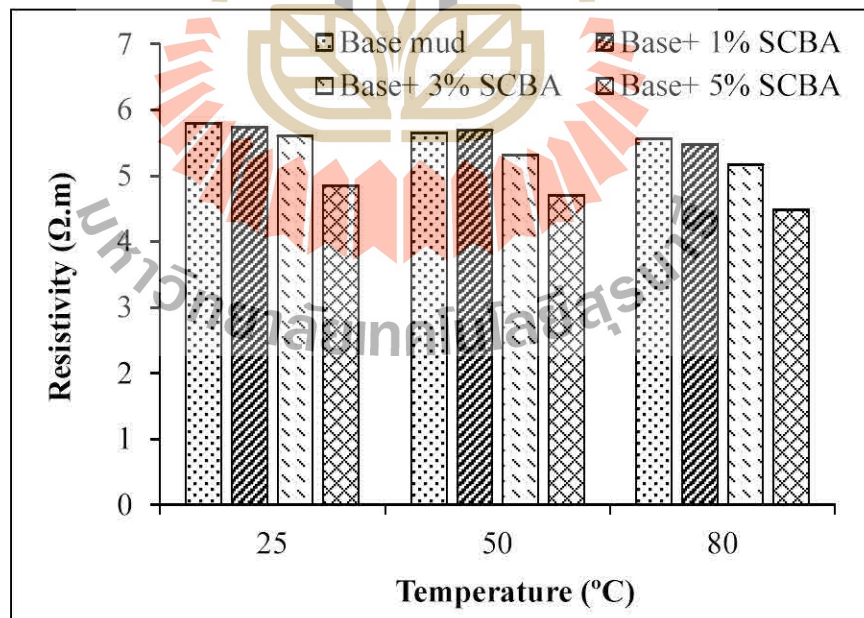


Figure 4.56 Resistivity of mud filtrate of base mud mixed with SCBA versus temperature.

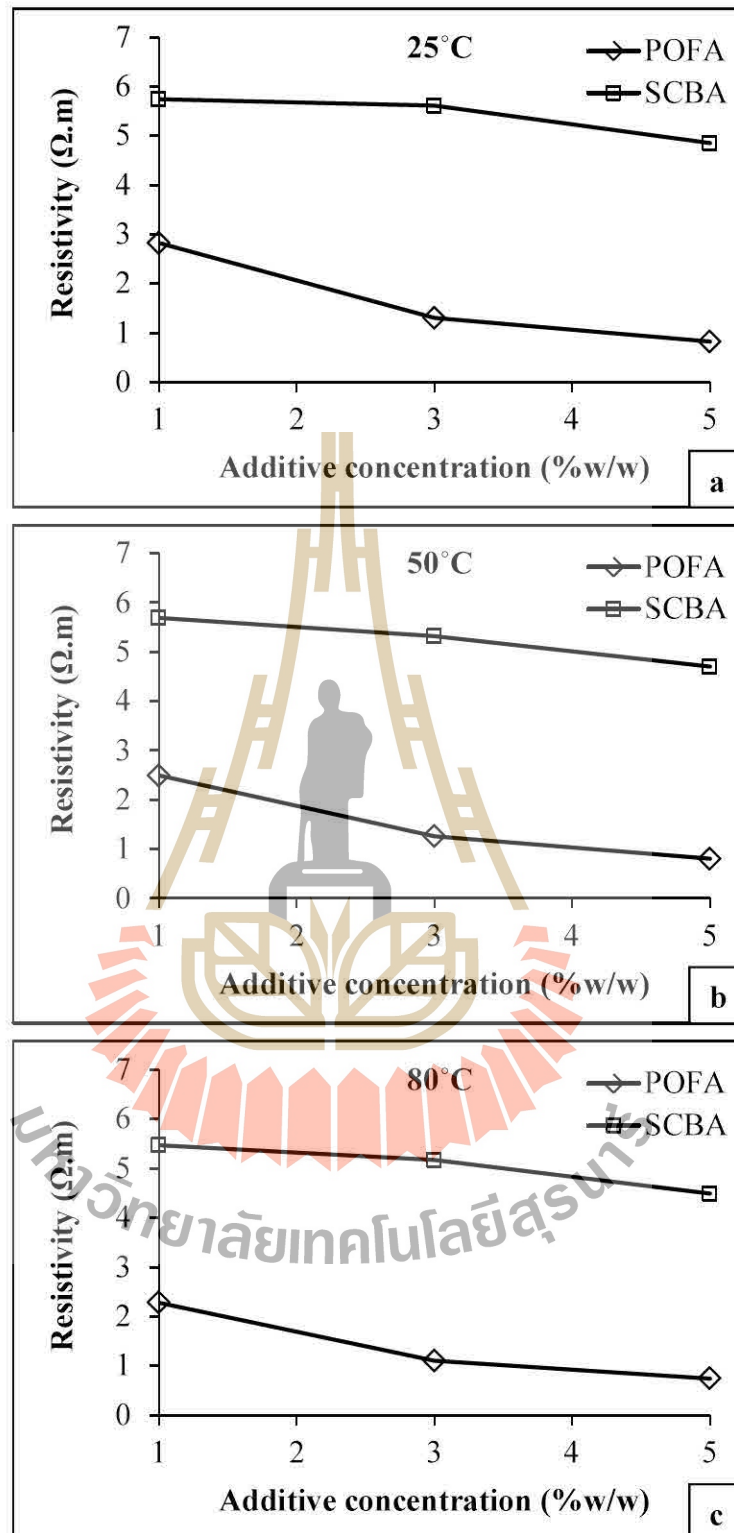


Figure 4.57 Resistivity of mud filtrate versus additive concentration at (a) 25°C, (b) 50°C and (c) 80°C.

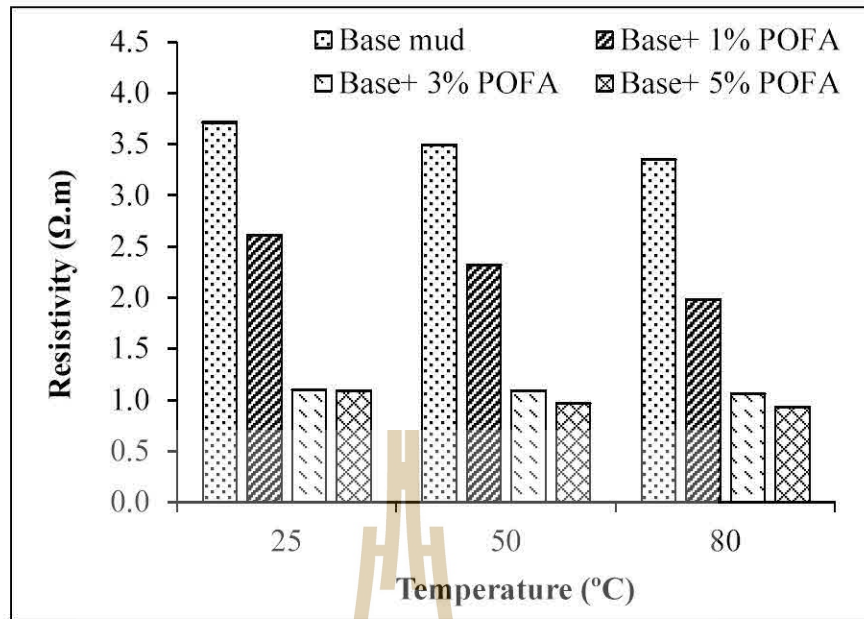


Figure 4.58 Resistivity of mud filter cake of base mud mixed with POFA versus temperature.

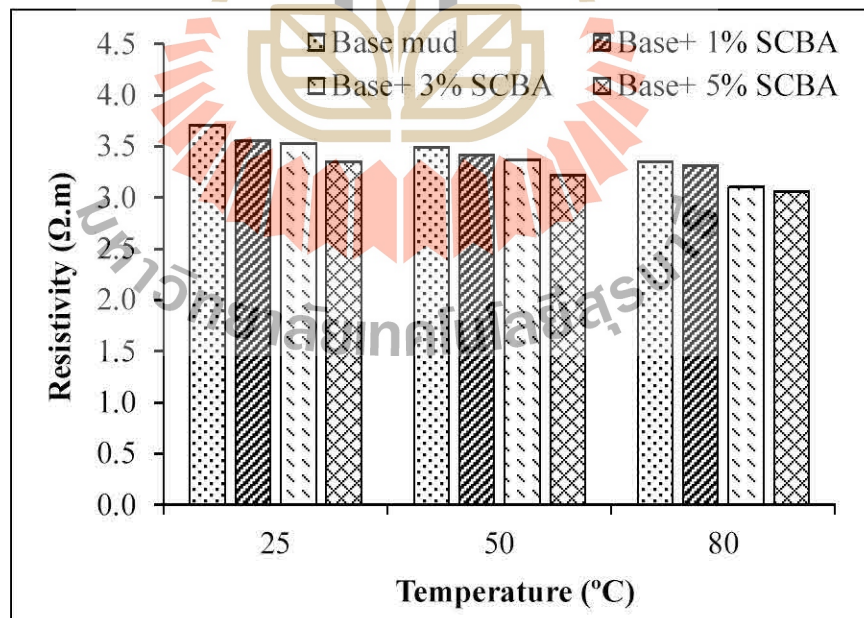


Figure 4.59 Resistivity of mud filter cake of base mud mixed with SCBA versus temperature.

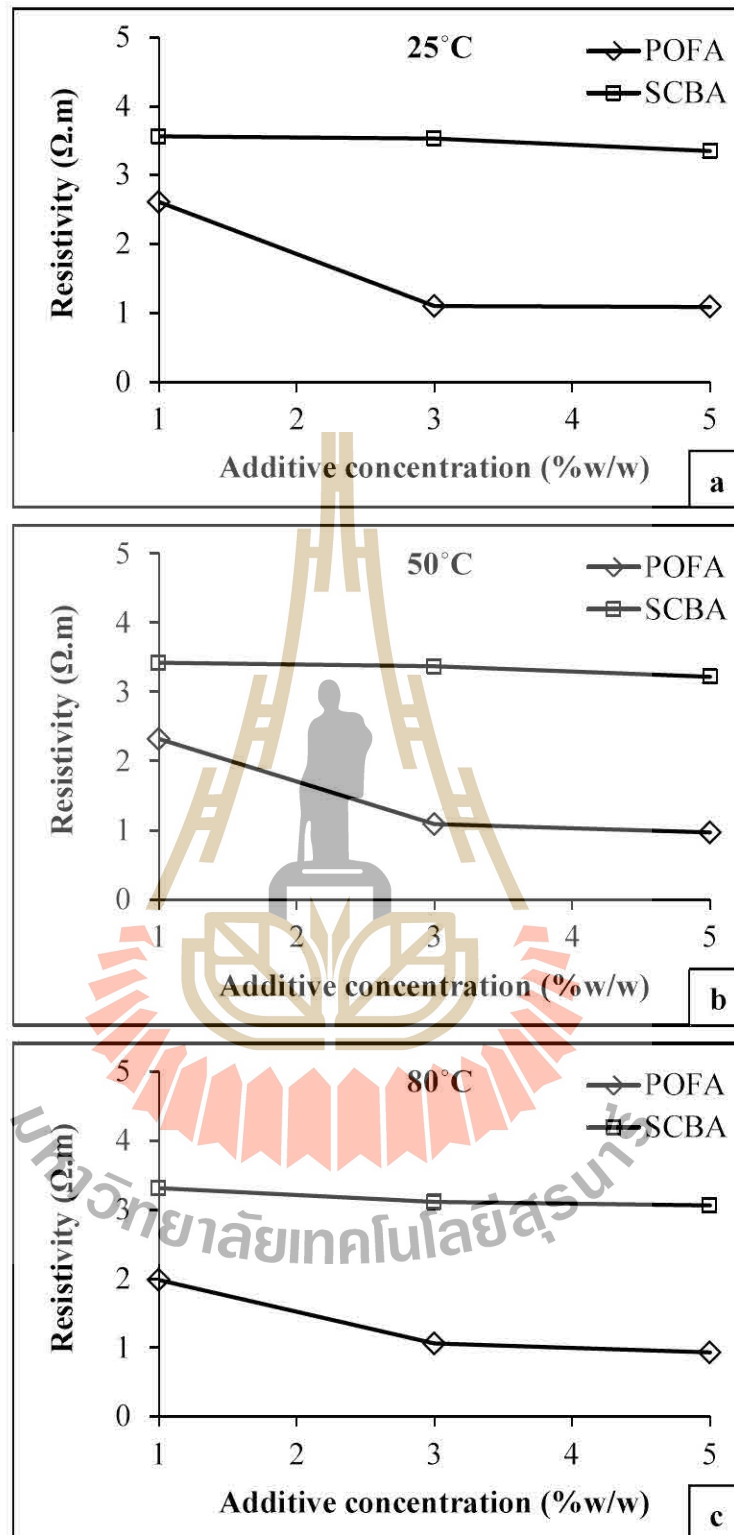


Figure 4.60 Resistivity of mud filter cake versus additive concentration at (a) 25°C, (b) 50°C and (c) 80°C.

4.3.7 Solid content properties

Three types of solid content were usually classified as soluble material such as salt. Insoluble high gravity solid (HGS) referred to barite, hematite and other weighting agents. Insoluble low gravity solid (LGS) consists of clays, polymers and bridging materials deliberately put in the drilling mud or drilled solid as solid particles from cuttings. The amount and type of solids in the drilling mud affect a number of drilling mud properties.

High solids content was increase plastic viscosity and gel strength. High solids mud has a much thicker mud filter cake and slower drilling rates. Meanwhile, much effort is expended to maintain low solids mud. It has been proved faster ROPs in all areas of operations. Low solids mud has a near-minimum amount of bentonite, clay or other low gravity solids. However, the total solids content is determined, to a great extent, by the density needed to control formation pressures (Azar and Samuel, 2007).

The results of solid content are presented in Figure 4.61 to 4.63. If a pipe sticking is to be avoided, the proportion of solids in the drilling mud should not exceed 10 percent (King Petroleum Services, www, 2014). The POFA and SCBA containing mud had a solid content in a normal range of 2.68 to 10.0 percent except SCBA 5%w/w containing mud at 80°C. For all test temperatures, the result indicates a significant increase in the solid content as the additive concentration increase. It clearly sees that for all of POFA compositions, the solid content to become less than base mud, but the solid content of SCBA containing mud was more than the base mud. A higher solids content affects the drilling mud efficiency by negatively impacting penetration rates, equivalent circulating density, high volumes of mud being

lost, large amounts of drilling waste generated and less mud able to be reused within the system.

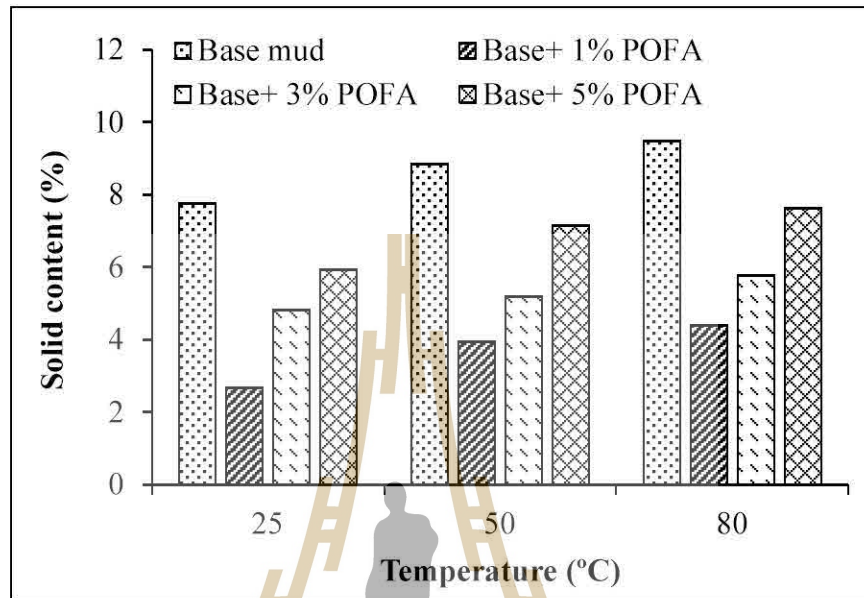


Figure 4.61 Solid content of base mud mixed with POFA versus temperature.

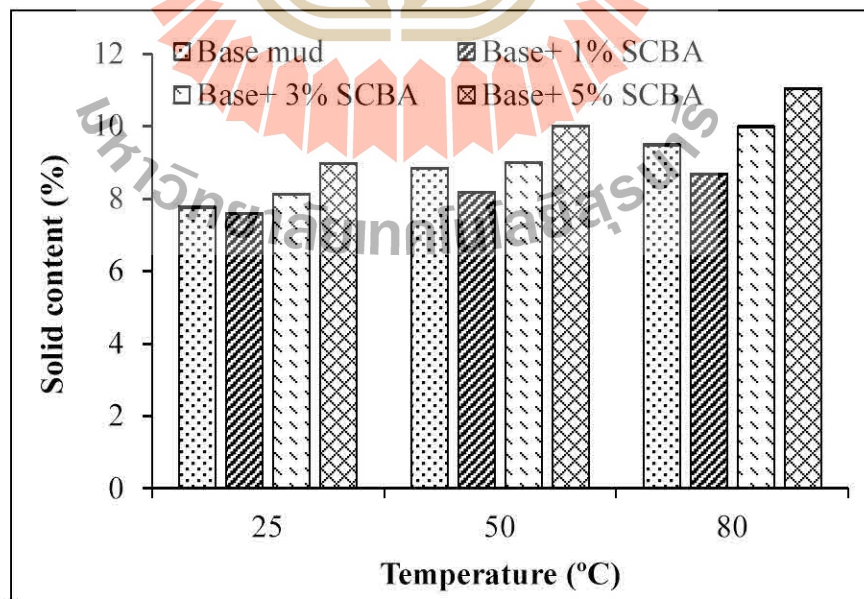


Figure 4.62 Solid content of base mud mixed with SCBA versus temperature.

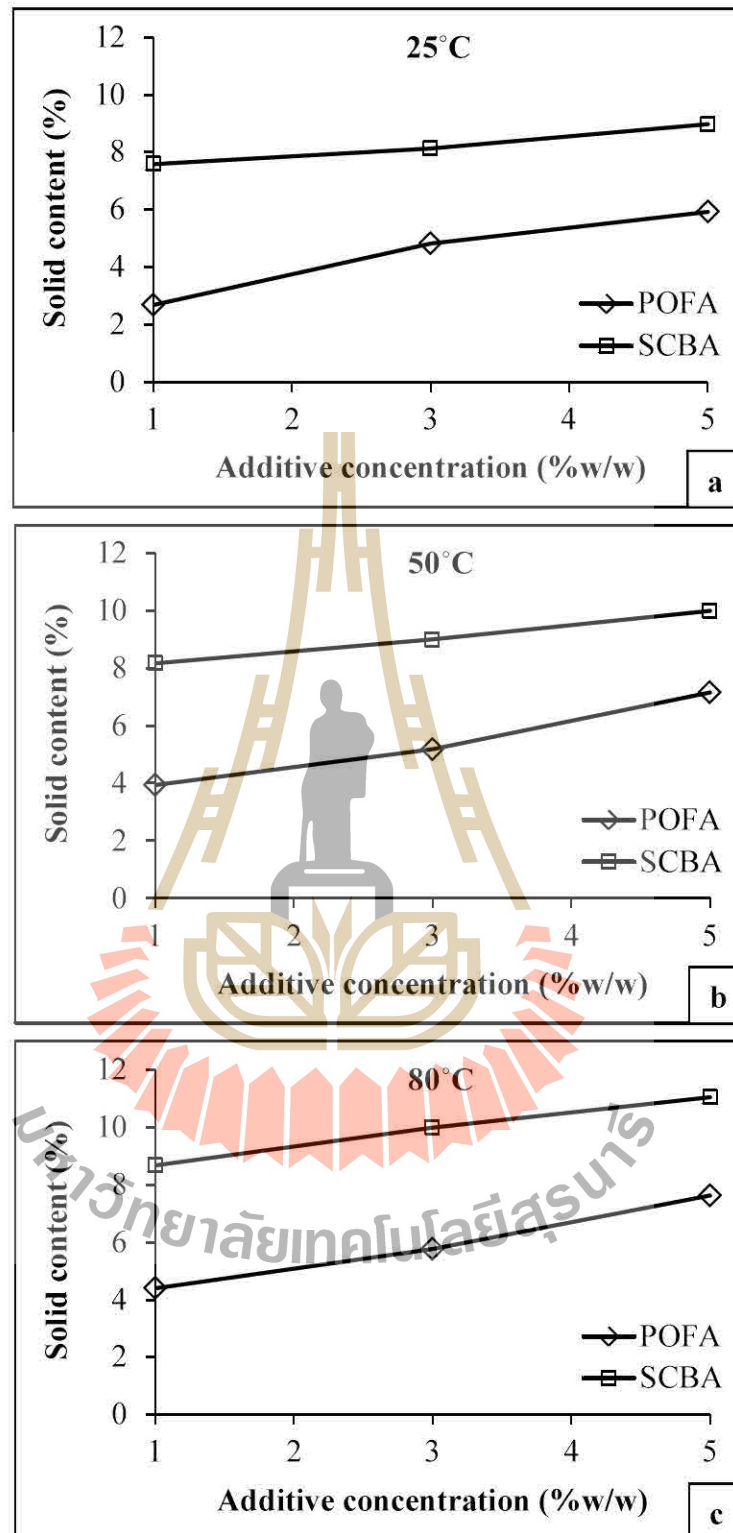


Figure 4.63 Solid content of drilling mud versus additive concentration at (a) 25°C, (b) 50°C and (c) 80°C.

4.3.8 Morphology properties

The morphology (texture), crystalline structure and orientation of drilling mud both before and after mixed with POFA and SCBA by using Scanning Electron Microscope (SEM) and Field Emission Scanning Electron Microscope (FE-SEM).

Figure 4.64 shows that the surface mud filter cake of the base mud shows uneven, thin sheet of bentonite clay larger and smaller particles of barite with the compactness of individual grains and remains of the grains of the material is even though heating at 50 and 80°C.

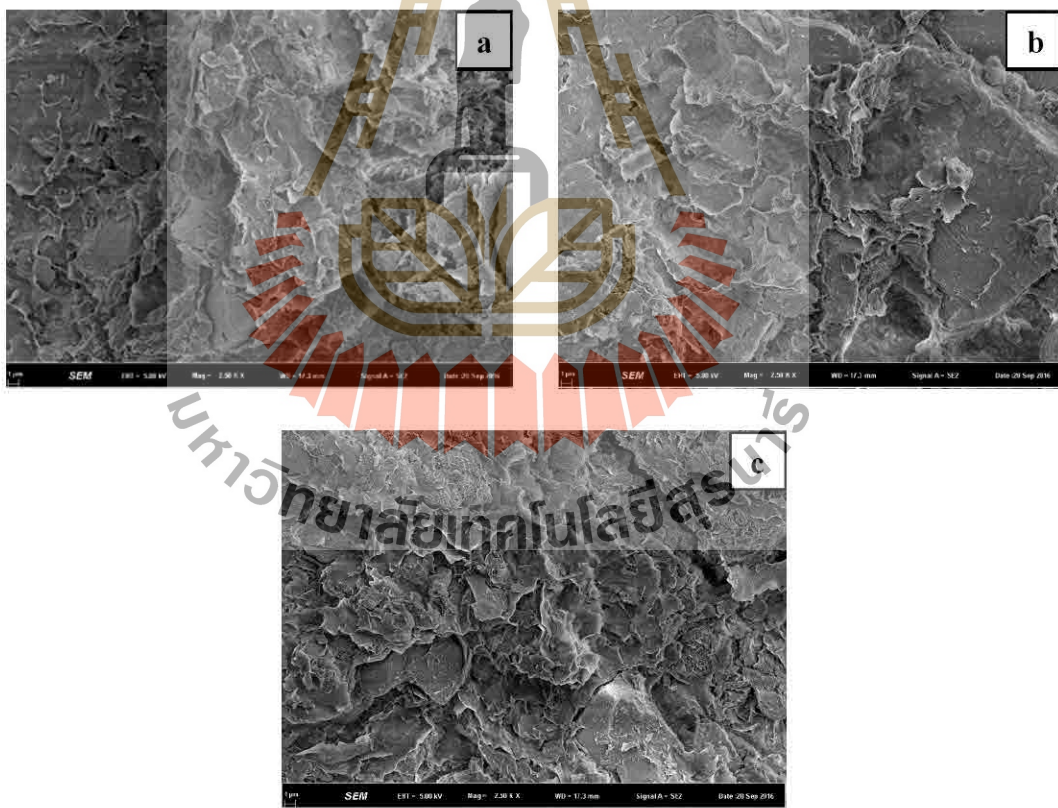


Figure 4.64 SEM image of mud filter cake (size 1 μm) formed by base mud on at (a) 25°C, (b) 50°C and (c) 80°C.

POFA and mud filter cake mixed with POFA are shown in Figure 4.65 and Figure 4.66. POFA particles were round, irregular and angular particle shapes. Some particles are rounded and contiguous clusters represented in Figure 4.65 (a) and (b). Figure 4.66 shows the mud filter cake after mixed with POFA, found the fine particle of POFA into the gap between bentonite and barite, but rough particle distributed on the surfaces of mud filter cakes, affect and engender to small pores between particle. However, POFA particle isn't even has a porous texture, thus can not absorb fluid, reduce filtration loss.

SCBA and mud filter cake mixed with SCBA are shown in Figure 4.67 and Figure 4.68. It reveals that the particle shape of SCBA has an irregular shape with rough surfaces and small porous textures represented in Figure 4.67 (a) and (b). Figure 4.68 shows that after mixed with SCBA, mud filter cakes are dense on their surfaces and distribution of particles SCBA into pores of mud filter cakes in tight connection, with no big pores and filtrate loss is less.

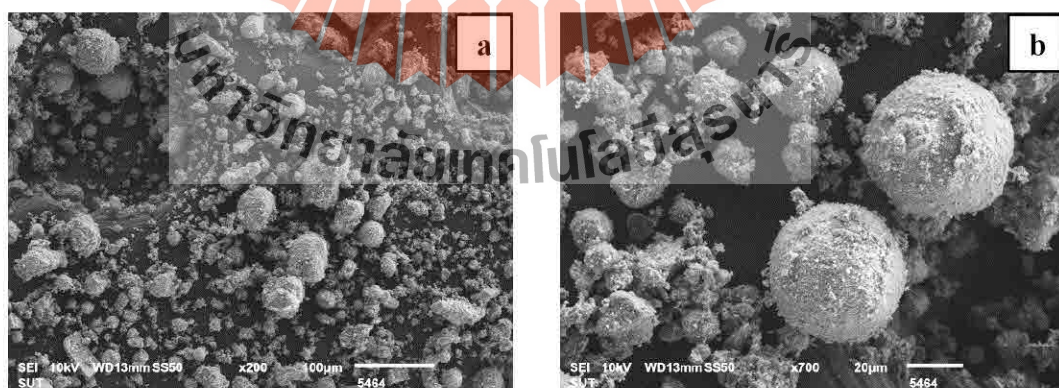


Figure 4.65 SEM image of POFA size (a) 100 μm and (b) 20 μm .

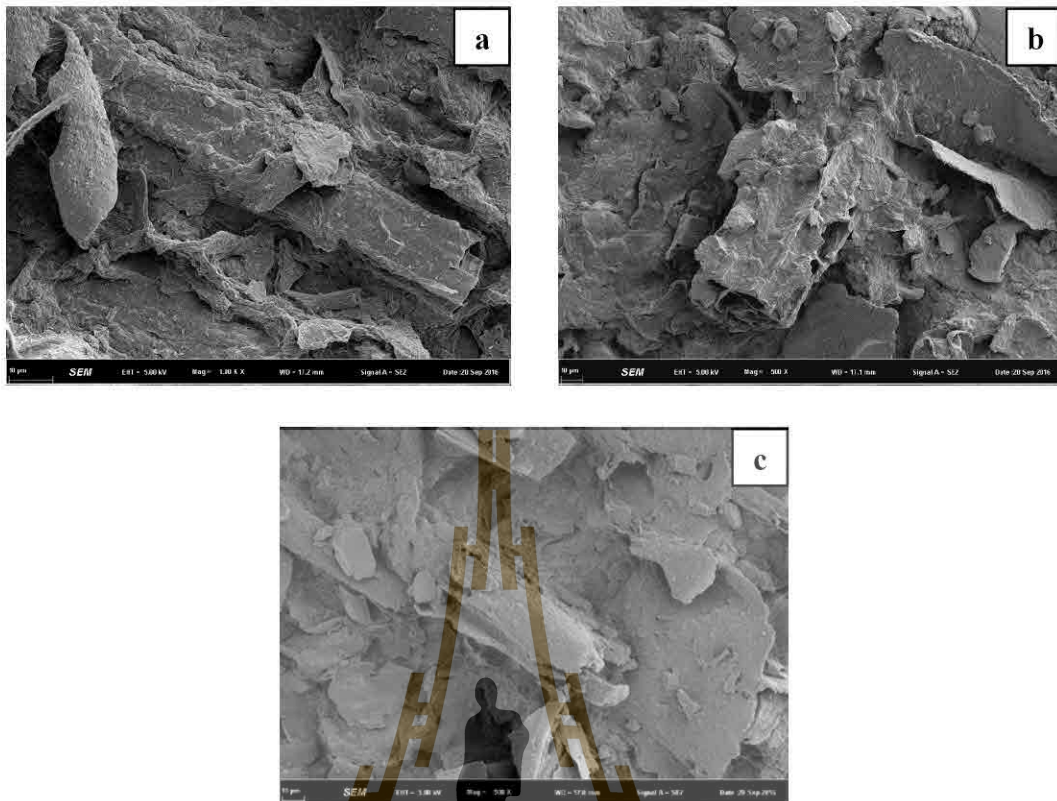


Figure 4.68 SEM image of mud filter cake (size 10 μm at temperature 25°C) formed by (a) base+ 1% SCBA, (b) base+ 3% SCBA and (c) base+ 5% SCBA.

4.4 Cost analysis

It is very important to improve the properties of drilling fluids in order to satisfy the increasing demands and need to cut drilling costs, not least of which in economics. In general, drilling mud may represent about one-fifth (15-18%) of the total cost of petroleum well drilling, but many causes 100% of drilling problems. Table 4.7 demonstrates the cost of chemicals used in drilling mud. It is essential to compare its cost between POFA and SCBA with a drilling mud system that generally

used in drilling well to analyze and conclusively this system during the term of economic consideration.

Table 4.7 Cost of chemical additives in drilling mud.

Chemical	Cost (Baht)	Unit (Kg)	Cost/Kg (Baht/Kg)
Bentonite	8,000	1,000	8
Barite	5,000	1,000	5
PAC Polymer	72,000	25	2,880
Guar Gum	350	1	350
Xanthan Gum	320	1	320
CMC HV	200,000	1,000	200
POFA	1,000	1,000	1
SCBA	150	1,000	0.15

From Table 4.7 presents the net cost of each material in drilling mud that including all operations cost, but the cost of POFA and SCBA were the ex-factory cost that it does not include the cost of material process, storage, packaging, transport and other indirect materials. Comparative cost of POFA and SCBA with other additives found that the net cost of POFA and SCBA still are expensive than chemical additives for viscosifier and fluid loss control agent. However, if the POFA and SCBA could be produced in commercial, which it could be able to reduce the cost use these materials as additive in drilling mud. In addition, the POFA and SCBA can also add value to these additives and ecologically friendly.

4.5 Summary of chemical and physical properties of drilling mud mixed with POFA and SCBA

The analysis result of drilling mud mixed with POFA and SCBA additives can be summarized the chemical and physical properties in Table 4.8.

The results obtained showed that POFA and SCBA produced a significantly higher density compared with base mud. The density of the 5%w/w of these additives is higher than other samples concentrations. Effect on density an optimum weight 5%w/w was recommended for application of the POFA or SCBA if they are to serve as weight control additive.

The effects of POFA and SCBA on the rheological properties. The flow behavior of base mud mixed with these additives usually acted between the Bingham plastic model and the Power law model. The experimental results show that the 3%w/w in all tested temperature of POFA were a potential additive for improving the rheological properties. For example, the apparent viscosity has increased in range 71.9 cP to 103.8 cP.

The effect of SCBA concentration of filtration properties at all temperature an acceptable fluid loss, but POFA concentration in drilling mud was rejected because the fluid loss values are above base mud. The drilling mud mixed with 1%w/w of SCBA in all ranges tested the temperature have proved to possess good filtration control properties, which were major responsible for the thinner filter cake and minimal filtrate volume produced (18.50 ml to 21.50 ml).

The pH value of base mud mixed with POFA has increased in range 10.33 to 10.69. Likewise, the pH value of base mud mixed with SCBA has increased in range 10.17 to 10.74, which then conformed to numerical value standard specifications (between 8 and 11). This implies that the two additives can use a greener alternative to higher the pH of drilling fluid. Albeit the appropriate pH of drilling mud varies with the mud type.

Analysis of the resistivity properties, POFA can be used as an additive material with content up to 5%w/w to produce lower resistivity than base mud (0.82 Ω .m to 2.38 Ω .m). Nevertheless, SCBA does not apply because in all concentration has extremely effective on higher the resistivity more than base mud.

The POFA and SCBA were an acceptable solid content in all the temperature. Except for 5%w/w of SCBA at 80°C was rejected because the solid content was above 10 percent. Represent, that the base mud mixed with 1%w/w of POFA was a high potential additive for LGS improving rheological properties of drilling mud.

The cost of the POFA is cheaper than viscosifier chemicals. While, the cost of SCBA is cheaper than fluid loss control agents. Cost comparison of POFA and SCBA with other viscosifier and filtration loss control agent shows that both these additives are cheaper than chemical additives, but not commercial. Because the cost of POFA and SCBA, it does not include a cost of materials process and other indirect materials. However, the utilization of both POFA and SCBA as additives in drilling mud can also add value to these additives and ecologically friendly.

Table 4.8 Summarized comparison of the chemical and physical properties of drilling mud mixed with POFA and SCBA additives.

Samples	Temperature (°C)	Chemical property		Physical property										Cost analysis	Remarks	
		XRF	XRD	Density	Viscosity					Filtrate loss	pH	Resistivity	Solid content			SEM
					AV	PV	YP	n	K							
Base	25	SiO ₂ = 66.53 Al ₂ O ₃ = 14.69 Fe ₂ O ₃ = 4.77 MgO = 4.91 BaO = 5.07	Bar = 48.73 Tal = 17.27 Qua = 14.52 Cal = 5.21 Kao = 2.68	1.11	15.0	8.8	12.5	0.51	1.1	19.75	10.34	4.64	7.76	Surface mud filter cake of the base mud shows uneven, thin sheet of bentonite clay larger and smaller particles of barite with compactness of individual grains and remains of the grains of the material is even though heating at 50 and 80°C.	Bentonite = 8 baht/kg. Barite = 5 baht/kg.	API Standard
	50	SiO ₂ = 65.77 Al ₂ O ₃ = 15.28 Fe ₂ O ₃ = 5.95 MgO = 4.65 BaO = 3.25	Bar = 55.52 Tal = 20.52 Qua = 8.89 Cal = 1.67 Kao = 3.87	1.10	19.5	8.0	23.0	0.33	4.7	21.25	10.26	4.42	8.84			
	80	SiO ₂ = 67.56 Al ₂ O ₃ = 14.99 Fe ₂ O ₃ = 5.93 MgO = 5.25 BaO = 2.03	Bar = 53.51 Tal = 14.29 Qua = 11.72 Cal = 5.60 Kao = 4.73	1.09	28.6	5.3	46.8	0.13	24.4	23.25	10.14	4.38	9.48			

Table 4.8 Summarized comparison of the chemical and physical properties of drilling mud mixed with POFA and SCBA additives

(continued).

Samples	Temperature (°C)	Chemical property		Physical property										Cost analysis	Remarks	
		XRF	XRD	Density	Viscosity					Filtrate loss	pH	Resistivity	Solid content			SEM
					AV	PV	YP	n	K							
POFA (1%)	25	SiO ₂ = 61.52 Al ₂ O ₃ = 13.69 BaO = 7.91 MgO = 5.18 Fe ₂ O ₃ = 5.44	Bar = 25.05 Qtz = 21.06 Cal = 10.26 Nac = 10.95 Tob = 7.81	-	↑	↑	↑	↑	↑	↓	↑	↑	↑	Fine particle of POFA into the gap between bentonite and barite, but rough particle distributed on the surfaces of mud filter cakes, affect and engender to small pores between particle. However POFA particle not even have a porous texture, thus can not absorb fluid, reduce filtration loss.	Cost of POFA is cheaper than guar gum and xanthan gum (viscosifier), but not commercial. Because the cost of POFA does not include the operations cost.	Addition of 1% POFA to the base mud samples improved the properties of density (at 80°C), apparent viscosity, plastic viscosity (at 25 and 80°C), yield point, n (at 25 and 50°C), K, pH, resistivity and solid content.
	50	SiO ₂ = 58.54 Al ₂ O ₃ = 13.42 BaO = 11.26 MgO = 5.31 Fe ₂ O ₃ = 5.78	Bar = 36.30 Qtz = 21.42 Cal = 8.40 Nac = 3.40 Tob = 2.46	-	↑	↓	↑	↑	↓	↑	↑	↑				
	80	SiO ₂ = 60.38 Al ₂ O ₃ = 13.73 BaO = 8.73 MgO = 4.77 Fe ₂ O ₃ = 6.11	Bar = 39.98 Qtz = 21.75 Cal = 3.05 Nac = 8.67 Tob = 4.65	↑	↑	↑	↑	↓	↑	↓	↑	↑	↑			

↑ = Better, ↓ = Worse, - = Unaltered

Table 4.8 Summarized comparison of the chemical and physical properties of drilling mud mixed with POFA and SCBA additives

(continued).

Samples	Temperature (°C)	Chemical property		Physical property										Cost analysis	Remarks	
		XRF	XRD	Density	Viscosity					Filtrate loss	pH	Resistivity	Solid content			SEM
					AV	PV	YP	n	K							
POFA (3%)	25	SiO ₂ = 68.73 Al ₂ O ₃ = 13.43 BaO = 4.20 MgO = 5.16 Fe ₂ O ₃ = 4.68	Bar = 28.60 Qtz = 22.68 Cal = 4.31 Nac = 8.87 Tob = 9.19	↑	↑	↑	↑	↑	↑	↓	↑	↑	↑	Fine particle of POFA into the gap between bentonite and barite, but rough particle distributed on the surfaces of mud filter cakes, affect and engender to small pores between particle. However POFA particle not even have a porous texture, thus can not absorb fluid, reduce filtration loss.	Cost of POFA is cheaper than guar gum and xanthan gum (viscosifier), but not commercial. Because the cost of POFA does not include the operations cost.	Addition of 3% POFA to the base mud samples improved the properties of density, apparent viscosity, plastic viscosity, yield point, n, K, pH, resistivity and solid content.
	50	SiO ₂ = 63.62 Al ₂ O ₃ = 11.80 BaO = 4.43 MgO = 5.20 Fe ₂ O ₃ = 4.99	Bar = 35.59 Qtz = 27.49 Cal = 5.02 Nac = 7.47 Tob = 4.09	↑	↑	↑	↑	↑	↓	↑	↑	↑				
	80	SiO ₂ = 60.60 Al ₂ O ₃ = 10.81 BaO = 9.84 MgO = 5.04 Fe ₂ O ₃ = 5.09	Bar = 38.80 Qtz = 22.99 Cal = 1.84 Nac = 7.33 Tob = 2.39	↑	↑	↑	↑	↑	↓	↑	↑	↑				

↑ = Better, ↓ = Worse, - = Unaltered

Table 4.8 Summarized comparison of the chemical and physical properties of drilling mud mixed with POFA and SCBA additives

(continued).

Samples	Temperature (°C)	Chemical property		Physical property										Cost analysis	Remarks	
		XRF	XRD	Density	Viscosity					Filtrate loss	pH	Resistivity	Solid content			SEM
					AV	PV	YP	n	K							
POFA (5%)	25	SiO ₂ = 63.87 Al ₂ O ₃ = 10.23 BaO = 5.02 MgO = 5.93 Fe ₂ O ₃ = 4.74	Bar = 22.81 Qtz = 27.57 Cal = 2.23 Nac = 6.48 Tob = 8.05	↑	↑	↑	↑	↑	↑	↓	↑	↑	↑	Fine particle of POFA into the gap between bentonite and barite, but rough particle distributed on the surfaces of mud filter cakes, affect and engender to small pores between particle. However POFA particle not even have a porous texture, thus can not absorb fluid, reduce filtration loss.	Cost of POFA is cheaper than guar gum and xanthan gum (viscosifier), but not commercial. Because the cost of POFA does not include the operations cost.	Addition of 5% POFA to the base mud samples improved the properties of density, apparent viscosity, plastic viscosity, yield point, n, K, pH, resistivity and solid content.
	50	SiO ₂ = 62.97 Al ₂ O ₃ = 9.76 BaO = 4.14 MgO = 6.90 Fe ₂ O ₃ = 4.27	Bar. = 33.99 Qtz = 28.11 Cal = 4.02 Nac = 6.09 Tob = 4.71	↑	↑	↑	↑	↑	↓	↑	↑	↑				
	80	SiO ₂ = 64.98 Al ₂ O ₃ = 9.78 BaO = 3.85 MgO = 5.96 Fe ₂ O ₃ = 4.32	Bar. = 30.96 Qtz = 33.05 Cal = 1.74 Nac = 6.71 Tob = 3.71	↑	↑	↑	↑	↑	↓	↑	↑	↑				

↑ = Better, ↓ = Worse, - = Unaltered

Table 4.8 Summarized comparison of the chemical and physical properties of drilling mud mixed with POFA and SCBA additives

(continued).

Samples	Temperature (°C)	Chemical property		Physical property										Cost analysis	Remarks		
		XRF	XRD	Density	Viscosity					Filtrate loss	pH	Resistivity	Solid content			SEM	
					AV	PV	YP	n	K								
SCBA (1%)	25	SiO ₂ = 65.61 Al ₂ O ₃ = 14.41 Fe ₂ O ₃ = 5.73 MgO = 4.65 BaO = 5.17	Bar = 48.88 Qtz = 15.53 Tob = 12.52 Kao = 9.60 Cal = 3.82	↑	↑	↑	↑	↑	↑	↑	↑	↑	↓	↑	Mud filter cakes are dense on their surfaces and distributed of particles SCBA into pores of mud filter cakes in tight connection, with no big pores and filtrate loss is less.	Cost of SCBA is cheaper than PAC polymer and CMC (fluid loss control agent), but not commercial. Because the cost of SCBA does not include the operations cost.	Addition of 1% SCBA to the base mud samples improved the properties of density (at 25 and 50°C), apparent viscosity (at 25 and 50°C), plastic viscosity (at 25 and 80°C), yield point (at 25 and 50°C), n (at 25 and 50°C), K (at 25 and 50°C), filtrate loss, pH and solid content.
	50	SiO ₂ = 68.70 Al ₂ O ₃ = 13.23 Fe ₂ O ₃ = 5.03 MgO = 4.12 BaO = 4.97	Bar = 49.22 Qtz = 16.46 Tob = 12.01 Kao = 6.08 Cal = 3.49	↑	↑	↓	↑	↑	↑	↑	↑	↑	↓	↑			
	80	SiO ₂ = 69.80 Al ₂ O ₃ = 12.59 Fe ₂ O ₃ = 4.91 MgO = 3.82 BaO = 4.98	Bar = 47.68 Qtz = 15.73 Tob = 12.40 Kao = 6.48 Cal = 3.72	-	↓	↑	↓	↓	↓	↓	↑	↑	↓	↑			

↑ = Better, ↓ = Worse, - = Unaltered

Table 4.8 Summarized comparison of the chemical and physical properties of drilling mud mixed with POFA and SCBA additives

(continued).

Samples	Temperature (°C)	Chemical property		Physical property										Cost analysis	Remarks		
		XRF	XRD	Density	Viscosity					Filtrate loss	pH	Resistivity	Solid content			SEM	
					AV	PV	YP	n	K								
SCBA (3%)	25	SiO ₂ = 65.73 Al ₂ O ₃ = 14.61 Fe ₂ O ₃ = 4.64 MgO = 5.72 BaO = 4.04	Bar = 48.29 Qtz = 15.04 Tob = 13.03 Kao = 6.55 Cal = 3.92	↑	↑	↑	↑	↑	↑	↑	↑	↑	↓	↓	Mud filter cakes are dense on their surfaces and distributed of particles SCBA into pores of mud filter cakes in tight connection, with no big pores and filtrate loss is less.	Cost of SCBA is cheaper than PAC polymer and CMC (fluid loss control agent), but not commercial. Because the cost of SCBA does not include the operations cost.	Addition of 3% SCBA to the base mud samples improved the properties of density (at 25 and 50°C), apparent viscosity (at 25 and 50°C), plastic viscosity (at 25 and 80°C), yield point (at 25 and 50°C), n (at 25 and 50°C), K (at 25 and 50°C), filtrate loss, pH and resistivity (at 50 and 80°C).
	50	SiO ₂ = 69.08 Al ₂ O ₃ = 14.08 Fe ₂ O ₃ = 4.44 MgO = 4.57 BaO = 3.23	Bar = 46.37 Qtz = 16.60 Tob = 12.34 Kao = 6.33 Cal = 3.27	↑	↑	↓	↑	↑	↑	↑	↑	↑	↑	↓			
	80	SiO ₂ = 68.50 Al ₂ O ₃ = 13.40 Fe ₂ O ₃ = 4.65 MgO = 4.55 BaO = 4.04	Bar = 47.94 Qtz = 14.85 Tob = 12.17 Kao = 6.04 Cal = 2.63	-	↓	↑	↓	↓	↓	↓	↑	↑	↑	↓			

↑ = Better, ↓ = Worse, - = Unaltered

Table 4.8 Summarized comparison of the chemical and physical properties of drilling mud mixed with POFA and SCBA additives

(continued).

Samples	Temperature (°C)	Chemical property		Physical property										Cost analysis	Remarks	
		XRF	XRD	Density	Viscosity					Filtrate loss	pH	Resistivity	Solid content			SEM
					AV	PV	YP	n	K							
SCBA (5%)	25	SiO ₂ = 69.87 Al ₂ O ₃ = 12.38 Fe ₂ O ₃ = 4.71 MgO = 4.75 BaO = 3.72	Bar = 48.84 Qtz = 15.85 Tob = 12.24 Kao = 6.57 Cal = 3.17	↑	↑	↑	↑	↑	↑	↑	↑	↑	↓	Mud filter cakes are dense on their surfaces and distributed of particles SCBA into pores of mud filter cakes in tight connection, with no big pores and filtrate loss is less.	Cost of SCBA is cheaper than PAC polymer and CMC (fluid loss control agent), but not commercial. Because the cost of SCBA does not include the operations cost.	Addition of 5% SCBA to the base mud samples improved the properties of density, apparent viscosity, plastic viscosity (at 25 and 80°C), yield point (at 25 and 50°C), n (at 25 and 50°C), K (at 25 and 50°C), filtrate loss, pH and resistivity.
	50	SiO ₂ = 70.43 Al ₂ O ₃ = 11.57 Fe ₂ O ₃ = 4.25 MgO = 3.97 BaO = 5.98	Bar = 45.00 Qtz = 17.78 Tob = 12.34 Kao = 5.24 Cal = 2.89	↑	↑	↓	↑	↑	↑	↑	↑	↑	↓			
	80	SiO ₂ = 71.46 Al ₂ O ₃ = 12.23 Fe ₂ O ₃ = 4.47 MgO = 3.29 BaO = 4.08	Bar = 47.77 Qtz = 14.11 Tob = 12.33 Kao = 7.19 Cal = 3.23	↑	↑	↑	↓	↓	↓	↓	↑	↑	↑			

↑ = Better, ↓ = Worse, - = Unaltered

CHAPTER V

CONCLUSIONS AND RECOMMENDATIONS

5.1 Introduction

This chapter is divided into two parts, which are conclusions and recommendations. In conclusion part, it presents the conclusion from two main sections (1) chemical property of drilling mud mixed with various additives and (2) physical property of drilling mud mixed with various additives, respectively. In recommendation part, it consists of some recommendations for the future study.

5.2 Conclusions

It is based on the results of drilling mud mixed with additive properties tested obtains from the previous chapter. The conclusions of this study are as follows.

5.2.1 Chemical property

In terms of chemical composition, base mud was dominantly filled with silica, followed by aluminium oxide, iron oxide, magnesium oxide, barium oxide and a slight other chemical was found. The major elements of base mud include barite, talc, quartz, calcite, kaolinite and microcline.

The POFA was constituted mainly of silica (up to 57.583%), followed by potassium oxide, calcium oxide, chloride and magnesium oxide. Analysis by XRD in the POFA was obtained a mineral that has the greatest is a sylvite with a 35.479%, followed by quartz, anorthite, kaolinite, gypsum and calcite. The drilling mud mixed with POFA showed a typical composition rich in silica, aluminium oxide,

barium oxide, magnesium oxide and iron oxide. Meanwhile, the drilling mud mixed with POFA testing with the XRD; giving results that mineral that has the greatest is barite, followed by quartz, calcite, nacrite and tobermorite.

The SCBA contains a high amount of silica (SiO_2) of 88.38% and very small proportions of other chemical compositions. Meanwhile, the major minerals of SCBA with the predominance of quartz (73.123%) and shows the amorphous silica formation. The main chemical components of the drilling mud mixed with SCBA in three temperatures have the cognate components dominantly are silica, aluminum oxide, iron oxide, magnesium oxide and barium oxide. Testing by XRD, the drilling mud mixed with SCBA provides results, that mineral which has the largest barite followed by quartz, tobermorite, kaolinite, calcite and nacrite.

From XRF and XRD analysis, the drilling mud mixed with POFA and SCBA was found to have an increase in magnesium oxide, kaolinite and tobermorite. These increased was result in advocate increasing the strength of drilling mud, which effects to the rheology properties. In addition, the results of chemical and mineral analysis found that the temperature in the study, which does not change the structure of chemical and mineral of drilling mud. However, the drilling mud after mixed with these additives has changed the content of chemical and minerals that depended on the mixed ratio.

5.2.2 Physical property

The density of drilling mud shows that the density slightly decreased with an increase of temperature. The other noticeable effect is the increase in density with increase in additive concentration for both mud (particle of POFA and SCBA having a specific gravity to be in the range of 2.20-2.78). Comparison of POFA and

SCBA indicated that a similar amount of density at 25 and 50°C, but POFA will give a higher mud density than SCBA in all the concentration at 80°C. If the POFA was to serve as weight control agent, 5%w/w of POFA at 25 and 50°C are recommended. Moreover, it was observed that for weight control, 5%w/w of SCBA at 25°C can also use as weight control agents as well.

The drilling mud mixed POFA and SCBA additives exhibited pseudo-plastic flow and shear thinning fluid with flow behavior index less than 1. In terms of several concentrations, increasing the POFA and SCBA concentration in base mud gives rise to increasing the apparent viscosity, yield point, gel strength and as does slightly increased the plastic viscosity. When changing the temperature from 25 to 80°C, the apparent viscosity, yield point and gel strength of base mud mixed with these additives increased with increasing temperature, while the plastic viscosity slightly decreased with increasing temperature. At 1, 3 and 5%w/w of concentrations of the rheological properties (apparent viscosity, plastic viscosity, yield point and gel strength), the drilling mud mixed with POFA was generally greater than SCBA throughout a temperature range. The drilling mud mixed with 3%w/w of POFA in all ranges tested the temperature; give appropriate rheological properties for water based drilling mud.

Physical examination of the filtrate volume indicates that filtrate volume and filter cake thickness increases as the concentration of these additives and temperature increases. Comparison of 1, 3 and 5 the percentages of SCBA concentration at all temperatures, which produced the least of filtrate volume and mud filter cake thickness, demonstrated better filtration control characteristics than POFA and base mud. At the temperature of 25°C, 1%w/w of SCBA, exhibited the best filtration

control characteristics with minimal filtrate volume (18.50 ml) and thinner and consistent mud filter cakes (1.44 mm). However, the thermal stability of the SCBA mixed with drilling mud indicated that the SCBA additive could be used in a subterranean well formation having the downhole temperature up to 80°C.

The result of pH in drilling mud mixed with POFA and SCBA was decreased when an elevated temperature and additive concentration increase. However, the pH of drilling mud and mud filtrate mixed with POFA at 25 and 50°C to be lower than of the SCBA additive, except at 80°C. From the pH value, the formulated drilling mud mixed with these additives is in an alkaline state. Thus, POFA and SCBA were recommended as maintain the pH of the mud and hence can be used without having any adverse effect on the equipment.

The resistivity of the drilling mud, mud filtrate and mud filter cake decreased with increasing POFA content, SCBA content and temperature and it can be implied that the resistivity of mud filtrate was more than the drilling mud and mud filter cake, respectively. The results indicated that the drilling mud mixed with POFA, it can be implied that the resistivity of drilling mud, mud filtrate and mud filter cake tended to become less than the drilling mud mixed with SCBA. From an analysis to improve efficiency the resistivity, which is the best 5%w/w of POFA at 80°C has an excellent percentage.

The result indicates a significant increase in the solid content as the additive concentration and temperature increase. For all of POFA compositions the solid content to become less than the solid content of the drilling mud mixed with SCBA. Thus, the POFA additive was an LGS is improving the rheological properties

of drilling mud and it indicated a certain 1%w/w at 25°C of POFA can control lowermost solid content.

The microstructure of base mud by using mud filter cake is characterized shows uneven, a thin sheet of bentonite clay larger and smaller particles of barite with the compactness of individual grains. The SEM image of POFA, it can be seen that POFA contains round, irregular and angular shaped particles with some of the particles are rounded and contiguous clusters. Meanwhile, the particle shape of SCBA has an irregular shape with rough surfaces and small porous textures. The particles in the SEM view of the mud filter cake after mixed with POFA observe the fine particle of POFA into the gap between bentonite and barite, but rough particle distributed on the surfaces of mud filter cakes, affect and engender to small pores between particle. The morphology of the mud filter cake after mixed with SCBA; mud filter cakes are dense on their surfaces and distribution of particles SCBA into pores of mud filter cakes in tight connection with no big pores.

From the physical properties test, it can be concluded that adding POFA in drilling mud can improve the property of density, rheology, pH, resistivity and solid content. While, adding SCBA in drilling mud can improve the property of density, rheology, filtration and pH. But in practice (in the field), there is a problem of availability of POFA and SCBA. Owing to these additives used in the study were raw materials obtained from the industry. It has not undergone the material preparation process to make it available.

5.2.3 Cost analysis

Comparative cost of POFA and SCBA with other additives found that the net cost of POFA and SCBA are expensive than chemical additives for viscosifier

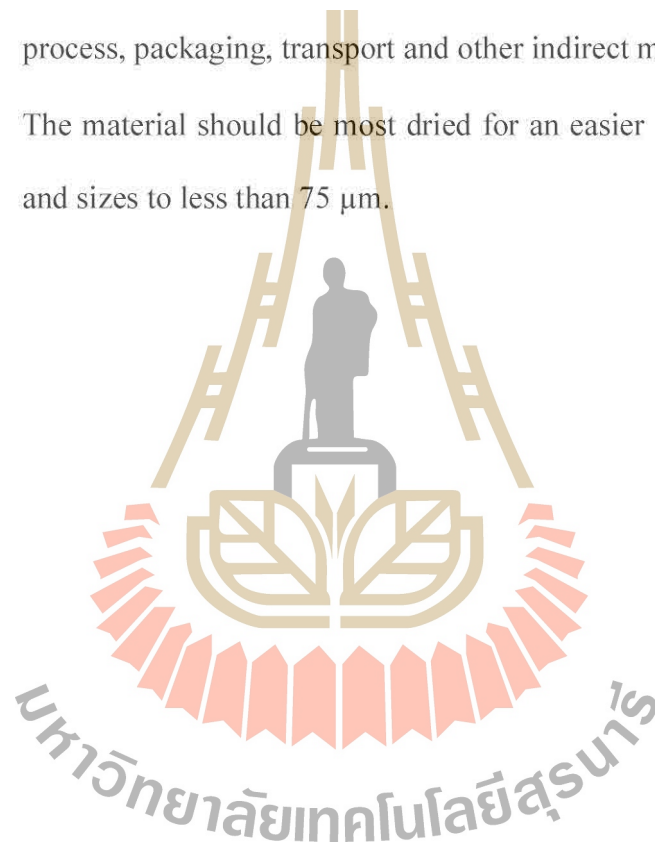
and fluid loss control agent. However, if the POFA and SCBA could be produced in commercial, which it could be able to reduce the cost use these materials as additive in drilling mud. Therefore, POFA was suitable to be additive in water based drilling mud for rheological properties. Meanwhile, SCBA was appropriate to be additive in water based drilling mud for fluid loss control properties and increased value to these additives.

5.3 Recommendations

The research, experimental and results lead to recommendation area for further studies including:

- Drilling mud mixed POFA and SCBA additives should be investigated at the elevated temperature more than 80°C.
- POFA and SCBA additive concentrations might be tested less than 1 percent and more than 5 percent.
- The dynamic filtration test should be performed to test under high temperature and pressure that represents the real circulated borehole condition.
- The formation damage is concerned and should be measured due to erodibility of mud filter cake these additive deposited are a presence.
- It should be investigated the drilling mud mixed other additives integrating with POFA and SCBA for performing the specific physical property.

- Using other ash additives comparisons with POFA and SCBA additive for the utility of better efficiency, availability, better environmental effects, and low cost factor.
- Comparison the rheology properties between adding POFA or SCBA and bentonite in drilling mud at the same concentration.
- Cost comparison of materials should include material preparation process, packaging, transport and other indirect materials.
- The material should be most dried for an easier crush to fine particles and sizes to less than 75 μm .



REFERENCES

- Abbasi, A., and Zargar, A. (2013). Using bagasse ash in concrete as pozzolan. **Middle-East Journal of Scientific Research**. 13(6): 716-719.
- Abdullah, K., Hussin, M.W., Zakaria, F., Muhamad, R., and Hamid, Z.A. (2006). POFA: A potential partial cement replacement material in aerated concrete. In **Proceedings of the Sixth Asia-Pacific Structural Engineering and Construction Conference** (pp. 132-140). Kuala Lumpur, Malaysia.
- API RP 13B-1. (1997). Recommended practice for field testing water-based drilling fluids (2nd ed.). In **API Recommended Practice 13B-1**. Washington, D.C.: American Petroleum Institute.
- Awal, A.S.M.A., and Hussin, M.W. (1999). Durability of high performance concrete containing palm oil fuel ash. In **Proceedings of the Eighth International Conference on Durability of Building Materials and Components** (pp. 465-474). Vancouver, Canada: NRC Research Press.
- Azar, J.J., and Samuel, G.R. (2007). **Drilling engineering**. Tulsa, Oklahoma: PennWell Books.
- Baker Hughes. (2006). **Drilling fluids reference manual** (rev. ed.). Houston, TX.
- Caenn, R., Darley, H.C.H., and Gray, G.R. (2016). **Composition and properties of drilling and completion fluids** (7th ed.). Cambridge, MA: Gulf Professional Publishing.

- Chindapasirt, P., Homwuttiwong, S., and Jaturapitakkul, C. (2007). Strength and water permeability of concrete containing palm oil fuel ash and rice husk-bark ash. **Construction and Building Materials**. 21(7): 1492-1499.
- Chindapasirt, P., Rukzon, S., and Sirivivatnanon, V. (2008). Resistance to chloride penetration of blended Portland cement mortar containing palm oil fuel ash, rice husk ash and fly ash. **Construction and Building Materials**. 22(5): 932-938.
- Chusilp, N., Jaturapitakkul, C., and Kiattikomol, K. (2009). Utilization of bagasse ash as a pozzolanic material in concrete. **Construction and Building Materials**. 23(11): 3352-3358.
- Cordeiro, G.C., Filho, R.D.T., Fairbairn, E.M.R., Tavares, L.M.M., and Oliveira, C.H. (2004). Influence of mechanical grinding on the pozzolanic activity of residual sugarcane bagasse ash. In **Proceedings of the International RILEM Conference on the Use of Recycled Materials in Buildings and Structures** (pp. 731-740). Barcelona, Spain: RILEM Publications.
- Fitton, T. (2007). **Tailings beach slope prediction**. Ph.D. Dissertation, RMIT University, Australia.
- Gatlin, C. (1960). **Petroleum engineering: Drilling and well completions**. Englewood Cliffs, NJ: Prentice-Hall.
- Goyal, A., Kunio, H., Ogata, H., and Mandula. (2007). Properties and reactivity of sugarcane bagasse ash. In **Proceeding of the Twelfth International Colloquium on Structural and Geotechnical Engineering** (pp. 1-5). Cairo, Egypt: Ain Shams University.

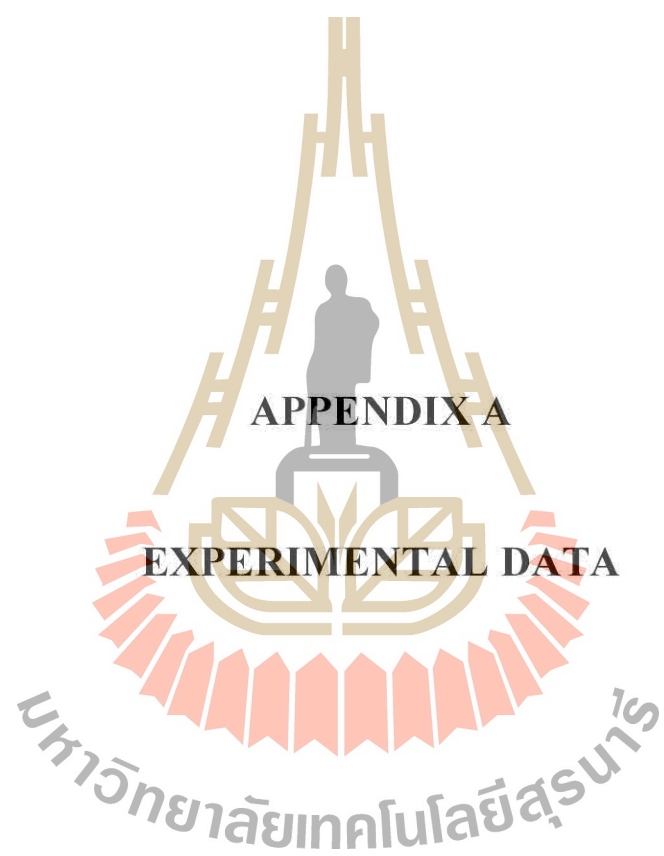
- Hallenburg, J.K. (1997). **Introduction to geophysical formation evaluation**. Boca Raton: Lewis Publishers.
- Hussein, A.A.E., Shafiq, N., Nuruddin, M.F., and Menon, F.A. (2014). Compressive strength and microstructure of sugar cane bagasse ash concrete. **Research Journal of Applied Sciences, Engineering and Technology**. 7(12): 2569-2577.
- Hussin, M.W., and Awal, A.S.M.A. (1996). Influence of palm oil fuel ash on strength and durability of concrete. In **Proceedings of the Seventh International Conference on Durability of Building Materials and Components** (pp. 291-298). Oxford, England: Taylor and Francis Group.
- Igwe, I., and Kinate, B.B. (2015). The use of periwinkle shell ash as filtration loss control agent in water-based drilling mud. **International Journal of Engineering Research and General Science**. 3(6): 375-381.
- Johnson, D.V. (2011). Palm ash: A humble product of many uses. **Palms**. 55(3): 117-121.
- Karagüzel, C., Çetinel, T., Boylu, F., Çinku, K., and Çelik, M.S. (2010). Activation of (Na, Ca)-bentonites with soda and MgO and their utilization as drilling mud. **Applied Clay Science**. 48: 398-404.
- Khodja, M., Khodja-Saber, M., Canselier, J.P., Cohaut, N., and Bergaya, F. (2010). Drilling fluid technology: Performances and environmental considerations. In I. Fuerstner (ed). **Products and services; from R&D to final solutions** (pp. 227-256). Rijeka, Croatia: Sciyo.

- Kiattikomol, K., Jaturapitakkul, C., Songpiriyakij, S., and Chutubtim, S. (2001). A study of ground coarse fly ashes with different fineness from various sources of pozzolanic materials. **Cement and Concrete Composites**. 23(4-5): 335-343.
- King Petroleum Services. (2014). **Drilling Fluids** [On-line]. Available: http://www.kingpetroleum.co.uk/training/wellEngHandout/training_chap09.php
- Kolias, S., Kasselouri-Rigopoulou, V., and Karahalios, A. (2005). Stabilisation of clayey soils with high calcium fly ash and cement. **Cement and Concrete Composites**. 27(2): 301-313.
- Korsinwattana, P., and Terakulsatit, B. (2014). Efficiency enhancement of drilling mud by using fly ash as an additive. In **Proceedings of International Conference on Advances in Civil Engineering for Sustainable Development** (pp. 531-536). Nakhon Ratchasima, Thailand: Suranaree University of Technology.
- Kumar, A.S., Mahto, V., and Sharma, V.P. (2003). Behaviour of organic polymers on the rheological properties of Indian bentonite-water based drilling fluid system and its effect on formation damage. **Indian Journal of Chemical Technology**. 10: 525-530.
- Luckham, P.F., and Rossi, S. (1999). The colloidal and rheological properties of bentonite suspensions. **Journal of Colloid and Interface Science**. 82: 43-92.
- Lyons, W.C., Plisga, G.J., and Lorenz, M.D. (2016). **Standard handbook of petroleum and natural gas engineering** (3rd ed.). Waltham, MA: Gulf Professional Publishing.
- Mahto, V. (2013). Effect of activated charcoal on the rheological and filtration properties of water based drilling fluids. **International Journal of Chemical and Petrochemical Technology**. 3(4): 27-32.

- Mahto, V., and Jain, R. (2013). Effect of fly ash on the rheological and filtration properties of water based drilling fluids. **International Journal of Research in Engineering and Technology**. 2(8): 150-156.
- Meng, X., Zhang, Y., Zhou, F., and Chu, P.K. (2012). Effects of carbon ash on rheological properties of water-based drilling fluids. **Journal of Petroleum Science and Engineering**. 100: 1-8.
- MI-Swaco. (1998). Rheology and hydraulics (rev. ed.). In **Drilling fluids engineering manual** (pp. 1-36). Houston, TX.
- Mian, M.A. (1992). **Petroleum engineering handbook for the practicing engineer** (Vol. II). Tulsa, Oklahoma: PennWell Books.
- Modani, P.O., and Vyawahare, M.R. (2013). Utilization of bagasse ash as a partial replacement of fine aggregate in concrete. **Procedia Engineering**. 51: 25-29.
- Payá, J., Monzó, J., Borrachero, M.V., Peris-Mora, E., and González-López, E. (1996). Mechanical treatment of fly ashes part II: Particles morphology in ground fly ashes (GFA) and workability of GFA-Cement mortars. **Cement and Concrete Research**. 26(2): 225-235.
- Penn, C., and Zhang, H. (2013). An introduction to the land application of drilling mud in Oklahoma. **OSU Fact Sheet, WREC-102**. Stillwater, OK: Oklahoma Cooperative Extension Service.
- Petchote, P., and Sikong, L. (2005). **Properties of drilling mud mixed with fly ash and dolomite powder**. Department of mining and materials engineering, Faculty of engineering, Prince of Songkla University. 1-6.

- Raheem, A.M., and Vipulanandan, C. (2014). Effect of salt contamination on the bentonite drilling mud shear strength and electrical resistivity. In **Proceedings of the Sixth Annual Texas Hurricane Conference and Exhibition** (pp. 1-2). Houston, Texas: University of Houston.
- Safiuddin, M., Salam, M.A., and Jumaat, M.Z. (2011). Utilization of palm oil fuel ash in concrete: A review. **Journal of Civil Engineering and Management**. 17(2): 234-247.
- Samavati, R., Abdullah, N., Nowtarki, K.T., Hussain, S.A., and Biak, D.R.A. (2014). The prospect of utilizing a cassava derivative (fufu) as a fluid loss agent in water based drilling muds. **International Journal of Chemical Engineering and Applications**. 5(2): 161-169.
- Sami, N.A. (2016). Effect of magnesium salt contamination on the behavior of drilling fluids. **Egyptian Journal of Petroleum**. 25(4): 453-458.
- Sata, V., Jaturapitakkul, C., and Kiattikomol, K. (2004). Utilization of palm oil fuel ash in high-strength concrete. **Journal of Materials in Civil Engineering**. 16(6): 623-628.
- Sata, V., Jaturapitakkul, C., and Kiattikomol, K. (2007). Influence of pozzolan from various by-product materials on mechanical properties of high-strength concrete. **Construction and Building Materials**. 21(7): 1589-1598.
- Sata, V., Jaturapitakkul, C., and Rattanasotinunt, C. (2010). Compressive strength and heat evolution of concretes containing palm oil fuel ash. **Journal of Materials in Civil Engineering**. 22(10): 1033-1038.

- Schettino, M.A.S., and Holanda, J.N.F. (2015). Processing of porcelain stoneware tile using sugarcane bagasse ash waste. **Processing and Application of Ceramics**. 9(1): 17-22.
- Srinivasan, R., and Sathiya, K. (2010). Experimental study on bagasse ash in concrete. **International Journal for Service Learning in Engineering**. 5(2): 60-66.
- Sumadi, S.R., and Hussin, M.W. (1995). Palm oil fuel ash (POFA) as a future partial cement replacement material in housing construction. **Journal of Ferrocement**. 25(1): 25-34.
- Tangchirapat, W., Jaturapitakkul, C., and Chindapasirt, P. (2009). Use of palm oil fuel ash as supplementary cementitious material for producing high-strength concrete. **Construction and Building Materials**. 23(7): 2641-2646.
- Tangchirapat, W., Saeting, T., Jaturapitakkul, C., Kiattikomol, K., and Siripanichgom, A. (2007). Use of waste ash from palm oil industry in concrete. **Waste Management**. 27(1): 81-88.
- Tay, J-H. (1990). Ash from oil-palm waste as concrete material. **Journal of Materials in Civil Engineering**. 2(2): 94-105.
- Tonnayopas, D., Nilrat, F., Putto, K., and Tantiwitayawanich, J. (2006). Effect of oil palm fiber fuel ash on compressive strength of hardening concrete. In **Proceedings of the Fourth Thailand Materials Science and Technology Conference** (pp. 1-3). Pathumthani, Thailand.



APPENDIX A

EXPERIMENTAL DATA

มหาวิทยาลัยเทคโนโลยีสุรนารี

Table A1 Compositions of drilling mud mixed with POFA and SCBA.

No.	Temperature (°C)	Base	POFA (%w/w)	SCBA (%w/w)
1	25	100 g of barite and 60 g of bentonite	-	-
2	50	100 g of barite and 60 g of bentonite	-	-
3	80	100 g of barite and 60 g of bentonite	-	-
4	25	100 g of barite and 60 g of bentonite	1	-
5	25	100 g of barite and 60 g of bentonite	3	-
6	25	100 g of barite and 60 g of bentonite	5	-
7	50	100 g of barite and 60 g of bentonite	1	-
8	50	100 g of barite and 60 g of bentonite	3	-
9	50	100 g of barite and 60 g of bentonite	5	-
10	80	100 g of barite and 60 g of bentonite	1	-
11	80	100 g of barite and 60 g of bentonite	3	-
12	80	100 g of barite and 60 g of bentonite	5	-
13	25	100 g of barite and 60 g of bentonite	-	1
14	25	100 g of barite and 60 g of bentonite	-	3
15	25	100 g of barite and 60 g of bentonite	-	5
16	50	100 g of barite and 60 g of bentonite	-	1
17	50	100 g of barite and 60 g of bentonite	-	3
18	50	100 g of barite and 60 g of bentonite	-	5
19	80	100 g of barite and 60 g of bentonite	-	1
20	80	100 g of barite and 60 g of bentonite	-	3
21	80	100 g of barite and 60 g of bentonite	-	5

Fann viscometer data and parameters for all tested.

Table A2 Water based drilling mud at 25°C (No.1).

RPM	Reading #1	Reading #2	Reading #3	Reading #4	Average reading	γ (sec ⁻¹)	τ (lb _f /ft ²)
600	29	29	31	31	30.00	1021.8	32.034
300	20	21	22	22	21.25	510.9	22.424
200	17	17	18	18	17.50	340.6	18.153
100	13	13	14	14	13.50	170.3	13.881
6	9	9	9	9	9.00	10.2	9.610
3	8	8	7	8	7.75	5.1	7.475
AV	14.5	14.5	15.5	15.5	15.0		
PV	9.0	8.0	9.0	9.0	8.8		
YP	11.0	13.0	13.0	13.0	12.5		
Gel _{in}	8						
Gel ₁₀	9						

Table A3 Water based drilling mud at 50°C (No.2).

RPM	Reading #1	Reading #2	Reading #3	Reading #4	Average reading	γ (sec ⁻¹)	τ (lb _f /ft ²)
300	31	31	31	31	31.00	510.9	33.102
200	27	28	27	28	27.50	340.6	28.831
100	23	23	23	23	23.00	170.3	24.559
6	17	18	18	17	17.50	10.2	18.153
3	14	14	14	14	14.00	5.1	14.949
AV	19.5	19.5	19.5	19.5	19.5		
PV	8.0	8.0	8.0	8.0	8.0		
YP	23.0	23.0	23.0	23.0	23.0		
Gel _{in}	13						
Gel ₁₀	14						

Table A4 Water based drilling mud at 80°C (No.3).

RPM	Reading #1	Reading #2	Reading #3	Reading #4	Average reading	γ (sec ⁻¹)	τ (lb _f /ft ²)
300	49	52	54	53	52.00	510.9	55.526
200	46	50	52	45	48.25	340.6	51.254
100	41	44	47	41	43.25	170.3	45.915
6	19	20	22	18	19.75	10.2	20.288
3	14	13	15	14	14.00	5.1	14.949
AV	27.5	28.5	29.0	29.5	28.6		
PV	6.0	5.0	4.0	6.0	5.3		
YP	43.0	47.0	50.0	47.0	46.8		
Gel _{in}	14						
Gel ₁₀	15						

Table A5 Water based drilling mud mixed with 1 percentage POFA at 25°C (No.4).

RPM	Reading #1	Reading #2	Reading #3	Reading #4	Average reading	γ (sec ⁻¹)	τ (lb _f /ft ²)
300	32	31	31	30	31.00	510.9	34.170
200	31	30	30	30	30.25	340.6	32.034
100	29	28	28	29	28.50	170.3	29.898
6	27	28	28	28	27.75	10.2	28.831
3	27	26	27	27	26.75	5.1	27.763
AV	21.0	20.0	19.5	19.5	20.0		
PV	10.0	9.0	8.0	9.0	9.0		
YP	22.0	22.0	23.0	21.0	22.0		
Gel _{in}	23						
Gel ₁₀	29						

Table A6 Water based drilling mud mixed with 3 percentage POFA at 50°C (No.5).

RPM	Reading #1	Reading #2	Reading #3	Reading #4	Average reading	γ (sec ⁻¹)	τ (lb _f /ft ²)
300	149	140	112	109	127.50	510.9	135.611
200	120	114	110	109	113.25	340.6	120.661
100	105	101	90	95	97.75	170.3	103.577
6	55	57	42	60	53.50	10.2	56.593
3	45	47	37	35	41.00	5.1	43.780
AV	80.0	77.0	74.0	56.5	71.9		
PV	11.0	14.0	36.0	4.0	16.3		
YP	138.0	126.0	76.0	105.0	111.3		
Gel _{in}	48						
Gel ₁₀	60						

Table A7 Water based drilling mud mixed with 5 percentage POFA at 80°C (No.6).

RPM	Reading #1	Reading #2	Reading #3	Reading #4	Average reading	γ (sec ⁻¹)	τ (lb _f /ft ²)
300	132	132	140	159	140.75	510.9	149.492
200	127	129	129	131	129.00	340.6	137.746
100	109	111	111	119	112.50	170.3	119.594
6	63	69	71	59	65.50	10.2	69.407
3	60	63	68	51	60.50	5.1	64.068
AV	74.5	77.5	77.5	88.0	79.4		
PV	17.0	23.0	15.0	17.0	18.0		
YP	115.0	109.0	125.0	142.0	122.8		
Gel _{in}	63						
Gel ₁₀	68						

Table A8 Water based drilling mud mixed with 1 percentage POFA at 50°C (No.7).

RPM	Reading #1	Reading #2	Reading #3	Reading #4	Average reading	γ (sec ⁻¹)	τ (lb _f /ft ²)
300	58	50	57	58	55.75	510.9	58.729
200	50	49	57	58	53.50	340.6	56.593
100	47	48	53	55	50.75	170.3	53.390
6	43	40	43	45	42.75	10.2	44.848
3	38	39	37	39	38.25	5.1	40.576
AV	31.0	32.5	30.5	31.0	31.3		
PV	4.0	15.0	4.0	4.0	6.8		
YP	54.0	35.0	53.0	54.0	49.0		
Gel _{in}	39						
Gel ₁₀	40						

Table A9 Water based drilling mud mixed with 3 percentage POFA at 50°C (No.8).

RPM	Reading #1	Reading #2	Reading #3	Reading #4	Average reading	γ (sec ⁻¹)	τ (lb _f /ft ²)
300	153	143	140	150	146.50	510.9	155.899
200	123	139	126	122	127.50	340.6	135.611
100	90	102	90	102	96.00	170.3	102.509
6	44	48	44	48	46.00	10.2	49.119
3	31	39	31	39	35.00	5.1	37.373
AV	78.5	79.0	78.5	79.0	78.8		
PV	4.0	15.0	17.0	8.0	11.0		
YP	149.0	128.0	123.0	142.0	135.5		
Gel _{in}	53						
Gel ₁₀	62						

Table A10 Water based drilling mud mixed with 5 percentage POFA at 50°C (No.9).

RPM	Reading #1	Reading #2	Reading #3	Reading #4	Average reading	γ (sec ⁻¹)	τ (lb _f /ft ²)
300	253	255	247	237	248.00	510.9	264.814
200	231	230	238	215	228.50	340.6	243.458
100	201	173	198	187	189.75	170.3	201.814
6	111	70	113	72	91.50	10.2	97.170
3	80	60	86	66	73.00	5.1	77.949
AV	131.5	136.0	127.5	127.5	130.6		
PV	10.0	17.0	8.0	18.0	13.3		
YP	243.0	238.0	239.0	219.0	234.8		
Gel _{in}	67						
Gel ₁₀	80						

Table A11 Water based drilling mud mixed with 1 percentage POFA at 80°C (No.10).

RPM	Reading #1	Reading #2	Reading #3	Reading #4	Average reading	γ (sec ⁻¹)	τ (lb _f /ft ²)
300	60	62	60	63	61.25	510.9	65.136
200	52	61	59	62	58.50	340.6	61.932
100	50	58	57	58	55.75	170.3	58.729
6	44	49	50	52	48.75	10.2	51.254
3	48	31	50	45	43.50	5.1	45.915
AV	33.0	33.5	34.0	34.5	33.8		
PV	6.0	5.0	8.0	6.0	6.3		
YP	54.0	57.0	52.0	57.0	55.0		
Gel _{in}	41						
Gel ₁₀	45						

Table A12 Water based drilling mud mixed with 3 percentage POFA at 80°C (No.11).

RPM	Reading #1	Reading #2	Reading #3	Reading #4	Average reading	γ (sec ⁻¹)	τ (lb _f /ft ²)
300	202	198	200	187	196.75	510.9	209.289
200	173	168	179	148	167.00	340.6	178.323
100	118	122	125	145	127.50	170.3	135.611
6	77	74	87	65	75.75	10.2	80.085
3	47	58	70	59	58.50	5.1	61.932
AV	106.0	102.5	104.0	102.5	103.8		
PV	10.0	7.0	8.0	18.0	10.8		
YP	192.0	191.0	192.0	169.0	186.0		
Gel _{in}	57						
Gel ₁₀	66						

Table A13 Water based drilling mud mixed with 5 percentage POFA at 80°C (No.12).

RPM	Reading #1	Reading #2	Reading #3	Reading #4	Average reading	γ (sec ⁻¹)	τ (lb _f /ft ²)
300	282	280	285	279	281.50	510.9	300.052
200	268	265	270	250	263.25	340.6	280.831
100	245	247	240	227	239.75	170.3	255.204
6	130	78	97	91	99.00	10.2	105.712
3	101	74	95	90	90.00	5.1	96.102
AV	147.5	145.0	147.5	145.5	146.4		
PV	13.0	10.0	10.0	12.0	11.3		
YP	269.0	270.0	275.0	267.0	270.3		
Gel _{in}	74						
Gel ₁₀	90						

Table A14 Water based drilling mud mixed with 1 percentage SCBA at 25°C (No.13).

RPM	Reading #1	Reading #2	Reading #3	Reading #4	Average reading	γ (sec ⁻¹)	τ (lb _f /ft ²)
300	28	28	28	29	28.25	510.9	29.898
200	24	25	24	25	24.50	340.6	25.627
100	20	22	20	20	20.50	170.3	21.356
6	18	14	14	17	15.75	10.2	16.017
3	14	13	13	15	13.75	5.1	13.881
AV	19.0	19.0	19.0	19.0	19.0		
PV	10.0	10.0	10.0	9.0	9.8		
YP	18.0	18.0	18.0	20.0	18.5		
Gel _{in}	15						
Gel ₁₀	16						

Table A15 Water based drilling mud mixed with 3 percentage SCBA at 25°C (No.14).

RPM	Reading #1	Reading #2	Reading #3	Reading #4	Average reading	γ (sec ⁻¹)	τ (lb _f /ft ²)
300	32	33	33	34	33.00	510.9	35.237
200	28	29	31	30	29.50	340.6	30.966
100	24	26	25	27	25.50	170.3	26.695
6	19	22	19	21	20.25	10.2	21.356
3	17	17	18	19	17.75	5.1	18.153
AV	22.0	22.0	21.5	21.0	21.6		
PV	12.0	11.0	10.0	8.0	10.3		
YP	20.0	22.0	23.0	26.0	22.8		
Gel _{in}	20						
Gel ₁₀	21						

Table A16 Water based drilling mud mixed with 5 percentage SCBA at 25°C (No.15).

RPM	Reading #1	Reading #2	Reading #3	Reading #4	Average reading	γ (sec ⁻¹)	τ (lb _f /ft ²)
300	36	38	35	35	36.00	510.9	38.441
200	31	33	30	34	32.00	340.6	34.170
100	26	29	25	30	27.50	170.3	28.831
6	18	23	19	28	22.00	10.2	23.492
3	17	22	16	21	19.00	5.1	20.288
AV	24.0	24.5	22.5	23.0	23.5		
PV	12.0	11.0	10.0	11.0	11.0		
YP	24.0	27.0	25.0	24.0	25.0		
Gel _{in}	23						
Gel ₁₀	28						

Table A17 Water based drilling mud mixed with 1 percentage SCBA at 50°C (No.16).

RPM	Reading #1	Reading #2	Reading #3	Reading #4	Average reading	γ (sec ⁻¹)	τ (lb _f /ft ²)
300	34	37	38	38	36.75	510.9	38.441
200	32	35	32	38	34.25	340.6	36.305
100	29	33	29	33	31.00	170.3	33.102
6	24	29	23	29	26.25	10.2	27.763
3	23	25	22	28	24.50	5.1	25.627
AV	19.5	21.5	22.5	23.0	21.6		
PV	5.0	6.0	7.0	8.0	6.5		
YP	29.0	31.0	31.0	33.0	30.3		
Gel _{in}	22						
Gel ₁₀	24						

Table A18 Water based drilling mud mixed with 3 percentage SCBA at 50°C (No.17).

RPM	Reading #1	Reading #2	Reading #3	Reading #4	Average reading	γ (sec ⁻¹)	τ (lb _f /ft ²)
300	37	39	36	38	37.50	510.9	39.509
200	34	37	33	36	35.00	340.6	37.373
100	31	34	30	35	32.50	170.3	34.170
6	24	29	26	29	27.00	10.2	28.831
3	24	27	23	32	26.50	5.1	26.695
AV	21.0	24.0	21.5	22.0	22.1		
PV	5.0	9.0	7.0	6.0	6.8		
YP	32.0	30.0	29.0	32.0	30.8		
Gel _{in}	27						
Gel ₁₀	31						

Table A19 Water based drilling mud mixed with 5 percentage SCBA at 50°C (No.18).

RPM	Reading #1	Reading #2	Reading #3	Reading #4	Average reading	γ (sec ⁻¹)	τ (lb _f /ft ²)
300	41	39	39	40	39.75	510.9	41.644
200	34	36	35	39	36.00	340.6	38.441
100	33	34	31	35	33.25	170.3	35.237
6	26	28	28	31	28.25	10.2	29.898
3	25	29	24	28	26.50	5.1	27.763
AV	24.5	23.5	23.0	24.0	23.8		
PV	8.0	8.0	7.0	8.0	7.8		
YP	33.0	31.0	32.0	32.0	32.0		
Gel _{in}	29						
Gel ₁₀	32						

Table A20 Water based drilling mud mixed with 1 percentage SCBA at 80°C (No.19).

RPM	Reading #1	Reading #2	Reading #3	Reading #4	Average reading	γ (sec ⁻¹)	τ (lb _f /ft ²)
300	42	42	42	42	42.00	510.9	44.848
200	39	40	40	38	39.25	340.6	41.644
100	36	32	36	35	34.75	170.3	36.305
6	25	29	25	29	27.00	10.2	28.831
3	24	25	25	25	24.75	5.1	26.695
AV	24.5	23.5	24.0	24.0	24.0		
PV	7.0	5.0	6.0	6.0	6.0		
YP	35.0	37.0	36.0	36.0	36.0		
Gel _{in}	25						
Gel ₁₀	27						

Table A21 Water based drilling mud mixed with 3 percentage SCBA at 80°C (No.20).

RPM	Reading #1	Reading #2	Reading #3	Reading #4	Average reading	γ (sec ⁻¹)	τ (lb _f /ft ²)
300	49	50	50	49	49.50	510.9	52.322
200	45	48	49	45	46.75	340.6	49.119
100	42	45	43	41	42.75	170.3	44.848
6	32	33	39	29	33.25	10.2	35.237
3	29	30	35	29	30.75	5.1	32.034
AV	28.0	28.0	28.0	27.5	27.9		
PV	7.0	6.0	6.0	6.0	6.3		
YP	42.0	44.0	44.0	43.0	43.3		
Gel _{in}	27						
Gel ₁₀	29						

Table A22 Water based drilling mud mixed with 5 percentage SCBA at 80°C (No.21).

RPM	Reading #1	Reading #2	Reading #3	Reading #4	Average reading	γ (sec ⁻¹)	τ (lb _f /ft ²)
300	55	51	53	51	52.50	510.9	55.526
200	52	50	46	51	49.75	340.6	52.322
100	40	46	43	50	44.75	170.3	46.983
6	30	35	31	45	35.25	10.2	37.373
3	28	30	30	40	32.00	5.1	34.170
AV	31.0	29.0	30.0	28.5	29.6		
PV	7.0	7.0	7.0	6.0	6.8		
YP	48.0	44.0	46.0	45.0	45.8		
Gel _{in}	30						
Gel ₁₀	40						



API static filtrate loss and mud filter cake thickness data for all tested

Table A23 Water based drilling mud in 25, 50 and 80°C.

No.	Filtrate loss (ml)					
	1 min	4 min	9 min	16 min	25 min	30 min
1	2.25	6.50	9.50	14.50	18.00	19.75
2	2.75	7.25	10.50	15.50	18.75	21.25
3	3.75	7.50	11.75	17.50	20.75	23.25

Table A24 Water based drilling mud mixed with 1, 3 and 5 percentage POFA at 25°C.

No.	Filtrate loss (ml)					
	1 min	4 min	9 min	16 min	25 min	30 min
4	3.00	7.50	12.00	16.75	21.25	23.50
5	6.25	14.00	21.50	29.75	37.00	40.50
6	12.25	24.75	37.50	50.25	63.75	69.50

Table A25 Water based drilling mud mixed with 1, 3 and 5 percentage POFA at 50°C.

No.	Filtrate loss (ml)					
	1 min	4 min	9 min	16 min	25 min	30 min
7	3.50	8.00	12.50	17.25	22.50	24.50
8	6.75	15.25	23.00	31.25	39.25	43.00
9	13.25	27.25	41.50	55.75	69.75	76.25

Table A26 Water based drilling mud mixed with 1, 3 and 5 percentage POFA at 80°C.

No.	Filtrate loss (ml)					
	1 min	4 min	9 min	16 min	25 min	30 min
10	4.25	9.50	14.75	20.00	25.00	27.75
11	8.25	16.50	25.25	34.00	42.50	46.50
12	14.75	31.00	47.25	60.50	76.00	83.00

Table A27 Water based drilling mud mixed with 1, 3 and 5 percentage SCBA at 25°C.

No.	Filtrate loss (ml)					
	1 min	4 min	9 min	16 min	25 min	30 min
13	2.00	5.70	9.40	13.00	16.75	18.50
14	2.25	5.75	9.50	13.25	17.00	18.75
15	2.50	6.00	10.00	13.75	17.25	19.25

Table A28 Water based drilling mud mixed with 1, 3 and 5 percentage SCBA at 50°C.

No.	Filtrate loss (ml)					
	1 min	4 min	9 min	16 min	25 min	30 min
16	2.30	6.20	10.00	14.00	18.00	19.50
17	2.40	6.50	10.50	14.50	18.50	20.00
18	2.50	6.80	10.75	15.00	19.00	21.00

Table A29 Water based drilling mud mixed with 1, 3 and 5 percentage SCBA at 80°C.

No.	Filtrate loss (ml)					
	1 min	4 min	9 min	16 min	25 min	30 min
19	2.60	7.00	11.00	15.50	19.50	21.50
20	3.00	7.50	11.50	15.75	19.75	21.75
21	3.25	7.75	12.00	16.50	20.50	22.50

Table A30 Water based drilling mud in 25, 50 and 80 °C.

No.	Mud filter cake thickness (mm)			Average (mm)
	#1	#2	#3	
1	1.84	1.88	1.78	1.83
2	2.16	2.20	2.36	2.24
3	2.34	2.62	2.66	2.54

Table A31 Water based drilling mud mixed with 1, 3 and 5 percentage POFA at 25°C.

No.	Mud filter cake thickness (mm)			Average (mm)
	#1	#2	#3	
4	2.50	2.94	2.78	2.74
5	3.02	3.00	3.04	3.02
6	4.72	5.30	5.06	5.03

Table A32 Water based drilling mud mixed with 1, 3 and 5 percentage POFA at 50°C.

No.	Mud filter cake thickness (mm)			Average (mm)
	#1	#2	#3	
7	3.16	3.44	2.80	3.13
8	3.64	3.90	3.40	3.65
9	5.12	4.60	5.64	5.12

Table A33 Water based drilling mud mixed with 1, 3 and 5 percentage POFA at 80°C.

No.	Mud filter cake thickness (mm)			Average (mm)
	#1	#2	#3	
10	3.40	3.36	3.60	3.45
11	3.54	3.70	4.14	3.79
12	5.48	5.22	5.10	5.27

Table A34 Water based drilling mud mixed with 1, 3 and 5 percentage SCBA at 25°C.

No.	Mud filter cake thickness (mm)			Average (mm)
	#1	#2	#3	
13	1.44	1.48	1.40	1.44
14	1.62	1.74	1.72	1.69
15	1.58	1.88	1.70	1.72

Table A35 Water based drilling mud mixed with 1, 3 and 5 percentage SCBA at 50°C.

No.	Mud filter cake thickness (mm)			Average (mm)
	#1	#2	#3	
16	1.80	1.82	1.76	1.79
17	1.88	1.70	1.82	18.0
18	1.90	1.86	2.10	1.95

Table A36 Water based drilling mud mixed with 1, 3 and 5 percentage SCBA at 80°C.

No.	Mud filter cake thickness (mm)			Average (mm)
	#1	#2	#3	
19	2.06	2.00	2.08	2.05
20	2.28	2.06	2.12	2.15
21	2.30	2.24	2.48	2.34

Hydrogen ion concentration data for all tested

Table A37 Water based drilling mud in 25, 50 and 80°C.

No.	Sample	pH reading			Average
		#1	#2	#3	
1	Mud	10.32	10.35	10.36	10.34
	Mud filtrate	10.17	10.18	10.16	10.17
2	Mud	10.20	10.27	10.30	10.26
	Mud filtrate	10.07	10.08	10.08	10.08
3	Mud	10.12	10.14	10.15	10.14
	Mud filtrate	9.99	10.04	10.02	10.02

Table A38 Water based drilling mud mixed with 1, 3 and 5 percentage POFA at 25°C.

No.	Sample	pH reading			Average
		#1	#2	#3	
4	Mud	10.69	10.70	10.68	10.69
	Mud filtrate	10.56	10.57	10.58	10.57
5	Mud	10.59	10.54	10.57	10.57
	Mud filtrate	10.52	10.52	10.52	10.52
6	Mud	10.51	10.51	10.51	10.51
	Mud filtrate	10.47	10.47	10.46	10.47

Table A39 Water based drilling mud mixed with 1, 3 and 5 percentage POFA at 50°C.

No.	Sample	pH reading			Average
		#1	#2	#3	
7	Mud	10.57	10.58	10.58	10.58
	Mud filtrate	10.54	10.53	10.52	10.53
8	Mud	10.45	10.44	10.44	10.44
	Mud filtrate	10.43	10.43	10.42	10.43
9	Mud	10.40	10.39	10.40	10.40
	Mud filtrate	10.41	10.41	10.40	10.41

Table A40 Water based drilling mud mixed with 1, 3 and 5 percentage POFA at 80°C.

No.	Sample	pH reading			Average
		#1	#2	#3	
10	Mud	10.52	10.49	10.52	10.51
	Mud filtrate	10.50	10.48	10.53	10.50
11	Mud	10.39	10.37	10.38	10.38
	Mud filtrate	10.36	10.39	10.37	10.37
12	Mud	10.36	10.32	10.32	10.33
	Mud filtrate	10.35	10.32	10.30	10.32

Table A41 Water based drilling mud mixed with 1, 3 and 5 percentage SCBA at 25°C.

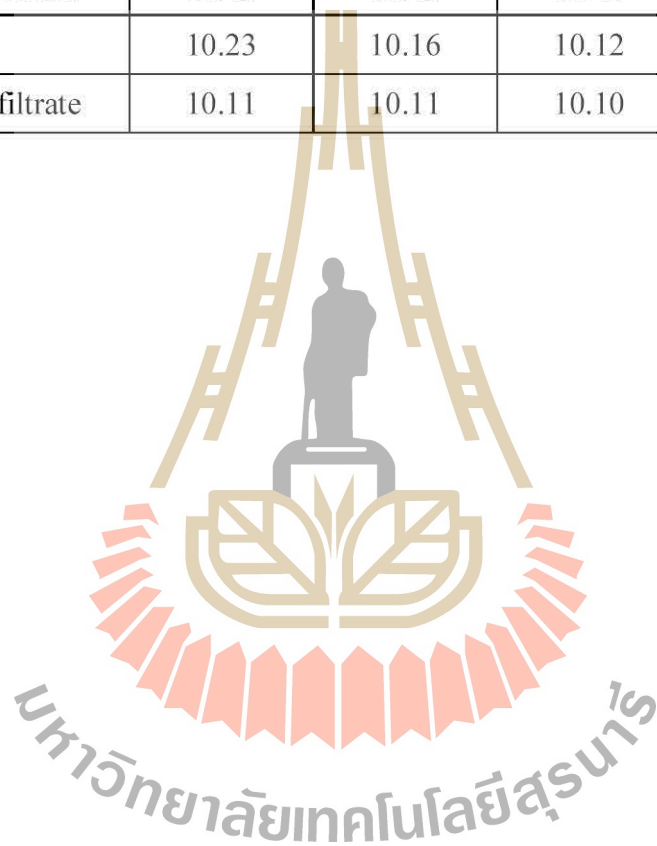
No.	Sample	pH reading			Average
		#1	#2	#3	
13	Mud	10.74	10.74	10.73	10.74
	Mud filtrate	10.61	10.61	10.60	10.61
14	Mud	10.60	10.60	10.60	10.60
	Mud filtrate	10.55	10.55	10.53	10.54
15	Mud	10.49	10.43	10.40	10.44
	Mud filtrate	10.31	10.32	10.32	10.32

Table A42 Water based drilling mud mixed with 1, 3 and 5 percentage SCBA at 50°C.

No.	Sample	pH reading			Average
		#1	#2	#3	
16	Mud	10.72	10.72	10.72	10.72
	Mud filtrate	10.61	10.60	10.57	10.59
17	Mud	10.58	10.58	10.57	10.58
	Mud filtrate	10.53	10.52	10.51	10.52
18	Mud	10.34	10.30	10.28	10.31
	Mud filtrate	10.19	10.16	10.18	10.18

Table A43 Water based drilling mud mixed with 1, 3 and 5 percentage SCBA at 80°C.

No.	Sample	pH reading			Average
		#1	#2	#3	
19	Mud	10.66	10.66	10.66	10.66
	Mud filtrate	10.55	10.54	10.52	10.54
20	Mud	10.45	10.42	10.40	10.42
	Mud filtrate	10.42	10.42	10.43	10.42
21	Mud	10.23	10.16	10.12	10.17
	Mud filtrate	10.11	10.11	10.10	10.11



Resistivity data for all tested

Table A44 Water based drilling mud at 25°C (No.1).

Sample	Temperature (°F)	#1	#2	#3	Average (Ω.m)
		(Ω.m)			
Mud	79.4	4.65	4.64	4.63	4.64
Mud filtrate	81.8	5.81	5.80	5.80	5.80
Mud filter cake	81.3	3.70	3.74	3.70	3.71

Table A45 Water based drilling mud at 50°C (No.2).

Sample	Temperature (°F)	#1	#2	#3	Average (Ω.m)
		(Ω.m)			
Mud	81.5	4.41	4.42	4.44	4.42
Mud filtrate	77.9	5.67	5.65	5.64	5.65
Mud filter cake	79.5	3.48	3.49	3.49	3.49

Table A46 Water based drilling mud at 80°C (No.3).

Sample	Temperature (°F)	#1	#2	#3	Average (Ω.m)
		(Ω.m)			
Mud	80.8	4.37	4.38	4.39	4.38
Mud filtrate	80.2	5.55	5.56	5.57	5.56
Mud filter cake	80.8	3.37	3.35	3.32	3.35

Table A47 Water based drilling mud mixed with 1 percentage POFA at 25°C (No.4).

Sample	Temperature (°F)	#1	#2	#3	Average (Ω.m)
		(Ω.m)			
Mud	75.8	2.44	2.38	2.31	2.38
Mud filtrate	74.7	2.82	2.82	2.82	2.82
Mud filter cake	75.6	2.88	2.86	2.09	2.61

Table A48 Water based drilling mud mixed with 3 percentage POFA at 25°C (No.5).

Sample	Temperature (°F)	#1	#2	#3	Average (Ω.m)
		(Ω.m)			
Mud	75.6	1.19	1.25	1.21	1.22
Mud filtrate	73.1	1.29	1.28	1.33	1.30
Mud filter cake	77.3	1.09	1.09	1.13	1.10

Table A49 Water based drilling mud mixed with 5 percentage POFA at 25°C (No.6).

Sample	Temperature (°F)	#1	#2	#3	Average (Ω.m)
		(Ω.m)			
Mud	78.6	1.06	1.04	1.06	1.05
Mud filtrate	75.3	0.84	0.81	0.81	0.82
Mud filter cake	76.8	1.11	1.10	1.07	1.09

Table A50 Water based drilling mud mixed with 1 percentage POFA at 50°C (No.7).

Sample	Temperature (°F)	#1	#2	#3	Average (Ω.m)
		(Ω.m)			
Mud	75.2	1.94	1.96	1.89	1.93
Mud filtrate	75.5	2.50	2.49	2.49	2.49
Mud filter cake	74.6	2.09	2.50	2.37	2.32

Table A51 Water based drilling mud mixed with 3 percentage POFA at 50°C (No.8).

Sample	Temperature (°F)	#1	#2	#3	Average (Ω.m)
		(Ω.m)			
Mud	76.0	1.06	1.06	1.08	1.07
Mud filtrate	74.2	1.29	1.27	1.21	1.26
Mud filter cake	76.8	1.08	1.09	1.09	1.09

Table A52 Water based drilling mud mixed with 5 percentage POFA at 50°C (No.9).

Sample	Temperature (°F)	#1	#2	#3	Average (Ω.m)
		(Ω.m)			
Mud	77.6	0.95	1.04	1.06	1.02
Mud filtrate	74.2	0.81	0.80	0.79	0.80
Mud filter cake	75.1	0.98	0.97	0.97	0.97

Table A53 Water based drilling mud mixed with 1 percentage POFA at 80°C (No.10).

Sample	Temperature (°F)	#1	#2	#3	Average (Ω.m)
		(Ω.m)			
Mud	84.3	1.57	1.43	1.48	1.49
Mud filtrate	77.6	2.19	2.32	2.33	2.28
Mud filter cake	76.8	1.98	1.97	1.99	1.98

Table A54 Water based drilling mud mixed with 3 percentage POFA at 80°C (No.11).

Sample	Temperature (°F)	#1	#2	#3	Average (Ω.m)
		(Ω.m)			
Mud	82.1	0.93	0.93	1.01	0.96
Mud filtrate	77.3	1.10	1.09	1.10	1.10
Mud filter cake	76.8	1.05	1.06	1.06	1.06

Table A55 Water based drilling mud mixed with 5 percentage POFA at 80°C (No.12).

Sample	Temperature (°F)	#1	#2	#3	Average (Ω.m)
		(Ω.m)			
Mud	79.3	0.81	0.83	0.83	0.82
Mud filtrate	75.4	0.73	0.75	0.73	0.74
Mud filter cake	75.5	0.93	0.94	0.92	0.93

Table A56 Water based drilling mud mixed with 1 percentage SCBA at 25°C (No.13).

Sample	Temperature (°F)	#1	#2	#3	Average (Ω.m)
		(Ω.m)			
Mud	77.7	4.80	4.78	4.84	4.81
Mud filtrate	75.7	5.73	5.75	5.74	5.74
Mud filter cake	76.0	3.60	3.54	3.55	3.56

Table A57 Water based drilling mud mixed with 3 percentage SCBA at 25°C (No.14).

Sample	Temperature (°F)	#1	#2	#3	Average (Ω.m)
		(Ω.m)			
Mud	76.2	4.76	4.74	4.81	4.77
Mud filtrate	74.3	5.67	5.59	5.56	5.61
Mud filter cake	73.4	3.47	3.54	3.58	3.53

Table A58 Water based drilling mud mixed with 5 percentage SCBA at 25°C (No.15).

Sample	Temperature (°F)	#1	#2	#3	Average (Ω.m)
		(Ω.m)			
Mud	76.1	4.53	4.45	4.63	4.54
Mud filtrate	77.0	4.86	4.82	4.87	4.85
Mud filter cake	76.6	3.35	3.35	3.35	3.35

Table A59 Water based drilling mud mixed with 1 percentage SCBA at 50°C (No.16).

Sample	Temperature (°F)	#1	#2	#3	Average (Ω.m)
		(Ω.m)			
Mud	79.2	4.88	4.68	4.68	4.75
Mud filtrate	77.6	5.69	5.69	5.69	5.69
Mud filter cake	72.0	3.42	3.42	3.43	3.42

Table A60 Water based drilling mud mixed with 3 percentage SCBA at 50°C (No.17).

Sample	Temperature (°F)	#1	#2	#3	Average (Ω.m)
		(Ω.m)			
Mud	80.0	4.33	4.39	4.39	4.37
Mud filtrate	76.7	5.31	5.32	5.32	5.32
Mud filter cake	76.5	3.37	3.37	3.37	3.37

Table A61 Water based drilling mud mixed with 5 percentage SCBA at 50°C (No.18).

Sample	Temperature (°F)	#1	#2	#3	Average (Ω.m)
		(Ω.m)			
Mud	80.1	4.21	4.23	4.24	4.23
Mud filtrate	76.6	4.70	4.69	4.70	4.70
Mud filter cake	72.1	3.22	3.22	3.23	3.22

Table A62 Water based drilling mud mixed with 1 percentage SCBA at 80°C (No.19).

Sample	Temperature (°F)	#1	#2	#3	Average (Ω.m)
		(Ω.m)			
Mud	80.6	4.50	4.46	4.50	4.49
Mud filtrate	77.0	5.48	5.47	5.47	5.47
Mud filter cake	77.7	3.28	3.34	3.32	3.31

Table A63 Water based drilling mud mixed with 3 percentage SCBA at 80°C (No.20).

Sample	Temperature (°F)	#1	#2	#3	Average (Ω.m)
		(Ω.m)			
Mud	78.3	4.24	4.25	4.26	4.25
Mud filtrate	74.6	5.16	5.15	5.19	5.17
Mud filter cake	76.6	3.12	3.09	3.11	3.11

Table A64 Water based drilling mud mixed with 5 percentage SCBA at 80°C (No.21).

Sample	Temperature (°F)	#1	#2	#3	Average (Ω.m)
		(Ω.m)			
Mud	79.6	4.14	4.17	4.21	4.17
Mud filtrate	75.1	4.45	4.48	4.53	4.49
Mud filter cake	74.0	3.06	3.06	3.06	3.06

Solid content data for all tested

Table A65 Solid contents all drilling mud.

No.	Average solid content	
	Solid (%)	Water (ml)
1	7.76	28.0
2	8.84	45.5
3	9.48	45.5
4	2.68	48.5
5	4.82	23.0
6	5.92	43.0
7	3.94	23.0
8	5.18	47.5
9	7.16	47.5
10	4.40	48.0
11	5.76	28.0
12	7.62	41.0
13	7.58	46.0
14	8.12	45.5
15	8.97	22.5
16	8.17	20.0
17	9.00	16.0
18	10.00	44.0
19	8.67	45.0
20	9.99	14.0
21	11.04	45.0

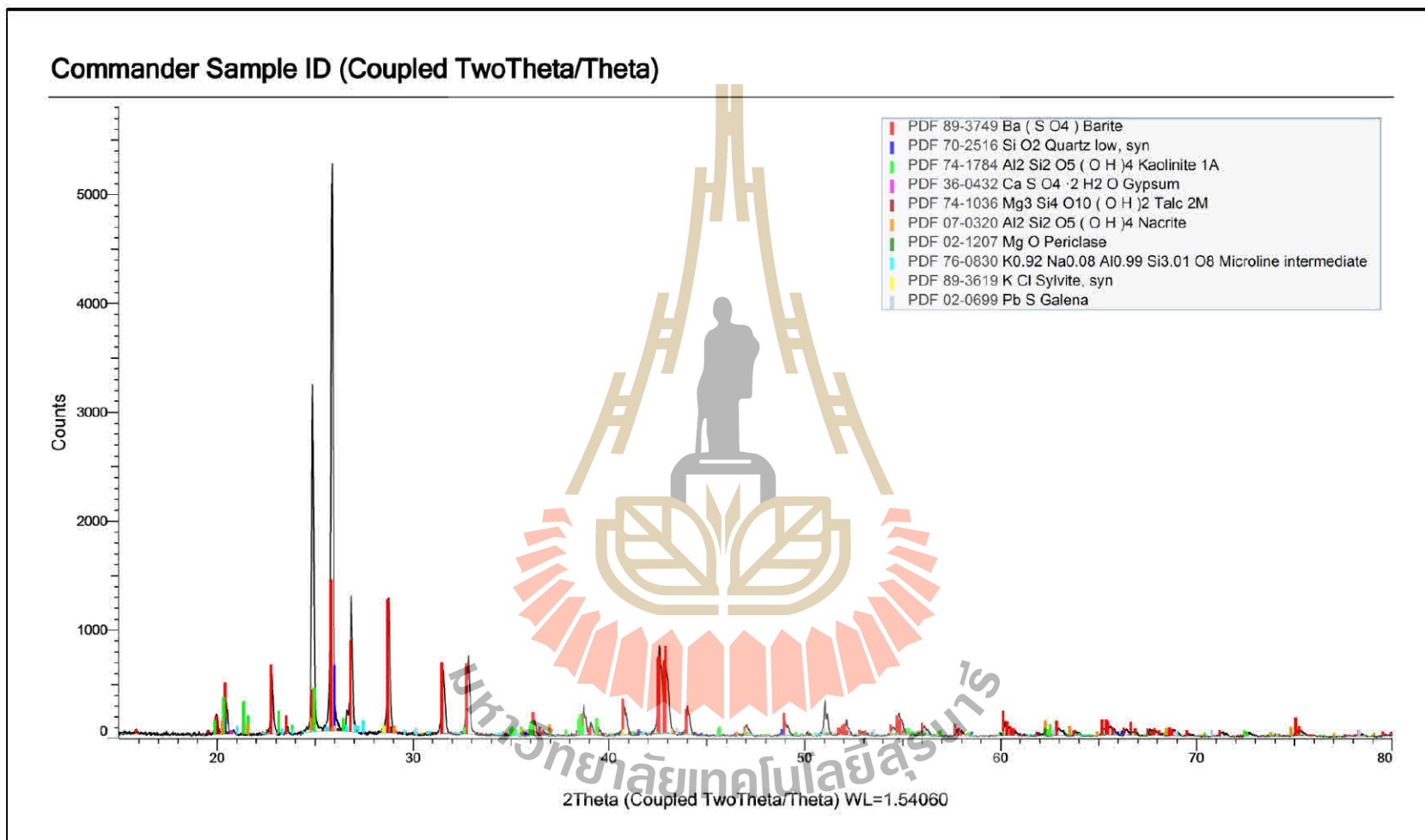


Figure A1 XRD pattern of barite.

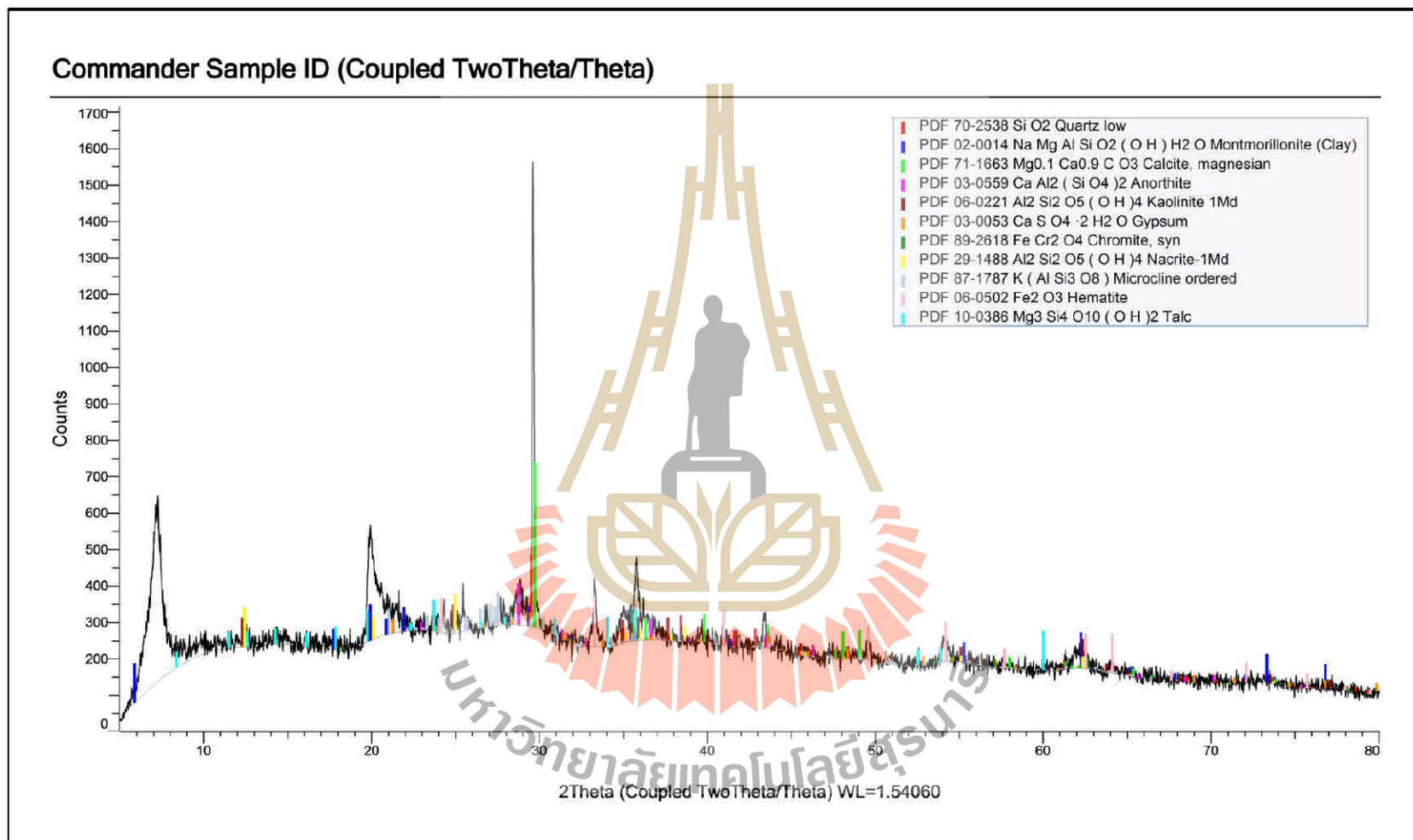


Figure A2 XRD pattern of bentonite.

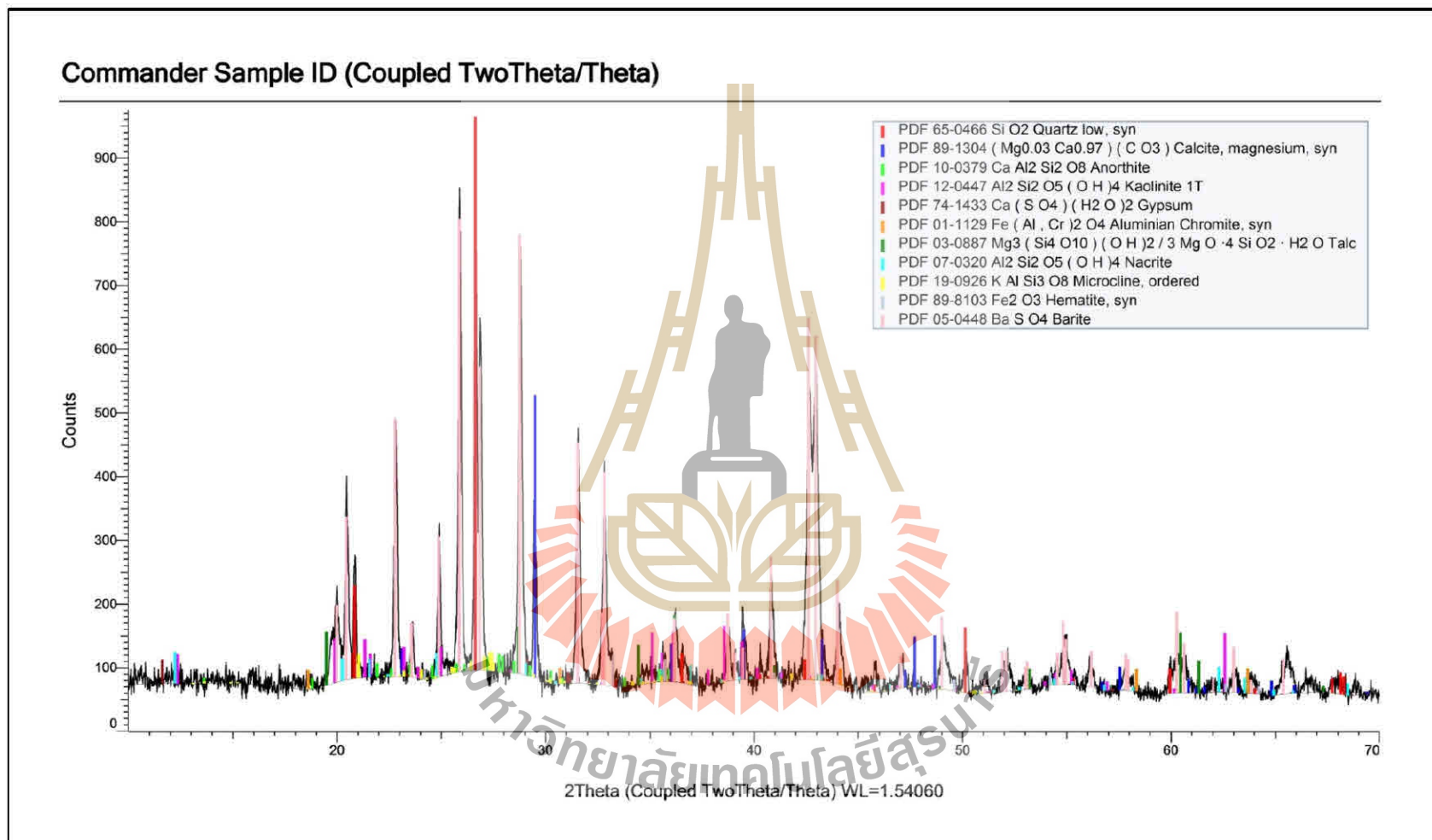


Figure A3 XRD pattern of water based drilling mud at 25°C (No.1).

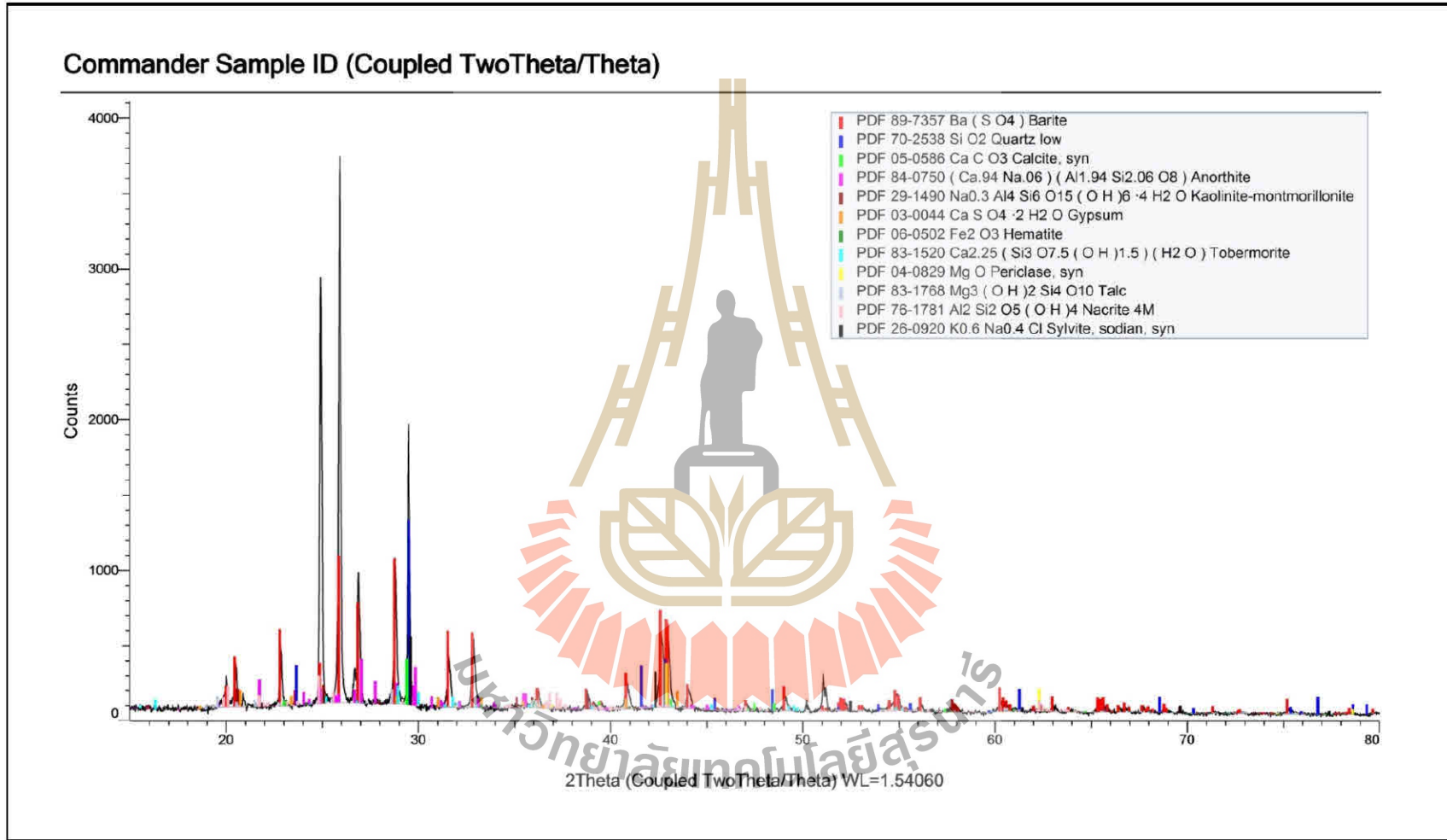


Figure A4 XRD pattern of water based drilling mud mixed with 1 percentage of POFA at 25°C (No.4).

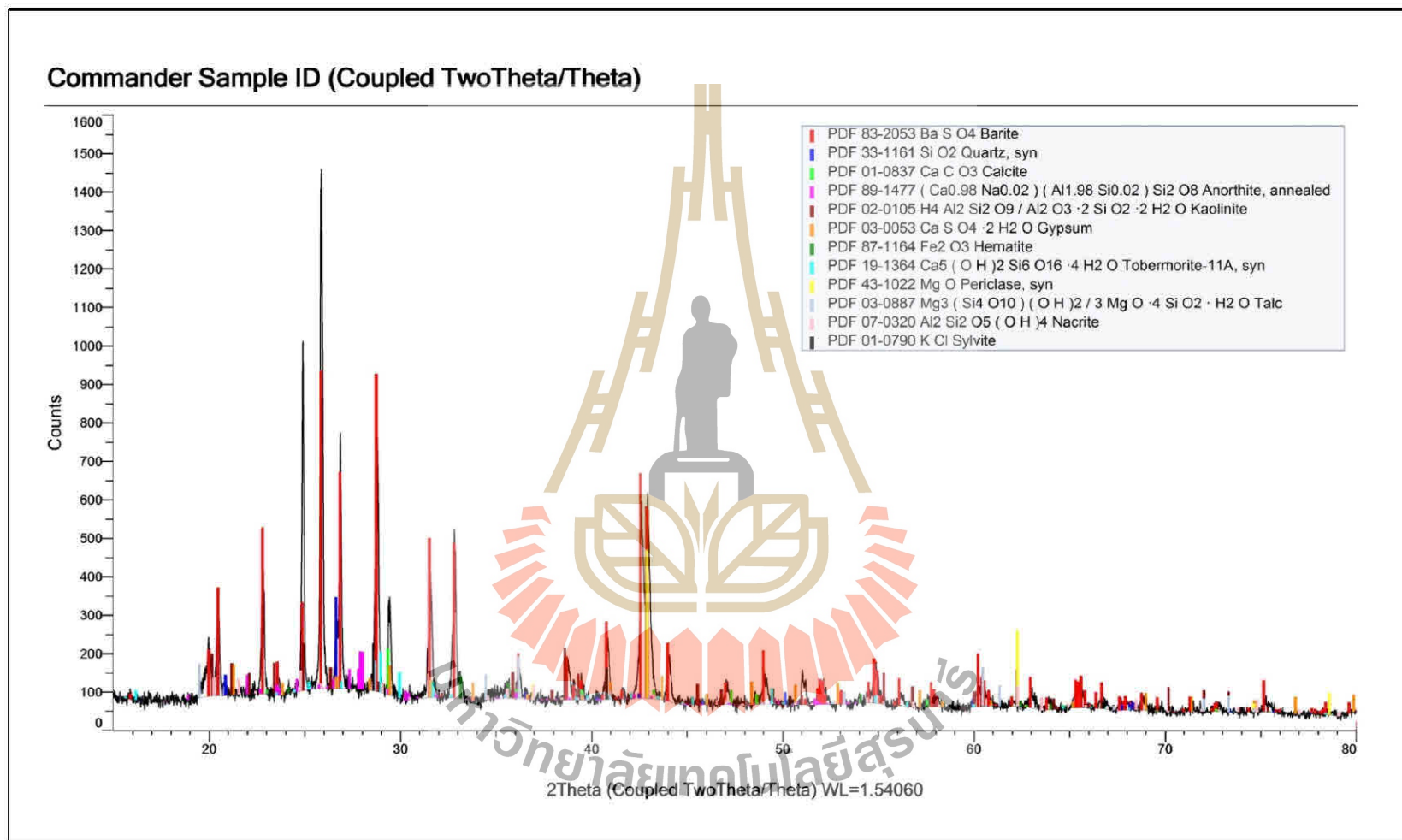


Figure A5 XRD pattern of water based drilling mud mixed with 3 percentage of POFA at 25°C (No.5).

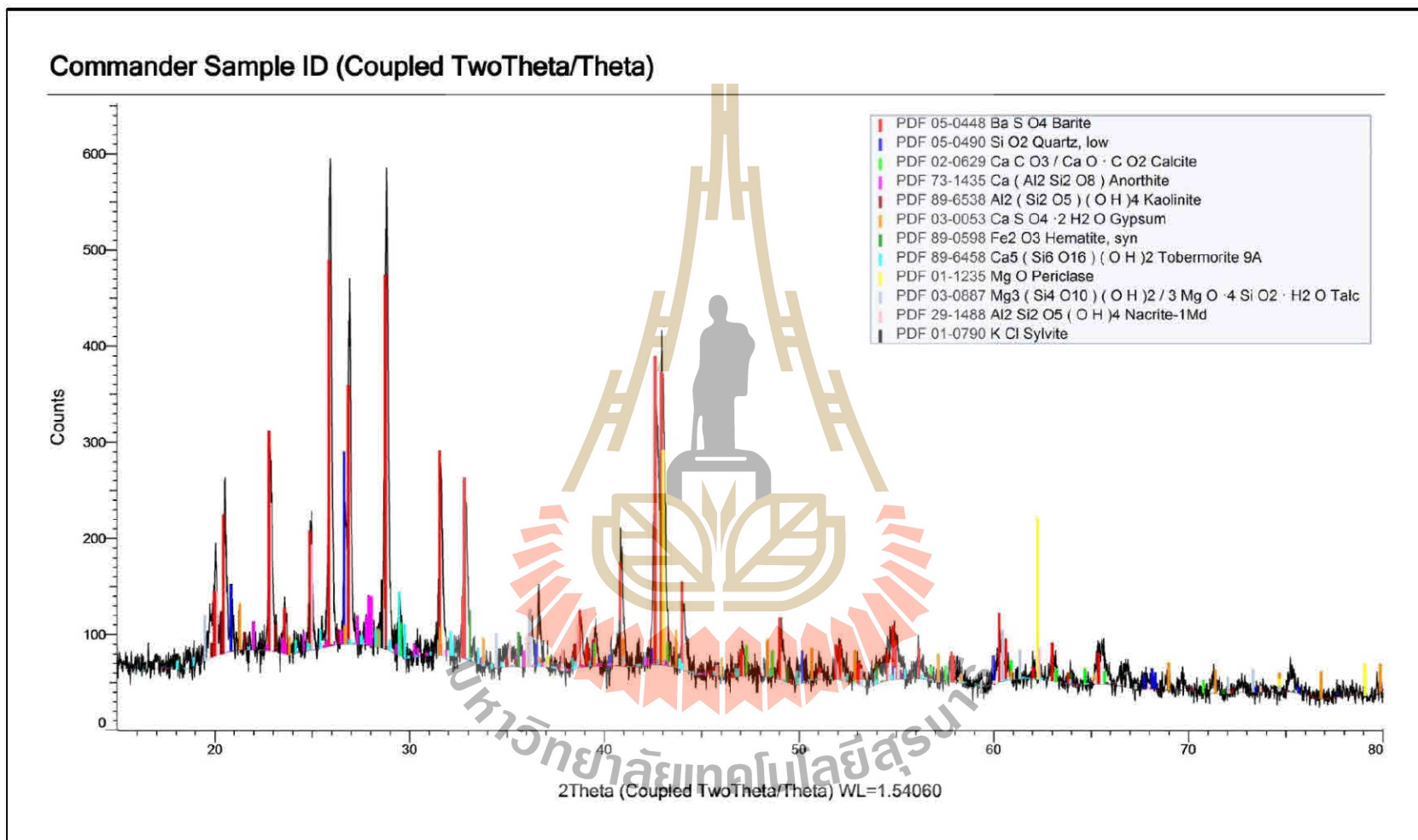


Figure A6 XRD pattern of water based drilling mud mixed with 5 percentage of POFA at 25°C (No.6).

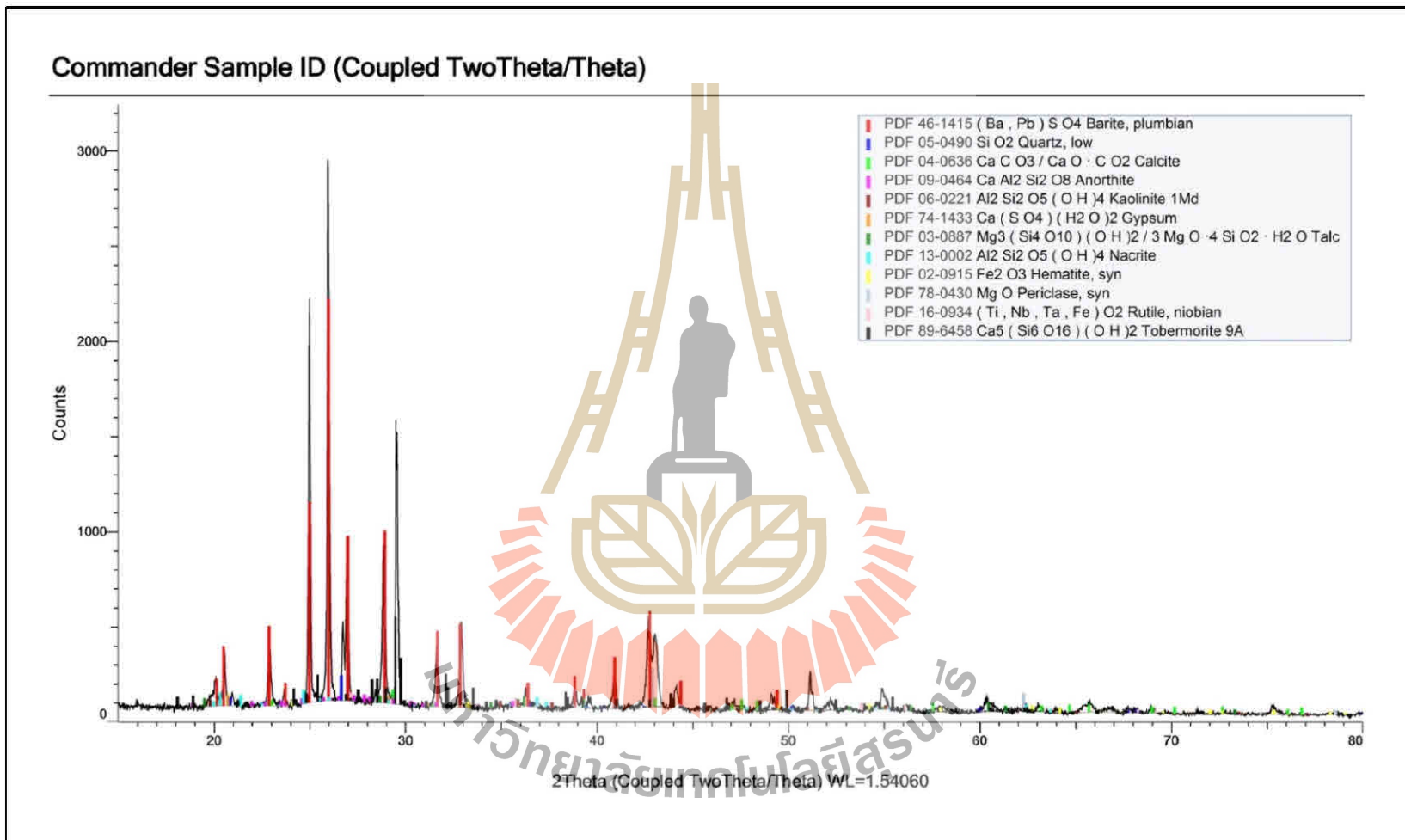


Figure A7 XRD pattern of water based drilling mud mixed with 1 percentage of SCBA at 25°C (No.13).

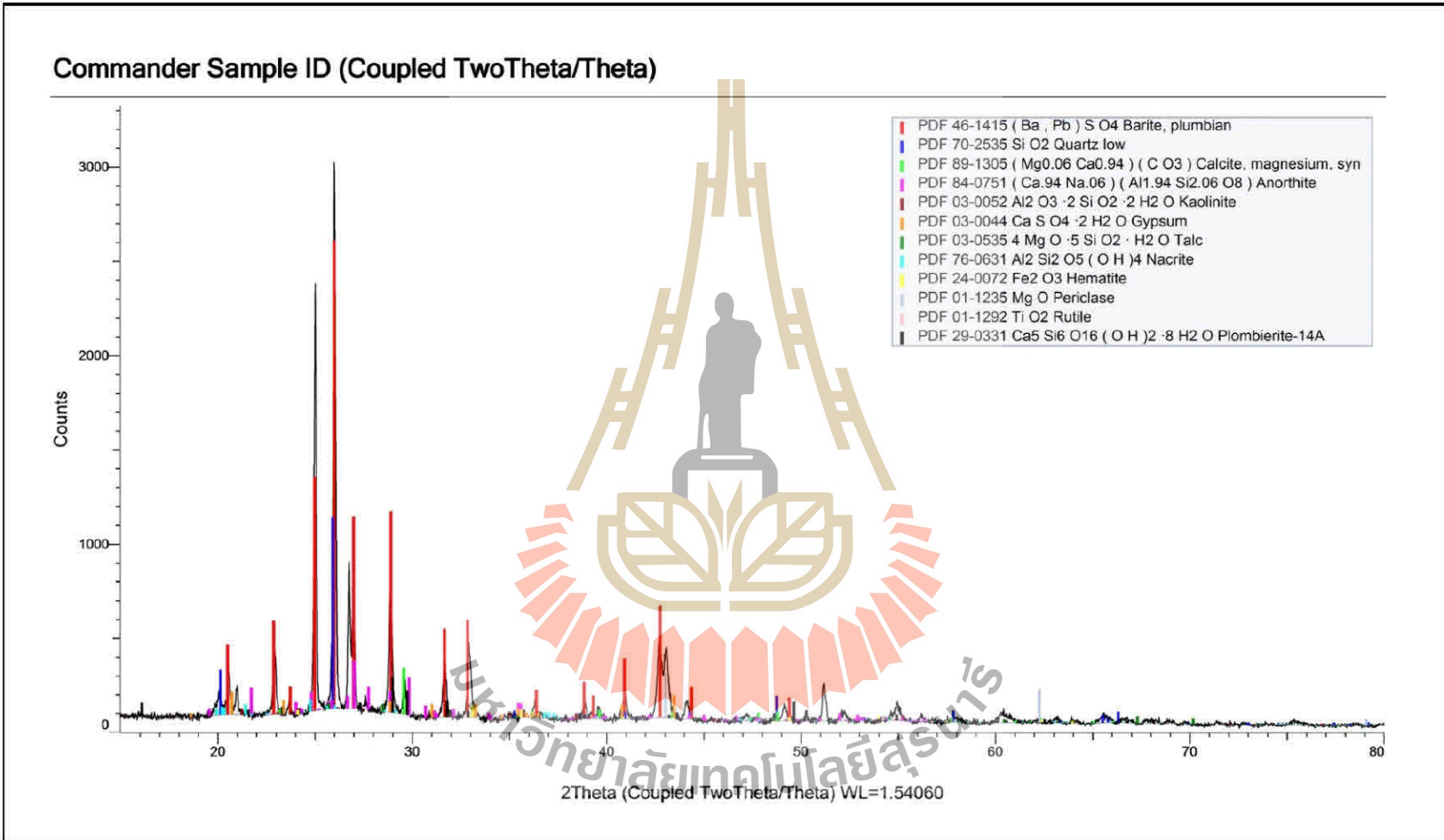


Figure A8 XRD pattern of water based drilling mud mixed with 3 percentage of SCBA at 25°C (No.14).

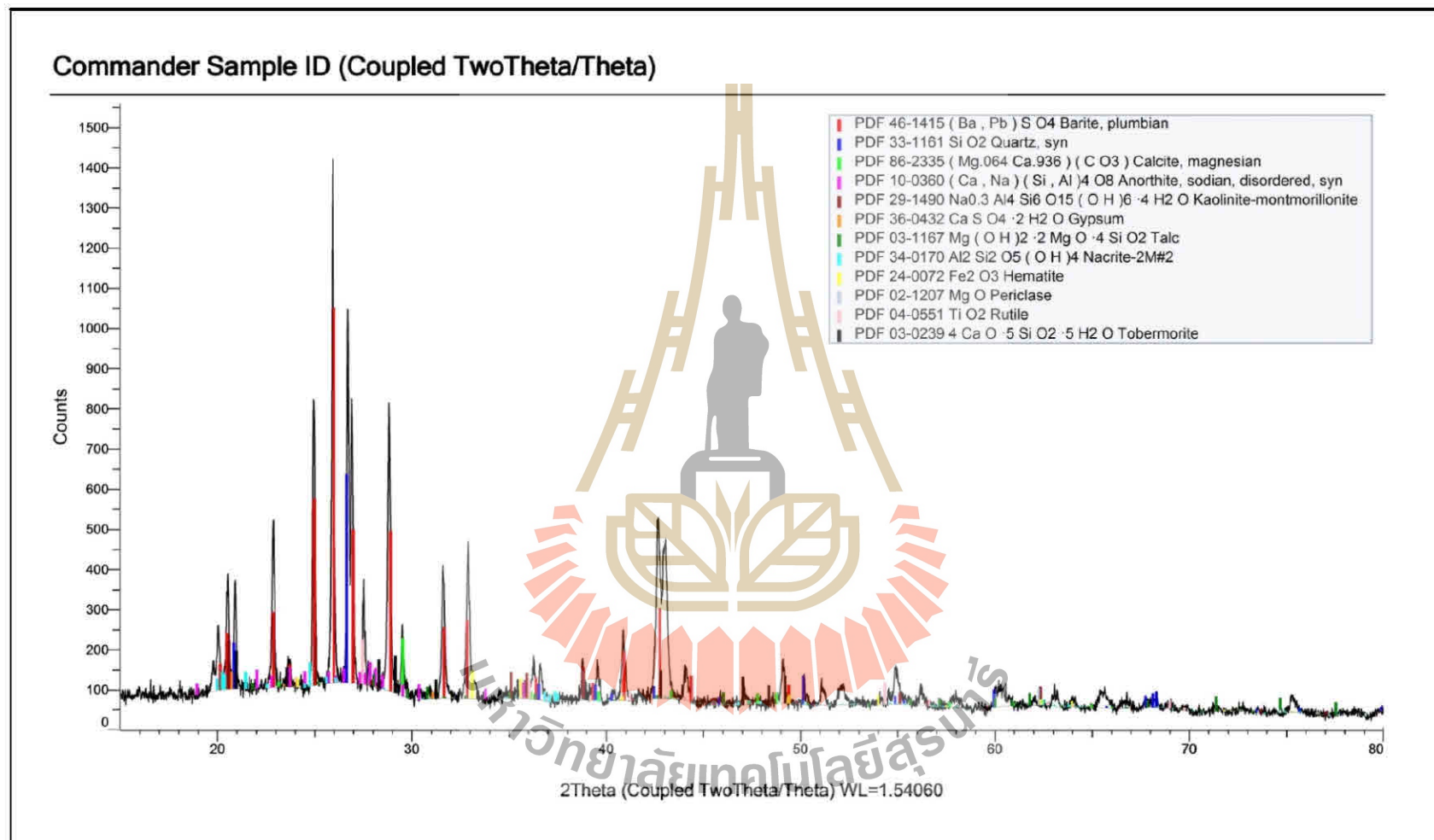
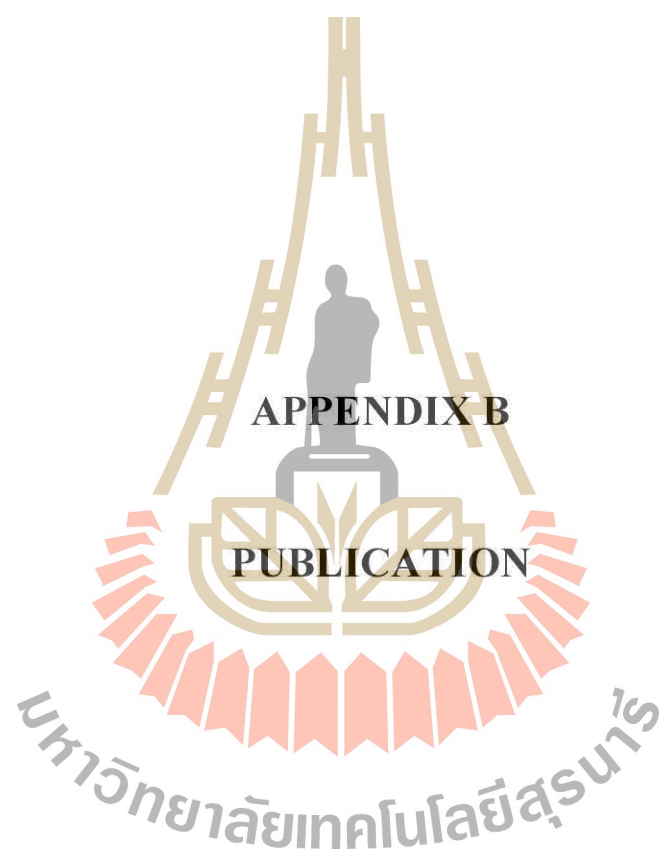


Figure A9 XRD pattern of water based drilling mud mixed with 5 percentage of SCBA at 25°C (No.15).



List of Publication

Saengdee, A., and Terakulsatit, B. (2017). Utilization of sugarcane bagasse ash as filtration loss control agent in water based drilling muds. **UBU Engineering Journal**. 10(1): 37-48.



BIOGRAPHY

Miss. Arada Saengdee was born on May 21, 1992 in Nonthaburi province, Thailand. She earned her Bachelor's Degree in Engineering (Geotechnology) from Suranaree University of Technology in 2014. After graduating, she continued to study for a Master's degree in the Petroleum Engineering Program, School of Geotechnology, Institute of Engineering, Suranaree University of Technology.

